S03020400-DAC10001-R01

Second Target Station Project: Analysis of Target Inconel-to-Tantalum Debonding

T. McManamy
J. Tipton

July, 2026

ORNL IS MANAGED BY UT-BATTELLE LLC FOR THE US DEPARTMENT OF ENERGY

S03020400-DAC10001-R01

Second Target Station Project

Analysis of Target Inconel-to-Tantalum Debonding

T. McManamy
J. Tipton

April 2026

Prepared by
OAK RIDGE NATIONAL LABORATORY
Oak Ridge, TN 37831
managed by
UT-BATTELLE LLC
for the
US DEPARTMENT OF ENERGY
under contract DE-AC05-00OR22725

CONTENTS

FIGURES

TABLES

LIST OF ACRONYMS

ASME/BPVC	=	American Society of Mechanical Engineers Boiler & Pressure Vessel Code
CTE	=	Coefficient of Thermal Expansion
DAC	=	Design Analysis Calculation
DBTT	=	Ductile-to-Brittle Transition Temperature
FEA	=	Finite Element Analysis
FOS	=	Factor of Safety
FTS	=	First Target Station
HCF	=	High Cycle Fatigue
HIP	=	Hot Isostatic Press
NUREG	=	United States Nuclear Regulatory Commission
OS	=	Operating System
PLM	=	Product Lifecycle Management
QA	=	Quality Assurance
UTS	=	Ultimate Tensile Strength
VHP	=	Vacuum Hot Press

ABSTRACT

A bounding analysis was done of the effect of total debonding in the target between the outer tantalum layer and the Inconel shell on the target fatigue life. Heat transfer between the tantalum and Inconel was assumed to be a function of pressure between contacting surfaces. An Abaqus transient coupled thermal temperature and displacement case with steady state heat loads was run until near steady state conditions were reached. The peak target temperature was 664 °C and the peak Inconel stress 475 MPa. These results were used as the initial configuration for a transient analysis with pulse heating over 1 μ second with stress evaluated over 700 μs. Fatigue analysis was then performed using fe-safe software. The fatigue lifetime for Inconel and 316L Stainless Steel was greater than 10 years. Some tungsten elements did not meet a 10-year criteria. Analyses show the target segment should be able to operate and meet requirements with the exception of cracks appearing in the tungsten even if the tantalum-to-Inconel surfaces debond.

1. INTRODUCTION

The STS Target has an outer water-cooled Inconel shroud. Inside of the Inconel there is a set of tungsten plates with .5mm tantalum plates between the tungsten plates surrounded by a 1mm tantalum layer as shown in Figure 1. The Inconel, tungsten and tantalum assembly are bonded together using HIP. Side Inconel flow covers and the rear stainless-steel section are later welded to the Inconel bonded assembly.

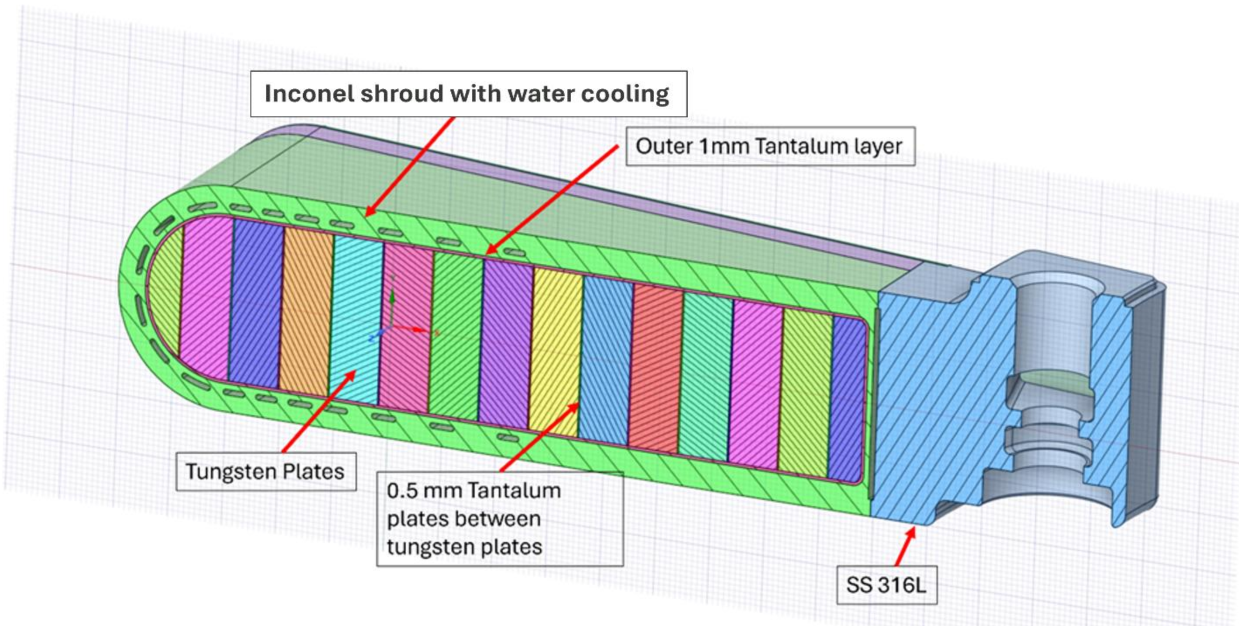

Figure 1 STS target configuration

The beam heating in the tungsten is transmitted through the outer tantalum layer by conduction to the Inconel shell. The HIP process is expected to make a good metallurgical bond between the Inconel and tantalum. Characterization of diffusion bonding between Inconel 718 and tantalum has been performed within the frame of STS Target R&D Program. Microstructural analyses and shear tests have been performed on VHP bonded specimens, which showed good metallurgical bonding between the two materials. This analysis was done to make a bounding estimate of the effect of the bond failing or not present. Heat transport between the Inconel and tantalum was modeled as a Surface-to-Surface contact with conductance as a function of pressure. There is no R&D data available for the surface conditions after a bond breaks or the surface conditions after the HIP process for bonds that are not made or any measured conductance without a bond. The model used for this analysis should be considered as a first order of magnitude estimate. Hard frictionless contact allowing separation was assumed. A transient calculation was done using the steady state heating and continued until quasi-steady state conditions were reached. Fixed film heat transport coefficients were assumed for the flow channels and side manifold surfaces. The results of this calculation were then used as the initial configuration for a transient analysis with the 47 KJ pulse energy deposition over 1 μs. Transient stress for 700 μs were found and used for fatigue analysis.

2. ASSUMPTIONS

The following conditions were assumed:

- Vacuum Core Vessel Operation
- 700 kW beam at 15 Hz with nominal beam profile
- Steady State heating loads used for initial transient analysis starting at 40 °C
- Pulse Energy deposition profiles used as volumetric heating loads over 1 μs with an initial condition from the steady state solution
- 3 bar normal water pressure for operation
- No thermal radiation included
- Fixed water sink temperature of 40 °C
- Initial cooling channel estimated film coefficients assumed constant and any boiling not evaluated
- No bond assumed anywhere between the outer tantalum layer and Inconel
- Contact conductance as a function of pressure assumed from literature data between tantalum and Inconel
- Quarter symmetry assumed with a simplified model of the SS316L which did not include all the structure near the Inconel connection
- Transient analysis assumed all manufacturing stresses relieved by radiation damage and analysis started with all parts stress free at 40 °C.

3. PHYSICAL MODEL DEFINITION

3.1 GEOMETRY

The same geometry was used for the initial analysis with steady state heat loads and for the transient analysis with pulse heating.

The CAD geometry of the target segment used for these analyses was downloaded from the Windchill PLM on 22 August 2025 with the version control as listed in Table 1. Figure 2 shows the geometry with Inconel side cover plates.

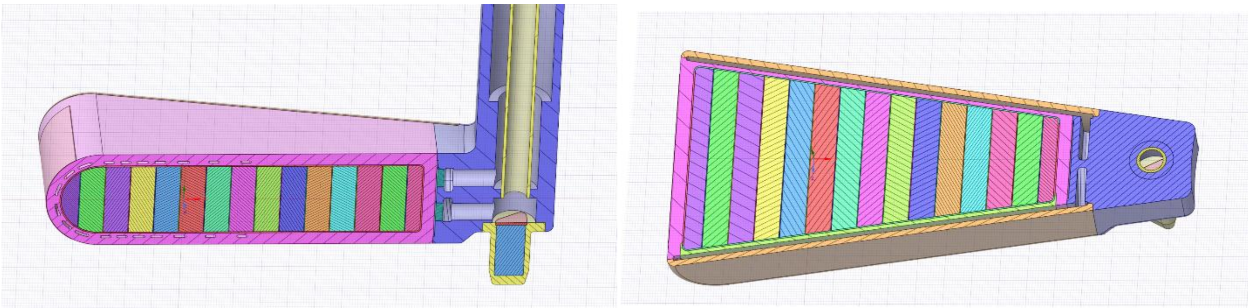

Figure 2 Target section view from 0000005039.asm "TARGET SEGMENT ASSEMBLY"

Table 1: Windchill CAD configuration used for analysis. Downloaded on 22 August 2025 from master assembly 0000005039.asm "TARGET SEGMENT ASSEMBLY".

File Name	Number	Version
0000005039.asm	5039	0.18
0000005999.asm	0000005999.ASM	1.8
0000006000.prt	6000	0.4
0000006867.prt	0000006867.PRT	0.8
0000006868.prt	0000006868.PRT	0.4
0000006869.prt	0000006869.PRT	0.6
0000006870.prt	0000006870.PRT	0.7
0000006871-sk.prt	0000006871-SK.PRT	0.2
0000006871.asm	6871	0.11
0000006994.prt	0000006994.PRT	0.4
0000008542.asm	8542	0.5
0000009216.prt	0000009216.PRT	0.6
0000009217.prt	0000009217.PRT	0.5
0000009218.prt	0000009218.PRT	0.4
0000009219.prt	0000009219.PRT	0.4
0000010279.prt	0000010279.PRT	1.3
0000010496.prt	0000010496.PRT	0.1
0000010497.prt	0000010497.PRT	0.3
0000010498.prt	0000010498.PRT	0.5
0000010499.prt	0000010499.PRT	0.1
0000010500.prt	0000010500.PRT	0.3

0000010506.prt	0000010506.PRT	1.1
0000010507.prt	0000010507.PRT	1.1
0000010518.prt	0000010518.PRT	0.4
0000010519.prt	0000010519.PRT	1.4
0000010520.prt	0000010520.PRT	0.2
0000010853.prt	0000010853.PRT	0.1
0000010854.prt	0000010854.PRT	0.4
0000010855.prt	0000010855.PRT	0.4
0000010856.prt	0000010856.PRT	0.1
0000010937.prt	0000010937.PRT	0.6
0000011300-1a.prt	0000011300-1A.PRT	0.2
0000011300-3.prt	0000011300-3.PRT	0.1
0000011300.asm	0000011300.ASM	0.9
0000011772.prt	11772	0.2
0000011774.prt	0000011774.PRT	0.1
0000011775.prt	0000011775.PRT	0.2
0000011778.prt	0000011778.PRT	0.1
0000011779.prt	0000011779.PRT	0.2
0000011781.prt	0000011781.PRT	0.2
0000011782.prt	0000011782.PRT	0.4
0000011783.prt	0000011783.PRT	0.2
0000015843.prt	15843	0.5
s03020000-m8u-8800-a10003-c_.prt	S03020000-M8U-8800-A10003-C_.PRT	0.1
s03020000-m8u-8800-a10003_skel.prt	S03020000-M8U-8800-A10003_SKEL.PRT	0.2
swagelok_ss-2-ut-a-4bt.prt	SWAGELOK_SS-2-UT-A-4BT.PRT	0.1

A hex mesh of this geometry to be used in a quarter symmetry model for the debonded case was made by A. Jacques and imported into Abaqus. Five separate Abaqus .inp part files were made as listed below. These files, along with all other input files, are archived with this document on the Windchill PLM.

- HEX_HEEL.inp
- HEX_COVER.inp
- hex_tungsten.inp
- hex_tantalum.inp
- hex_inconel.inp

The HEEL mesh as imported and as modified for a quarter symmetry model is shown in Figure 3. The modified version removed elements on or below the horizontal midplane and vertical sections which would not be expected to be affected by the debonded assumption. The mesh was done using mm as the space unit and no changes to the mesh were made for the elements retained. The hex mesh was simplified from the full model from the 4343 Step part in the heel area. Some material behind the surface that connects with the Inconel was not included as shown in Figure 4.

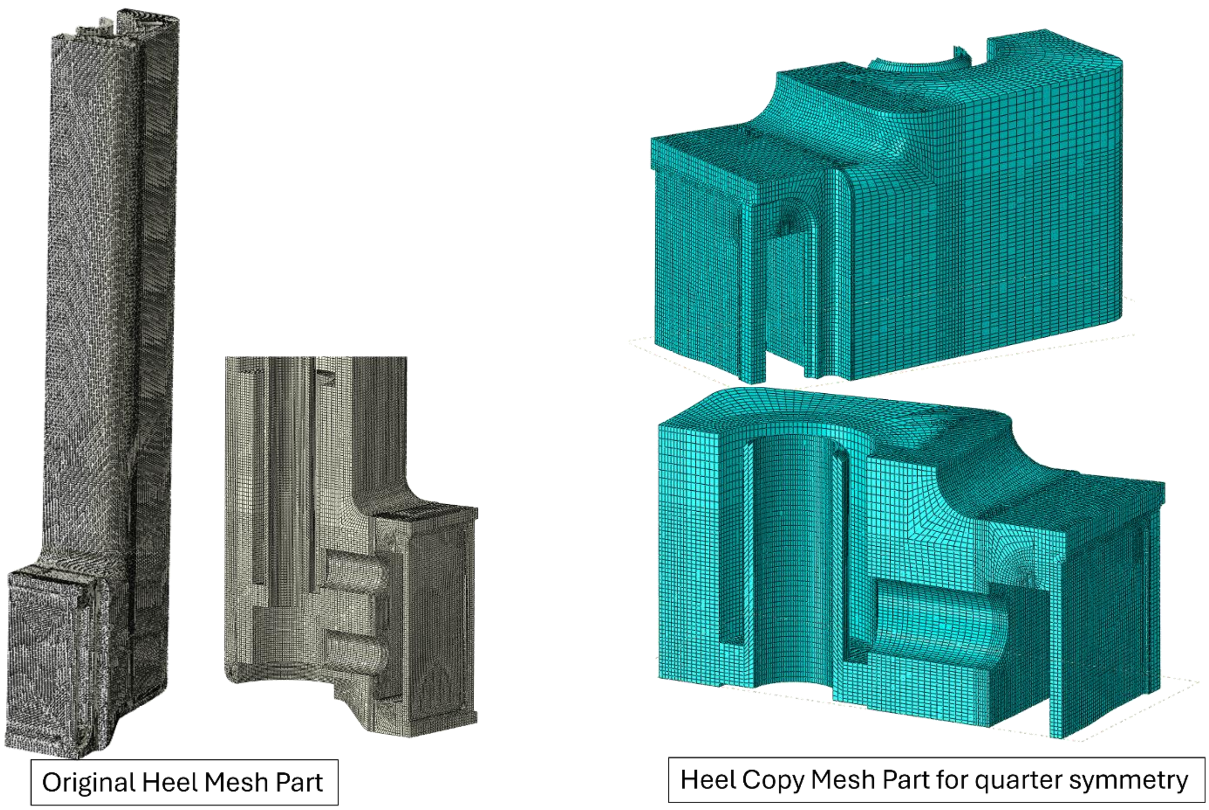

Figure 3 Heel mesh part

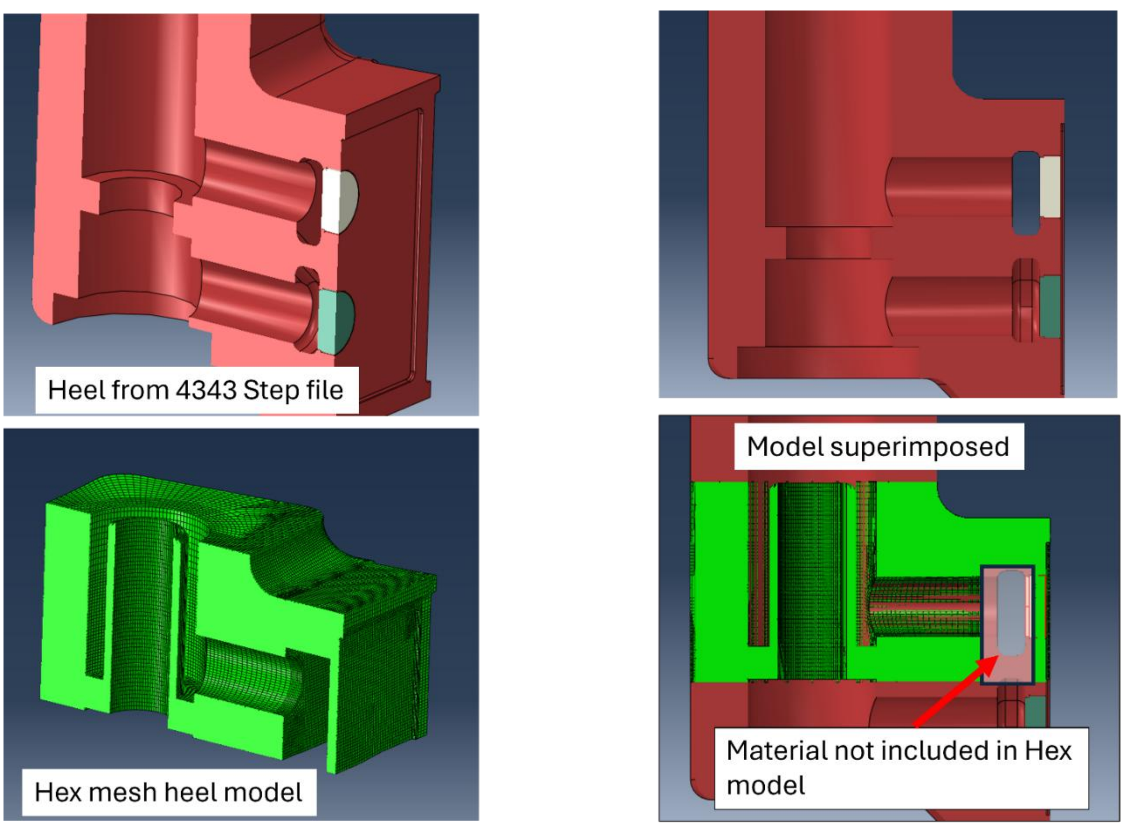

Figure 4 Heel hex and full models showing material not included in the hex mesh part

The Inconel cover part mesh as imported into Abaqus is shown in Figure 5.

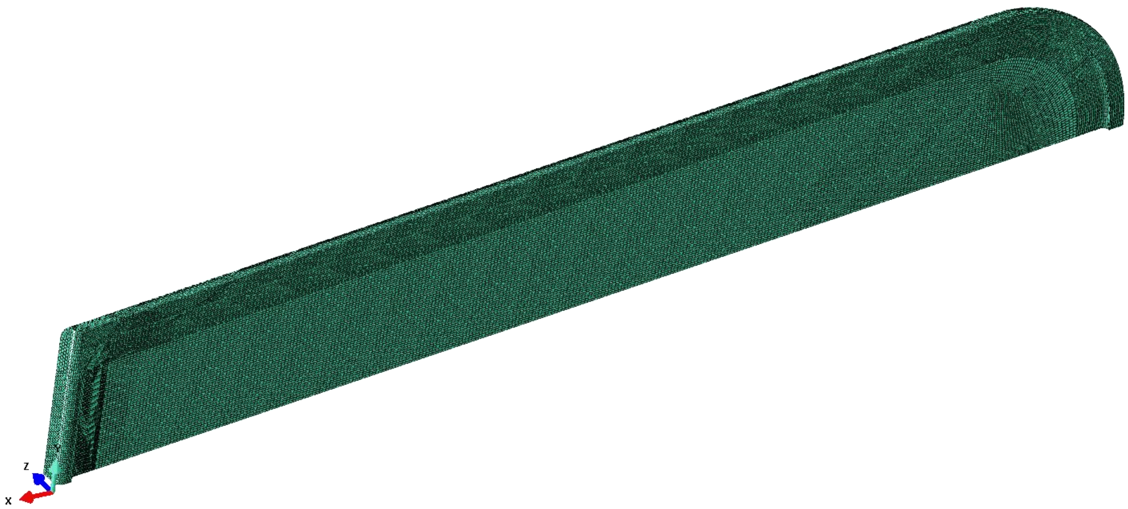

Figure 5 Cover mesh part

The tungsten mesh as imported is shown in Figure 6.

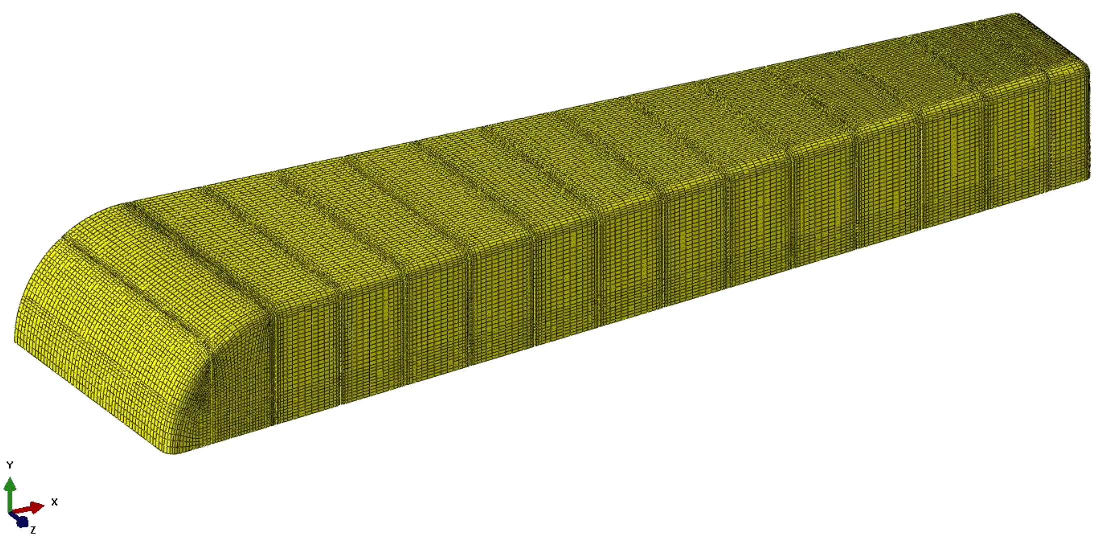

Figure 6 Tungsten mesh part

Figure 7 shows the tantalum mesh part with 0.5 mm between tungsten regions and 1 mm on the outside.

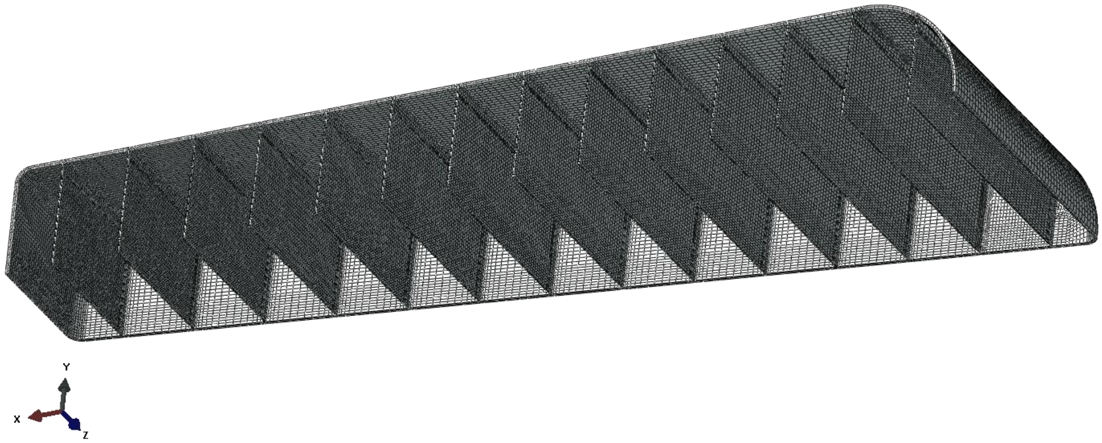

Figure 7 Tantalum mesh part

The Inconel mesh part which does not include the cover is shown in Figure 8.

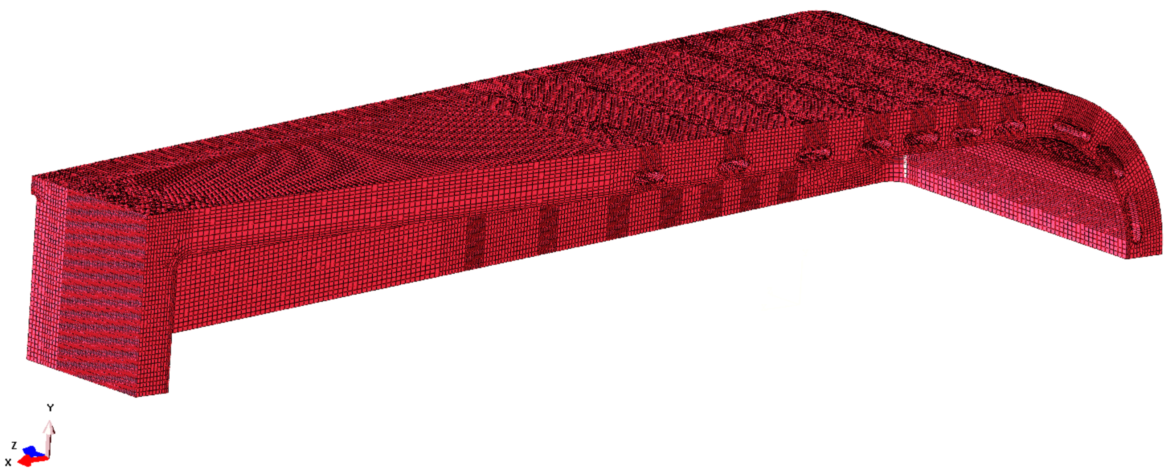

Figure 8 Inconel mesh

The overall assembly is shown in Figure 9. Figure 10 shows a view of the assembly cut on the X=0 plane and the coordinate directions with x axially, y vertically and z normal to the z=0 plane. The first tungsten node on the x axis is at -41 mm and the last at 175 mm.

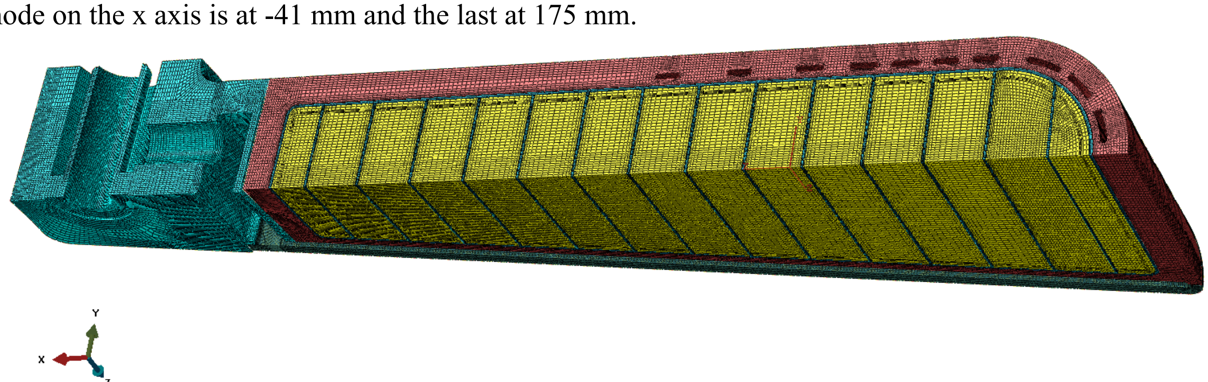

Figure 9 Assembly mesh

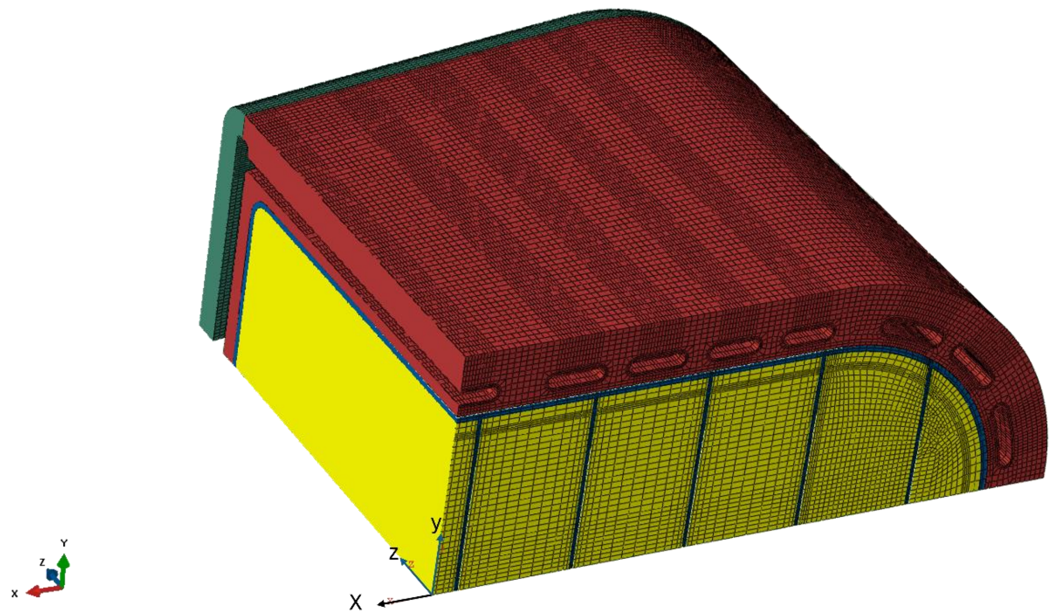

Figure 10 Assembly showing origin and coordinate system

3.2 MATERIAL PROPERTIES

3.2.1 Thermostructural Properties

The material properties used for the Abaqus analysis are derived from the "Target Systems Materials Library" [1] and are given in Appendix A. Temperature dependent elastic plastic properties were used for Inconel strength and thermal expansion, 316L strength and thermal expansion and tantalum modulus, strength and thermal expansion. Example of the plastic true stress stain curves for Inconel and 316L are shown in Figure 11. Tantalum temperature dependent Young's Modulus, CTE and plastic true stress strain curves of tantalum are shown in Figure 12.

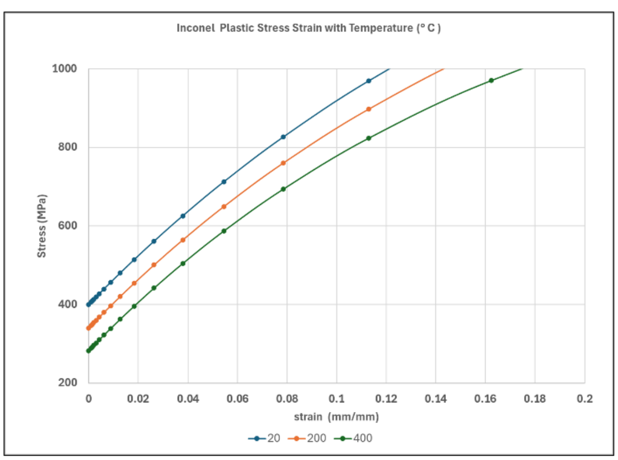

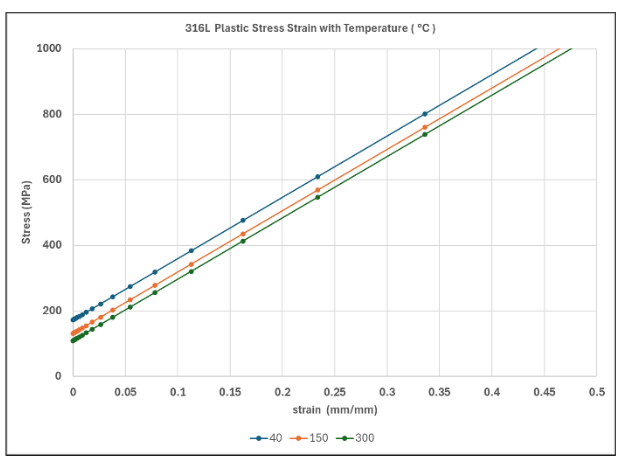

Figure 11 Inconel and 316L plastic stress strain data

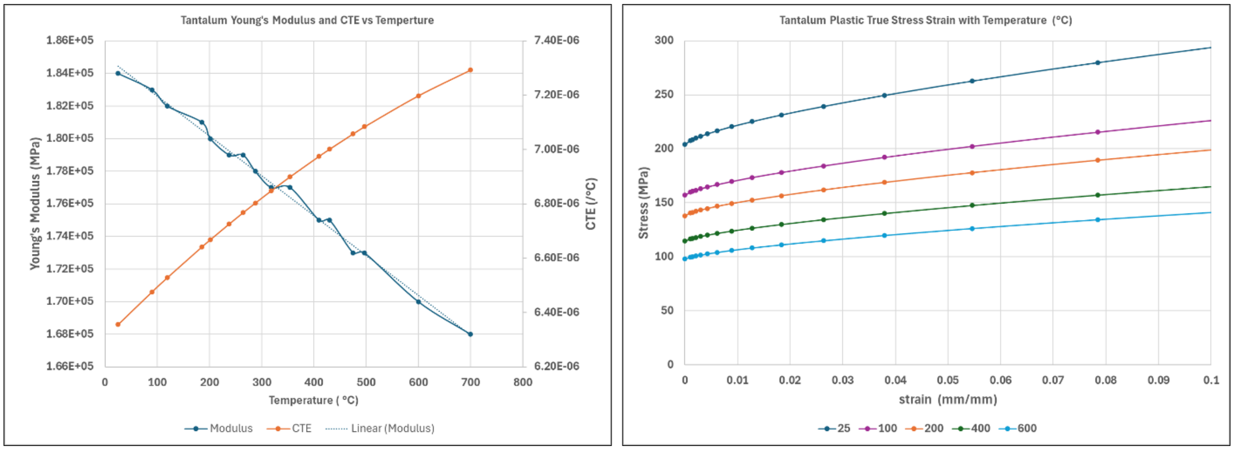

Figure 12 Tantalum Properties

Temperature dependent Modulus properties were not included for Inconel and 316L.

3.2.2 Fatigue Properties

The fatigue analyses in this report closely follow the methodology developed for the "Target Segment Thermostructural Analysis" DAC [2]. Only tungsten, Inconel, and stainless steel are considered for fatigue analyses. Inconel and stainless steel are the true structural materials of the target. Tungsten is also analyzed for historical reasons (as it is usually a structural material), and out of a desire to keep the spallation material well-defined. (For context, the brittle nature of tungsten led to the design choice of encasing the spallation package with structural Inconel.) Per the design requirements, all fatigue curves are based on the mean life. The fatigue models and properties used in the fe-safe fatigue analyses are fully documented (including references) in the "Target Systems Materials Library" [1] and are summarized below for convenience.

Tungsten

Tungsten will be well below the DBTT during operation in both unirradiated and irradiated conditions and is then assumed to follow brittle failure theory. A fatigue calculation should then calculate the largest normal stress amplitude. The stress plane in which that occurs, however, is unknown *a priori*. The stress plane orientation must be determined as part of the post-processing analysis (i.e. critical plane analysis).

Tungsten uses the Basquin HCF model shown in Equation (1),

$$\sigma_n = K_{irr}\sigma_f'(2N_f)^b \tag{1}$$

where the constants are listed in Equation (2) as:

$$\begin{aligned} K_{irr} &= 0.53 \\ \sigma_f' &= 677\ \text{MPa} \\ b &= -0.041508 \end{aligned} \tag{2}$$

Here, the effects of irradiation are accounted for as a knockdown factor (K_{irr}). The fatigue strength coefficient (σ'_f) is the fatigue strength for one half cycle and approximately represents the UTS of the material. It is chosen to match the weakest direction strength for 10-20 mm tungsten plate. Table 2 lists the important fatigue parameters in the fe-safe material definition.

Table 2: Tungsten fatigue model settings in fe-safe software.

Parameter Name	**Value**	**Comment**
fatigue strength coefficient (sf')	356 MPa	$K_{irr}\sigma_f'$ for 10-20mm plate
fatigue strength exponent (b)	-0.041508	Basquin fit
fatigue ductility coefficient (Ef')	0	Plasticity disabled
fatigue ductility exponent (c)	0	Plasticity disabled
K'	1.00E+20	Cyclic plasticity disabled
n'	1	Cyclic plasticity disabled
CAEL	1.00E+11	Constant amplitude endurance limit disabled
Young's modulus	398,000 MPa	
Poisson's ratio	0.28	
ultimate tensile strength	356 MPa	assume σ_f'= UTS
ultimate compressive strength	356 MPa	Assume same as UTS
algorithm	Normal Stress:-Goodman	Brittle failure mode

Type 316L Stainless Steel

The best source of fatigue data for SS316L comes from a NUREG sponsored study in the early 2000s that was then used to update the ASME/BPVC fatigue curves. In air, at temperatures up to 400°C, the mean fatigue life for austenitic stainless steels (e.g. SS304L, SS316L, SS316NG) is best represented by Equation 3,

$$\ln(\mathrm{N}) = 6.891 - 1.920\ln(\epsilon_a - 0.112) \tag{3}$$

where ϵ_a is the percent applied strain amplitude.

The present study seeks to design around the mean life curves. Also, the 10 year design life dictates a HCF regime that is predominantly elastic. Accordingly, the SS316L fatigue curve uses the mean fatigue curve given in Equation 4, where $\frac{\sigma_a}{E}$ is substituted for the applied strain amplitude. Equation 4 can then be used to solve fatigue life (N) for a given fully reversing stress amplitude (σ_a).

$$\ln(\mathrm{N}) = 6.891 - 1.920\ln\left(\frac{\sigma_a}{E} - 0.112\right) \tag{4}$$

In fe-safe software, the FEA stress results are used with the stress-based Brown-Miller model, and plasticity effects are disabled. This fatigue model is the " . . . preferred algorithm for most ductile metals at room temperature and is the default algorithm for most materials in the fe-safe material database" [3, pp. 14-16]. The Brown-Miller model ". . . proposes that the maximum fatigue damage occurs on the plane which experiences the maximum shear strain amplitude, and that the damage is a function of both this shear strain and the strain normal to this plane" [4, pp. 7-19]. Table 3 lists the important fatigue parameters in the fe-safe material definition. Since the fatigue curve equation is non-standard, the curve is input as an array of stress-cycle data points.

Table 3: Type 316L stainless steel fatigue model settings in fe-safe software.

Parameter Name	Value	Comment
stress -life table enabled	true	
sample series	*varies*	22 points log spaced from 1.0E+6 to 1.0E+11
control series	*varies*	Equation 4 solved for σ_a
K’	1.00E+20	Cyclic plasticity disabled
n’	1	Cyclic plasticity disabled
CAEL	1.00E+11	Constant amplitude endurance limit disabled
Young’s modulus	398,000 MPa	
Poisson’s ratio	0.31	
ultimate tensile strength	648.1 MPa	
ultimate compressive strength	648.1 MPa	Assume same as UTS
algorithm	(shear + direct) Stress: - Goodman	Stress based Brown-Miller

Inconel 718 (Solution Annealed)

A literature search was conducted to create a custom fatigue curve for Inconel 718 in the solution annealed condition (as opposed to the more conventional precipitation hardened condition). The mean-life fatigue curve was fit to the Basquin HCF model shown in Equation 5

$$\sigma_a = K_{grain}\sigma_f'(2N_f)^b \tag{5}$$

where the constants are defined in Equation 6.

$$\begin{aligned} K_{grain} &= 0.72 \\ \sigma_f' &= 657.16\ \text{MPa} \\ b &= -0.019635 \end{aligned} \tag{6}$$

Here, the effects of grain size are accounted for as a knockdown factor (K_{grain}). As with stainless steel in fe-safe software, the most appropriate model is the Brown-Miller fatigue model. Table 4 lists the important fatigue parameters in the fe-safe material definition.

Table 4: IN718SA fatigue model settings in fe-safe software.

Parameter Name	Value	Comment
fatigue strength coefficient (sf')	473.16 MPa	$K_{grain}\sigma_f'$ for ASTM 6
fatigue strength exponent (b)	-0.019635	Basquin fit
fatigue ductility coefficient (Ef')	0	Plasticity disabled
fatigue ductility exponent (c)	0	Plasticity disabled
K'	1.00E+20	Cyclic plasticity disabled
n'	1	Cyclic plasticity disabled
CAEL	1.00E+11	Constant amplitude endurance limit disabled
Young's modulus	209,628 MPa	
Poisson's ratio	0.3	
ultimate tensile strength	930 MPa	
ultimate compressive strength	930 MPa	Assume same as UTS
algorithm	(shear + direct) Stress: - Goodman	Stress based Brown-Miller

3.3 EXTERNAL LOADS

3.3.1 Steady State Heating

Steady-state heating loads are derived from the "NominalBeam" dataset in the "Neutronics Energy Deposition and DPA Data" DAC [5]. The steady state 700 kW heating loads in SI units were processed in a Python script as part of the "Target Assembly Thermo-Fluid Analysis" DAC [6]. The script summed the proton pulse energy deposition data for each of the 20 target segments and divided by the rotational period to create a time-averaged, steady-state rate of heat generation. For the Abaqus model in mm the spatial coordinates in meters were converted to mm and the heating rates in W/m^3 were converted to mW/mm^3 by multiplying by 1e-6. The original heating rates for tungsten (QW), Inconel without the cover (QInconel) and Tantalum (QTa) were converted to QWmm, QInconelmm and QTamm. These files are described further in Section 4.7.1 and are archived with this DAC on Windchill.

The Inconel cover and 316L heel heating rates were not included. There were mesh incompatibility problems and both regions are well cooled and away from the debonded region so that not including them should not affect the results significantly

3.3.2 Single Pulse Energy Deposition

Single pulse energy deposition comes from the "NominalBeam" dataset in the "Neutronics Energy Deposition and DPA Data" DAC [5]. The original data, given in J/cm^3, was converted to J/mm^3 by dividing by 1E+3. When used in Abaqus the data was Single pulse energy deposition from the "NominalBeam" dataset in the "Neutronics Energy Deposition and DPA Data" DAC [5]. When used for heating in Abaqus the energy data was converted to mW/mm^3 by multiplying by 1000 and dividing by 1E-6 seconds. (The division by 1E-6 seconds matches the analysis step duration in the Abaqus analysis.)

3.4 DESIGN CRITERIA AND ACCEPTABLE VALUES

STS requirements for the target segment are reported in controlled document S03020400-SRD10000 [7]. This report addresses two specific requirements:

- The steady state peak tungsten temperatures should be below 800°C so that tungsten vaporization in steam is not possible (see Requirement 3466).

- Fatigue lifetime for the Inconel and 316L Stainless Steel should be greater than 10 years (see Requirement 1574).

It should be noted that debonding is not a normal or anticipated operating condition and requirements are applied as an assurance of operating integrity. The normal design requirements do not strictly need to be met in the debonded condition. For example, tungsten was evaluated against a 10 year lifetime but not meeting this criterion with possible cracking was accepted for this bounding condition.

It should also be noted that the fatigue requirement (Requirement 1574) specifies analyses for several beam cases (nominal, offset, focused, diffuse). Only the nominal beam case will be used as a criterion for theses analyses as the “Target Segment Thermostructural Analysis” DAC has already shown the fatigue performance to be insensitive to these deviations from nominal beam [2].

4. NUMERICAL MODEL OR SIMULATION

4.1 SOFTWARE

All analyses were performed on the BERNIE.sns.gov cluster with the Red Hat Enterprise Linux 8.10 (Ootpa) operating system. The cluster consists of 6 compute nodes. Each node has 64 processors (Intel Xeon CPU E5-2637 v2 @ 3.50GHz) and 768-GB memory.

The software packages used for analysis include:

- *Abaqus 2025* (BUILD ID: 2024_09_20-09.00.46 RELr427 198590) was used for transient coupled temperature and displacement analysis with steady state heat loads and pulse energy deposition
- *Microsoft Excel* software was used to convert from SI to SI mm units for material properties and heating.
- *fe-safe 2025* (Buildstamp: 2025 2439.3) was used for fatigue analysis

4.2 UNIT SYSTEM

The Abaqus model length unit was mm. A consistent set of units needs to be used with the Abaqus model defined in mm. The table below shows the units for SI in m and SI in mm

Table 5 Unit Comparison

Parameter	SI (mm)	SI
Length	mm	m
Mass	tonne	kg
Temperature	°C	°C
Area	mm^2	m^2
Volume	mm^3	m^3
Density	tonne/mm^3	kg/m^3
Force	N	N
Pressure	MPa	Pa
Velocity	mm/s	m/2
Acceleration	mm/sec^2	m/sec^2
Moment	N-mm	N-m
Stress	MPa	Pa
Young's Modulus	MPa	Pa
Energy	mJ	J
Power	mW	W
Thermal Expansion	/°C	/°C
Thermal Conductivity	mW/mm °C	W/m °C
Specific Heat	mJ/tonne °C	J/kg °C
Heat Flux	mW/mm^2	W/m^2

All material property values and loads were used in SI mm consistent units.

4.3 DISCRETIZATION

4.3.1 Cover Mesh Part

The cover part as shown below has 142408 C3D8RT elements with most lengths approximately 1 mm. Shown below is the set of 2708 poor elements and geometry verification.

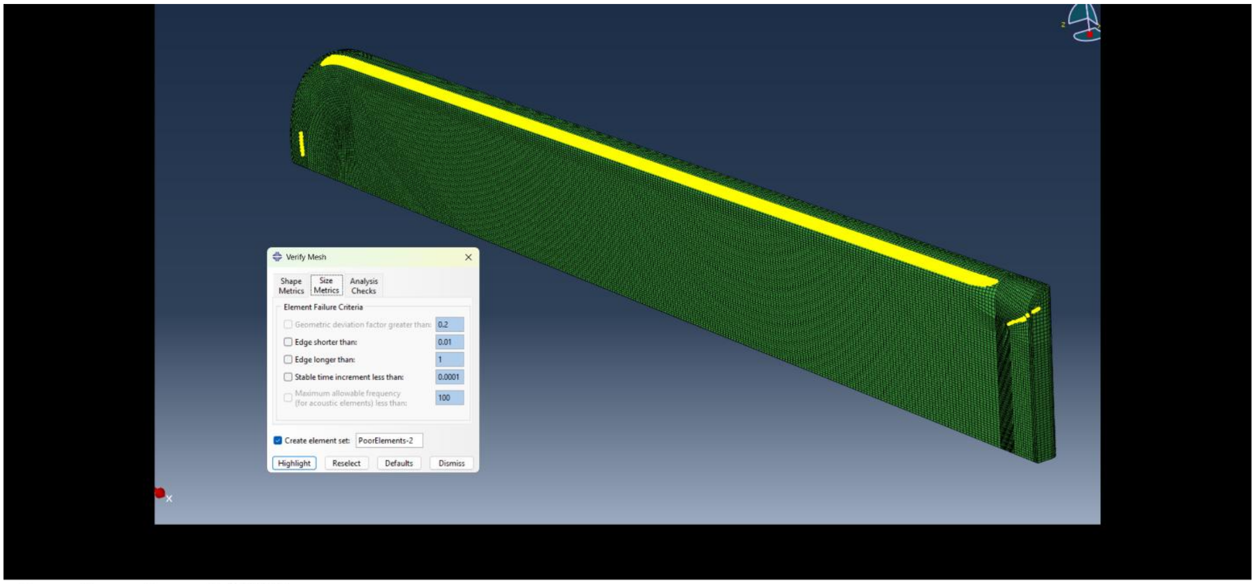


```
Hex elements:  142408
  Min angle on Quad Faces < 10:  0 (0%)
  Average min angle on quad faces:  78.43,  Worst min angle on quad faces:  21.86
  Max angle on Quad faces > 160:  0 (0%)
  Average max angle on quad faces:  102.11,  Worst max angle on quad faces:  156.44
  Aspect ratio > 10:  12 (0.00842649%)
  Average aspect ratio:  2.07,  Worst aspect ratio:  10.41
 Number of elements :  142408,   Analysis errors:  0 (0%),  Analysis warnings:  2708 (1.90158%)
```

Figure 13 Cover Poor elements and element verification

4.3.2 Heel Copy Mesh Part

The Heel mesh part has 130547 C3D8RT elements with sizes varying from approximately 0.3mm to 2 mm. Show below is the set of 5572 poor elements and mesh geometry verification.

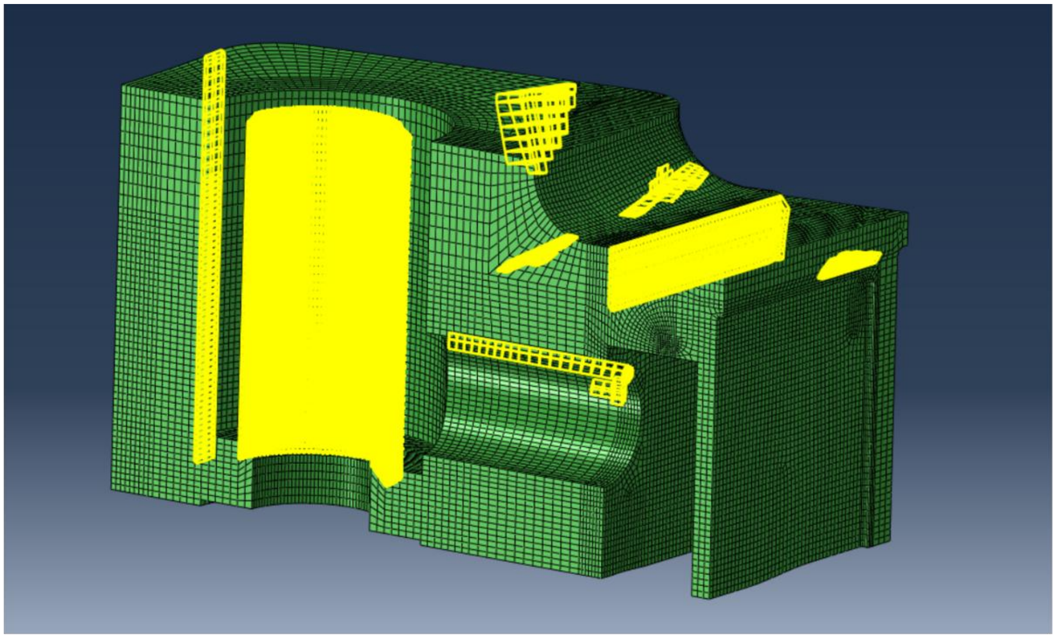

```
Part: heel-Copy
 Hex elements:  130547
   Min angle on Quad Faces < 10:  0 (0%)
   Average min angle on quad faces:  76.60,  Worst min angle on quad faces:  23.52
   Max angle on Quad faces > 160:  0 (0%)
   Average max angle on quad faces:  103.50,  Worst max angle on quad faces:  158.74
   Aspect ratio > 10:  0 (0%)
   Average aspect ratio:  2.03,  Worst aspect ratio:  8.39
  Number of elements :  130547,   Analysis errors:  0 (0%),  Analysis warnings:  5572 (4.26819%)
```

Figure 14 Heel mesh geometry verification

4.3.3 Inconel Mesh Part

The Inconel mesh part has 365702 C3D8RT elements varying in size from approximately 0.5 mm to 2 mm. Shown below is a view with the 588 poor elements highlighted and the geometry verification.

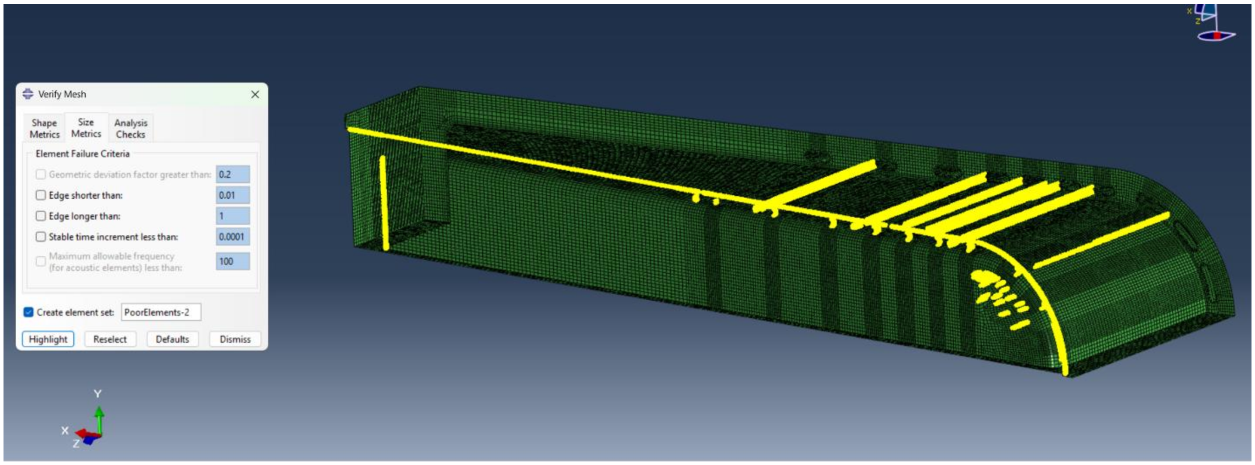


```
Part: inconel
 Hex elements:  365702
   Min angle on Quad Faces < 10:  0 (0%)
   Average min angle on quad faces:  81.49,  Worst min angle on quad faces:  19.21
   Max angle on Quad faces > 160:  5 (0.00136723%)
   Average max angle on quad faces:  98.27,  Worst max angle on quad faces:  160.96
   Aspect ratio > 10:  1727 (0.472242%)
   Average aspect ratio:  2.97,  Worst aspect ratio:  16.41
  Number of elements :  365702,   Analysis errors:  0 (0%),  Analysis warnings:  588 (0.160787%)
Created set 'PoorElements-2' containing 2315 elements
```

Figure 15 Inconel Part Mesh Verification

4.3.4 Tantalum Mesh Part

The tantalum part has 100234 C3D8RT elements with sizes varying from approximately .2 mm to 2 mm. Shown below is the shape verification with 588 poor elements highlighted.

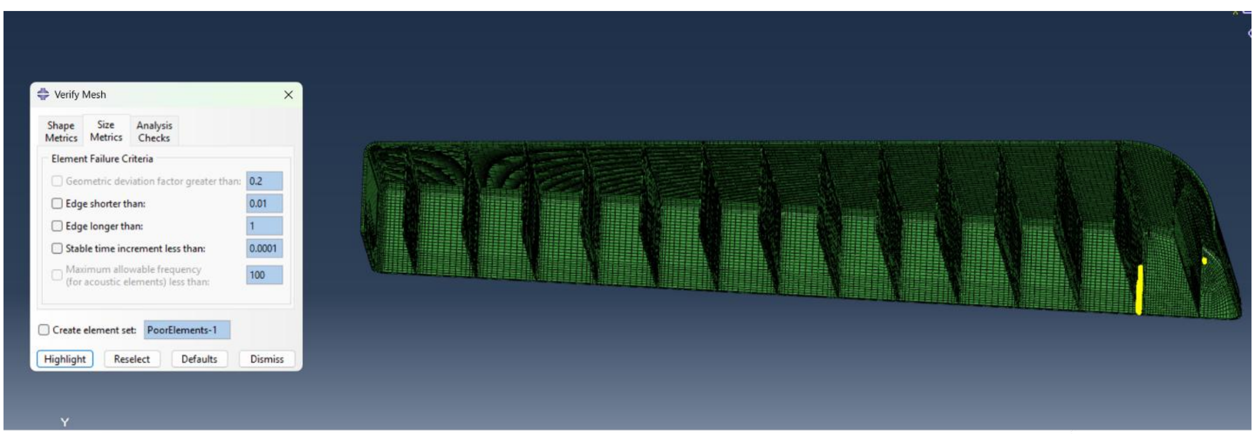


```
Part: tantalum
 Hex elements:  100234
   Min angle on Quad Faces < 10:  0 (0%)
   Average min angle on quad faces:  82.75,  Worst min angle on quad faces:  23.64
   Max angle on Quad faces > 160:  0 (0%)
   Average max angle on quad faces:  97.35,  Worst max angle on quad faces:  157.97
   Aspect ratio > 10:  0 (0%)
   Average aspect ratio:  3.56,  Worst aspect ratio:  8.00
  Number of elements :  100234,   Analysis errors:  0 (0%),  Analysis warnings:  46 (0.0458926%)
```

Figure 16 Tantalum mesh verification

4.3.5 Tungsten Mesh Part

The tungsten mesh has 424667 C3D8RT elements with sizes varying from approximately 0.4 mm to 2 mm. Shown below is the verification with 55 poor elements highlighted.

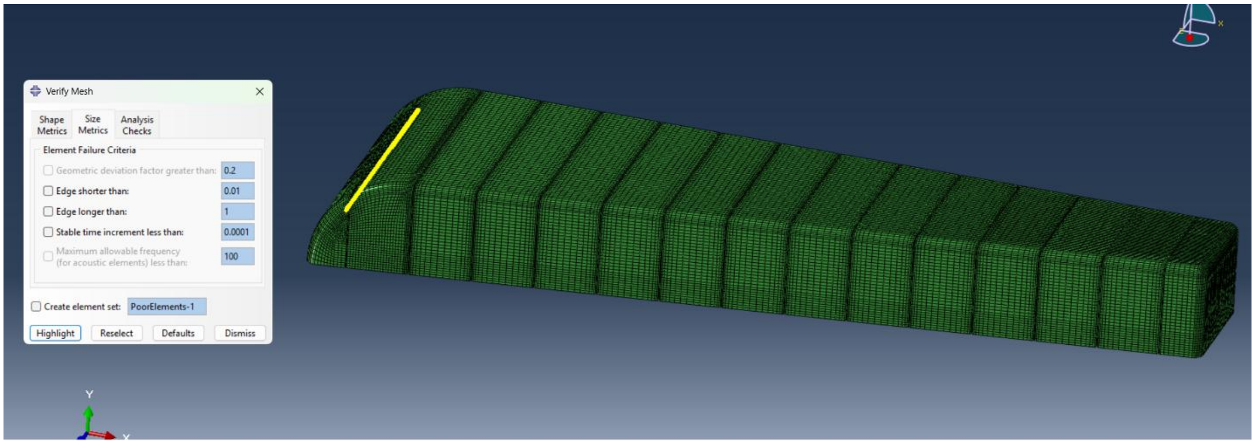


```
Part: tungsten
 Hex elements:  424667
   Min angle on Quad Faces < 10:  0 (0%)
   Average min angle on quad faces:  84.09,  Worst min angle on quad faces:  21.49
   Max angle on Quad faces > 160:  19 (0.00447409%)
   Average max angle on quad faces:  96.03,  Worst max angle on quad faces:  160.41
   Aspect ratio > 10:  0 (0%)
   Average aspect ratio:  2.39,  Worst aspect ratio:  7.98
  Number of elements :  424667,   Analysis errors:  0 (0%),  Analysis warnings:  55 (0.0129513%)
```

Figure 17 Tungsten mesh verification.

4.4 BOUNDARY AND INITIAL THERMAL CONDITION

There are 2 symmetry and one displacement boundary conditions. Figure 18 shows the Z symmetry constraint on nodes. Nodes ton tie boundaries between materials were excluded.

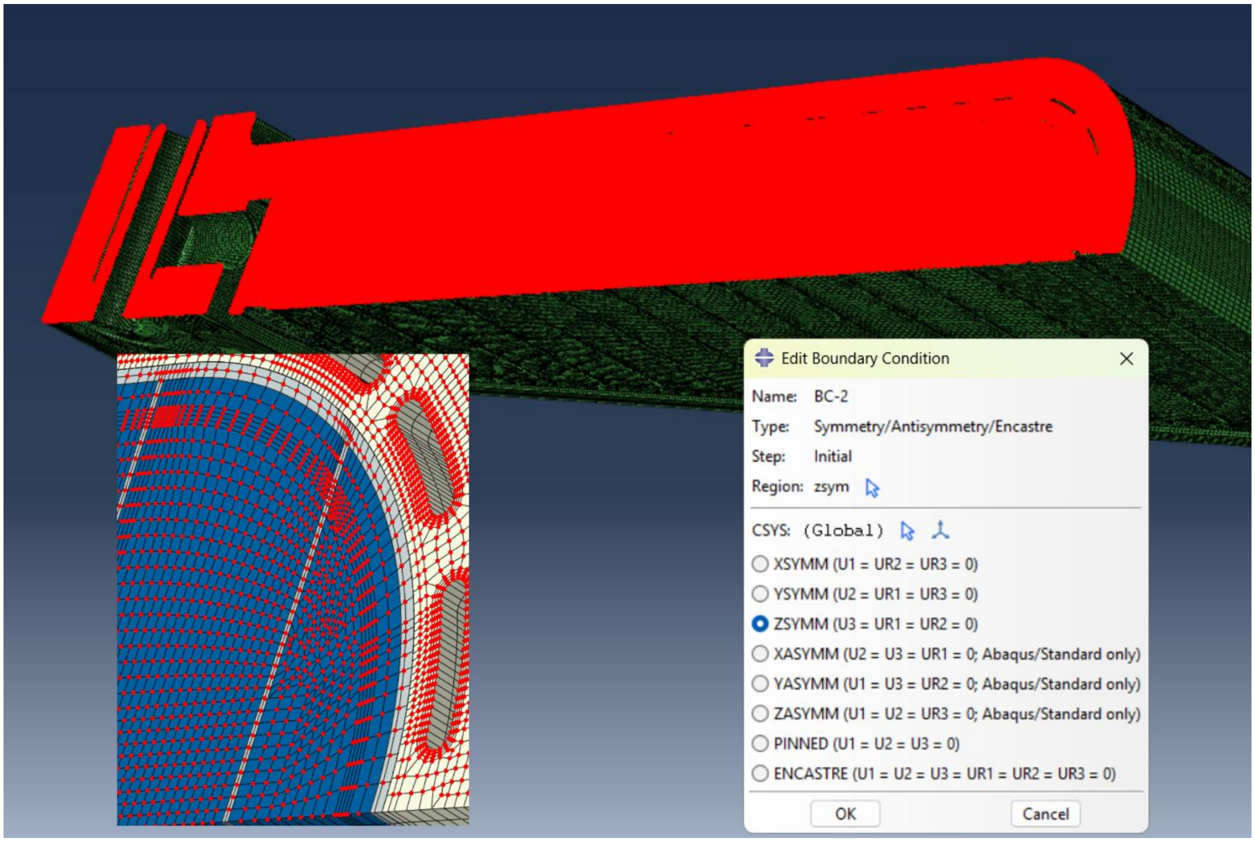

Figure 18 Z Symmetry Boundary constraint

The second symmetry boundary condition was in the vertical Y direction as shown in Figure 19.

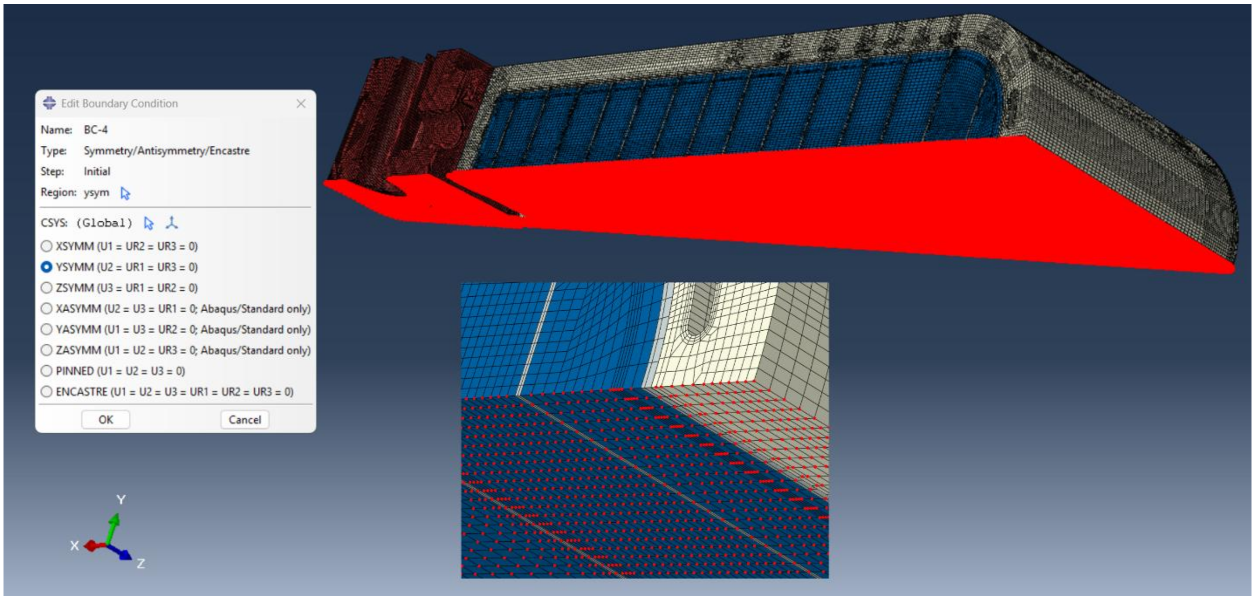

Figure 19 Y Symmetry Boundary Condition

The third boundary condition was on displacement in the axial direction as shown in Figure 20. The same boundary conditions were used for the initial analysis with steady state heating and for the second analysis with pulse energy deposition.

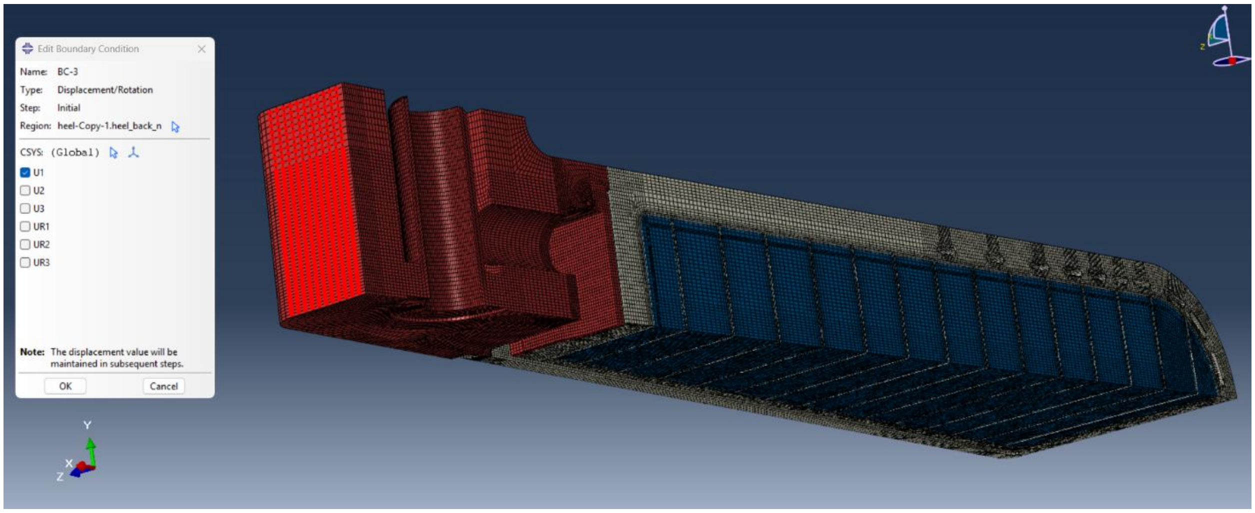

Figure 20 Boundary Condition on X (axial) displacement

The initial transient analysis with steady state heating was an Abaqus Standard coupled temperature and displacement analysis. The initial condition assumed all parts were stress free at 40 °C. This assumed that residual stresses from manufacturing had been relieved by radiation damage. The pulse heating analysis was a separate Abaqus explicit coupled temperature and displacement analysis with an initial configuration from the quasi-steady state results from the first analysis.

4.5 CONTACT CONDITIONS

4.5.1 Tie Constraints

There are four tie constraints in both models. Figure 21 shows the tie between the tungsten plates and tantalum.

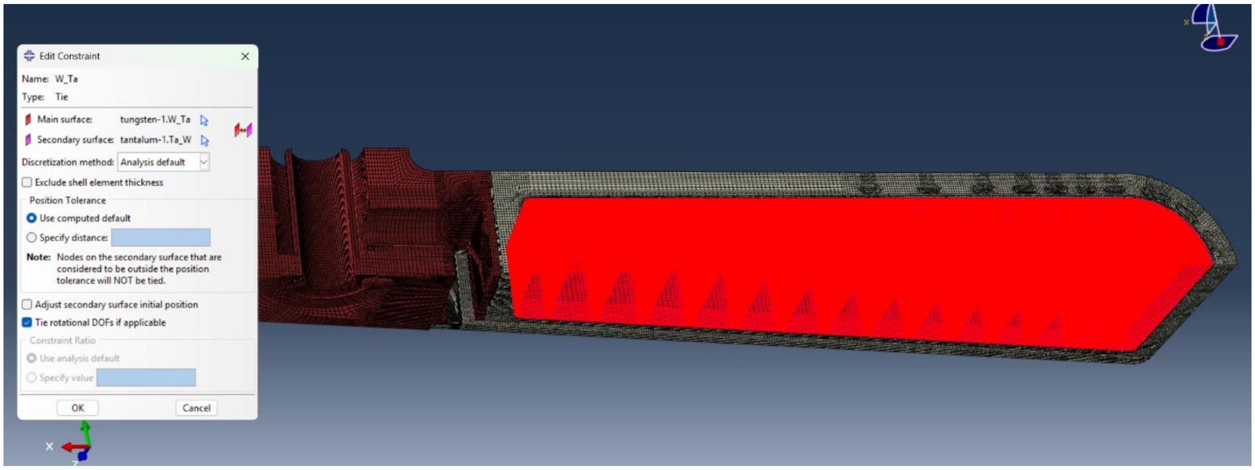

Figure 21 Tungsten to Tantalum tie constraint

The cover tie to the Inconel part is shown in Figure 22.

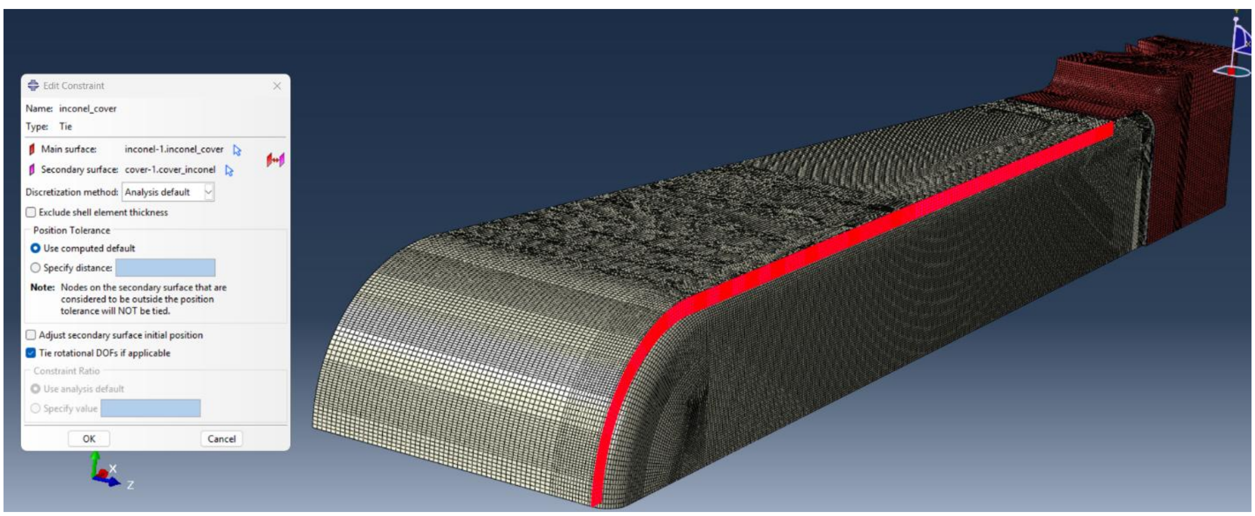

Figure 22Inconel to Cover tie

The cover and Inconel are both tied to the heel. Figure 23 shows these two tie constraints.

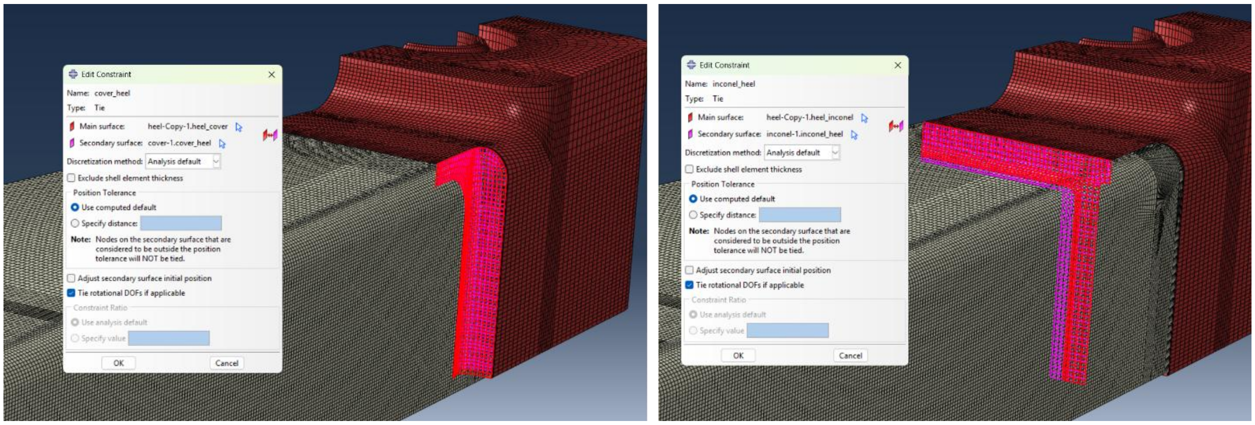

Figure 23 Cover to heel and Inconel to heel tie constraints

The separate mesh surfaces for the ties to the heel are shown in Figure 24.

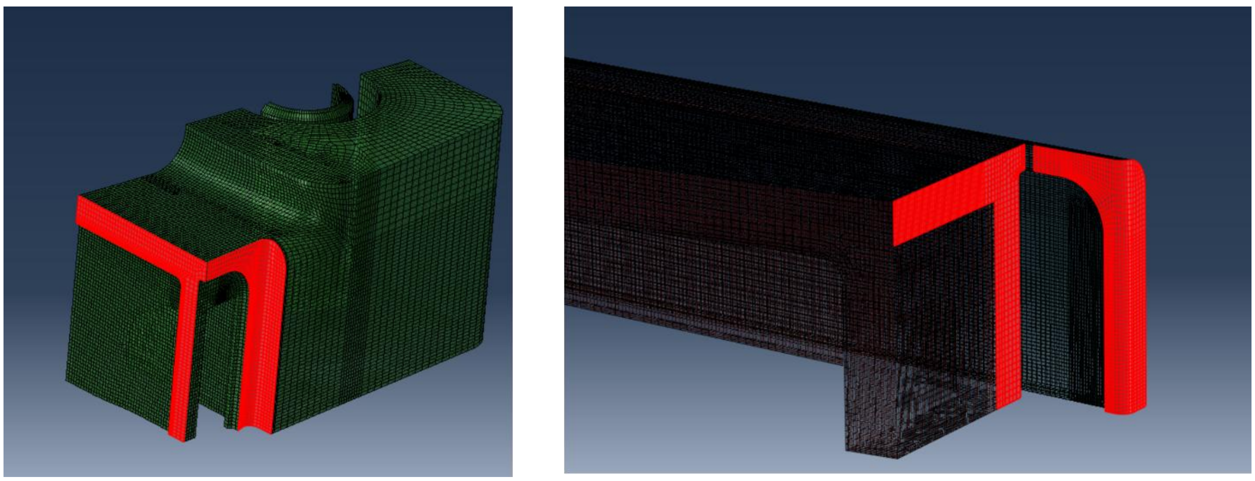
Figure 24 l Heel surfaces with tie constraints

4.5.2 Tantalum to Inconel Surface to Surface Interaction

The interface between the outer surface of the 1 mm tantalum layer and the inner surface of the Inconel was modeled as a hard, frictionless surface to surface contact with thermal conductance as a function of pressure. This is shown in Figure 25.

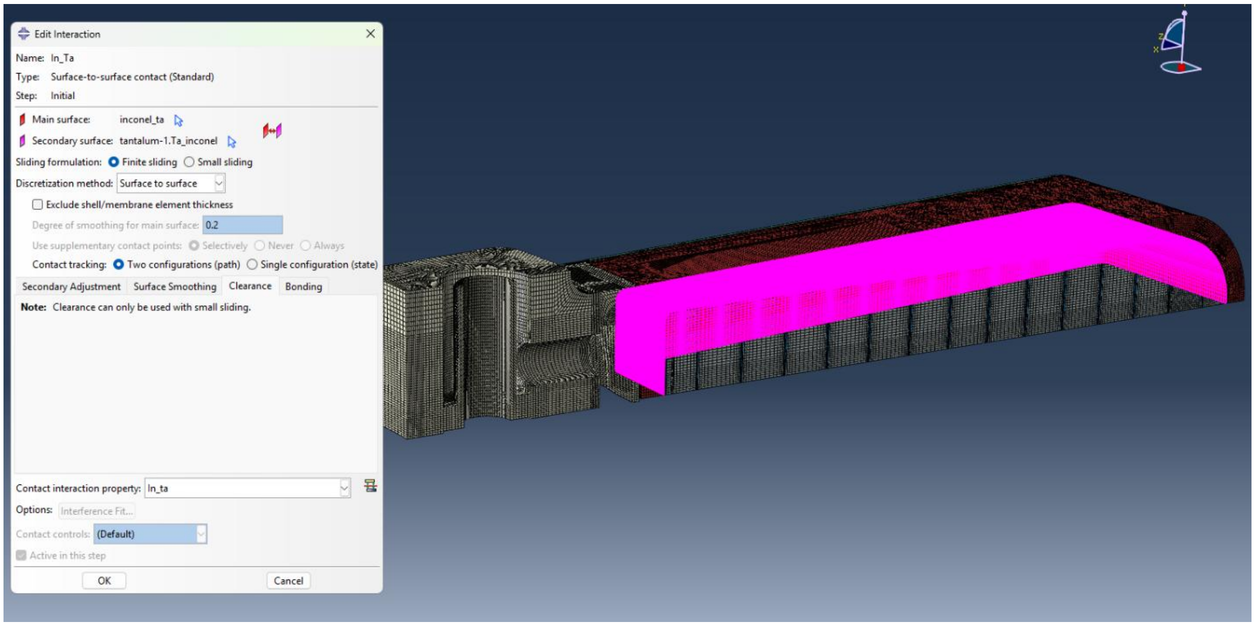

Figure 25 Tantalum to Inconel Surface to Surface Interaction

The interaction Normal mechanical and thermal properties are shown in Figure 26. To use consistent units, pressure is in MPa and conductance in mW/mm^2-K. The development of conductance between tantalum and Inconel as a function of pressure is given in the Appendix Contact Conductance. The Abaqus analysis used constant conductance of 93.9 mW/mm^2-K for pressure above 93.9 MPa. Tangential behavior was assumed frictionless.

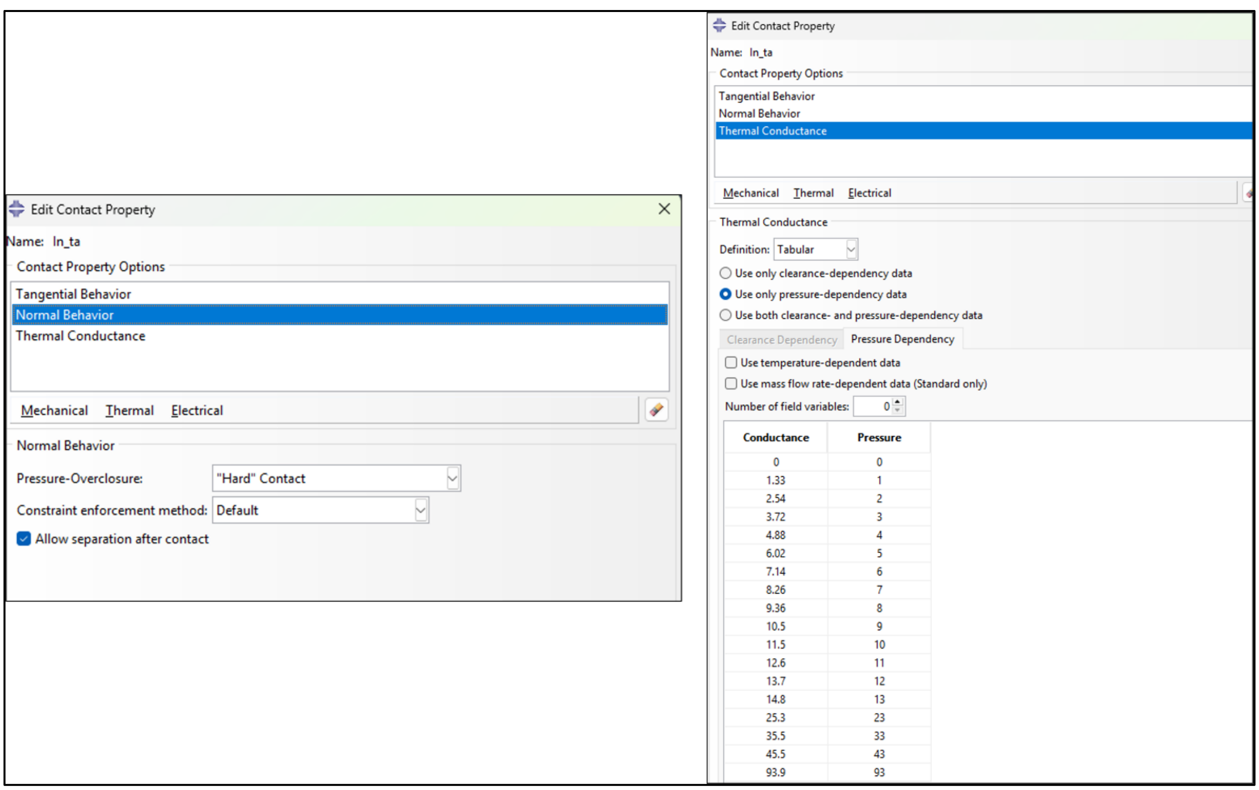

Figure 26 Tantalum to Inconel Interaction Properties

4.6 THERMAL INTERACTIONS FOR STEADY STATE SOLUTION

The target has 10 separate cooling channels across the width, manifold cooling on the sides and cooling for the 316L heel. The layout for the cooling channels was developed by J. Tipton using a script for a 1 D estimate which developed flow velocities and heat transfer coefficients for each channel. The results were compared to a full CFD analysis and found to give similar results for flow velocities. Figure 27 shows the comparison. The Python script used for the calculation is documented in Appendix C "Convection Heat Transfer Coefficients".

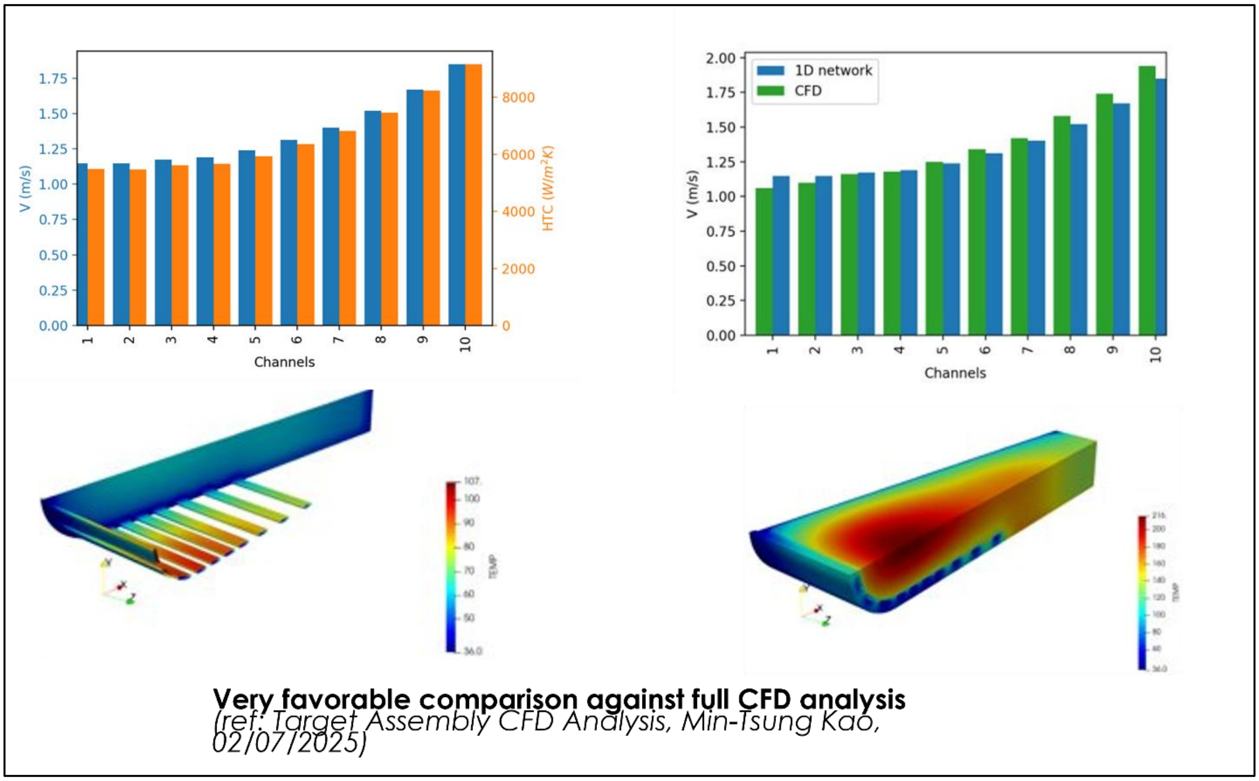

Figure 27 1D Channel Heat Transfer Coefficients Comparison

The script also predicted an HTC of 8000 for the side flow manifold. For the Abaqus analysis with steady state heat loads the 1D estimated Heat Transfer Coefficients were assumed with a 40 °C sink temperature. The manifold estimate was also applied to the cooled surfaces in the heel. Figure 28 shows the wetted surfaces and the Film Coefficients as mapped into Abaqus. The values in W/m^2-K go from 5485 for channel 1 to 9162 for channel 10 as shown. The manifold and heel regions film coefficient is 8000.

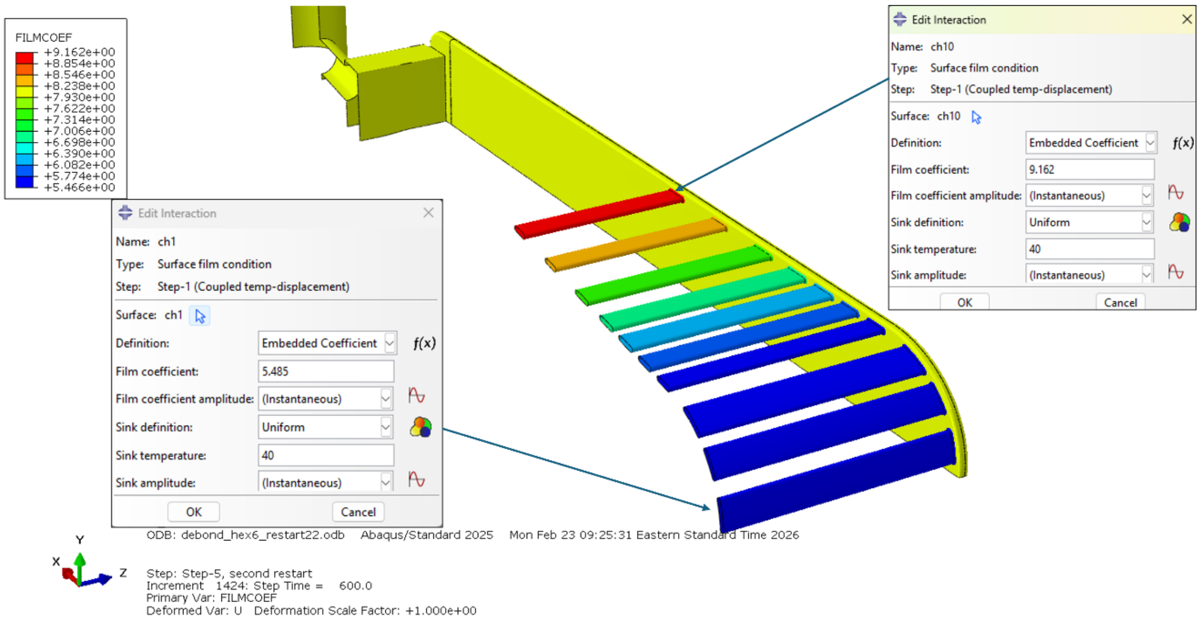

Figure 28 Applied Film Coefficients

4.7 LOAD DEFINITIONS

4.7.1 Initial Transient analysis with Steady State Heat Loads

This analysis used 3 bar water pressure on all wetted surfaces and steady state heating for the tungsten, tantalum and Inconel mesh parts. The pressure was assumed to ramp up over 10 seconds prior to heating. This avoided anomalous transient results from instantaneous pressure application. Figure 29 shows the pressure load.

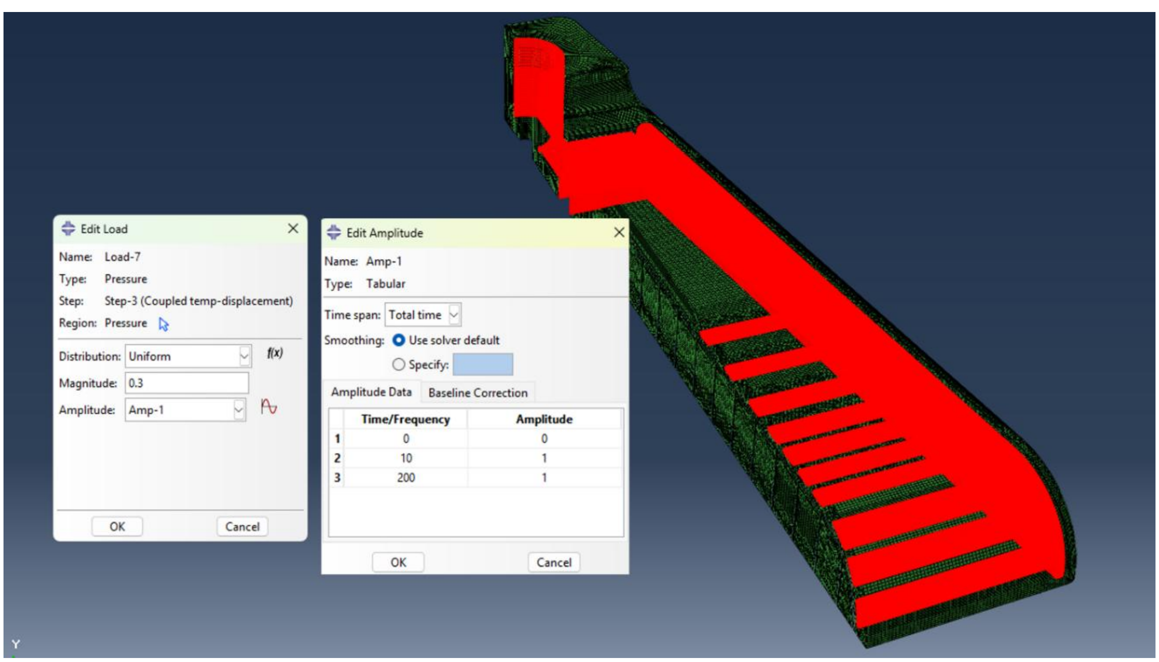

Figure 29 Pressure Load in MPa and time in seconds

A link to the target heat loads in SI standard units was used as described in Section 3.3. For use in SI (mm) units the spatial coordinates were multiplied by 1000 and the volumetric heating by 1e-6 to give coordinates in mm and heating in mW/mm^3 . The converted source Abaqus heating data files for tungsten (QWmm), tantalum (QTamm) and Inconel (Qinconel_mm) were plotted on the assembly model as shown in Figure 30. They are archived along with the other analysis input files for this DAC on the Windchill PLM.

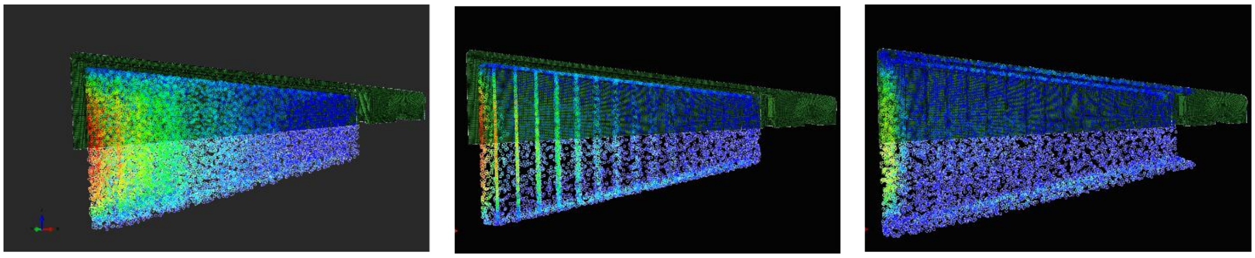

Figure 30 Heating source data plots

Abaqus was used to map the source data on the model elements. The result for tungsten is shown in Figure 31. The peak heating was equivalent to 28.4 MW/m^3. Most outer surface elements did not have a heating value mapped. The heating mesh and target mesh was different and the Abaqus mapping function could not interpolate values particularly on the outer surface elements. The total tungsten heating from the "Target Assembly Thermo-Fluid Analysis" DAC was 14.65 kW [6]. The sum of the volumetric heating mapped by Abaqus times the element volumes was 14.1 kW for a full target, approximately 4% low.

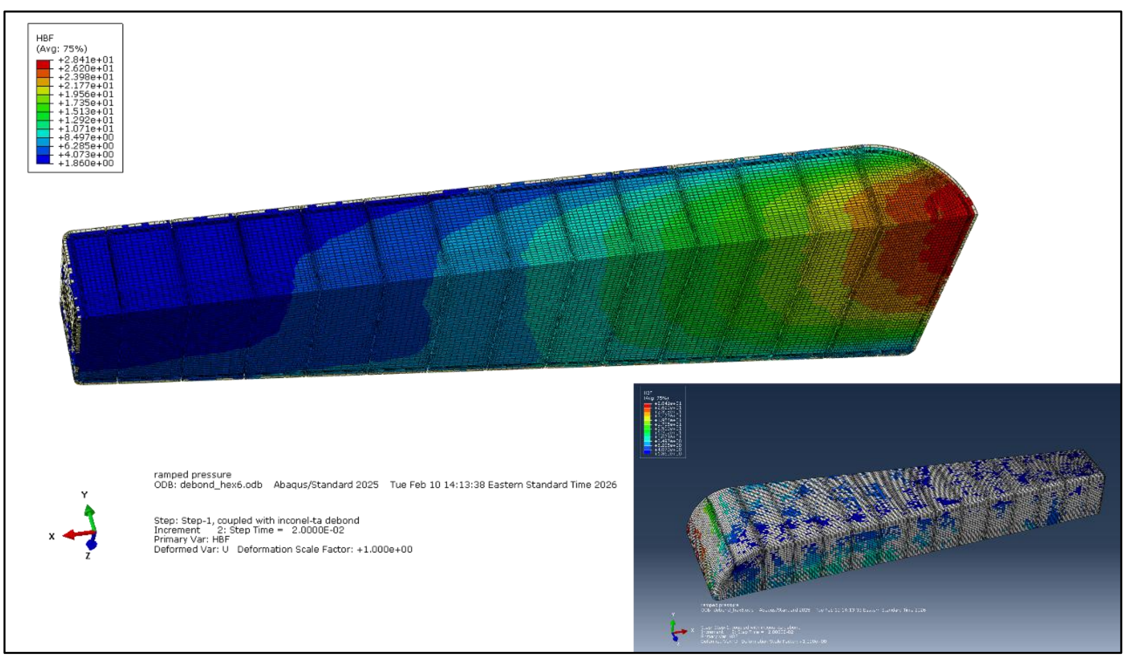

Figure 31 Tungsten Body Heat Flux

The tantalum heating is shown in Figure 32 with a peak of 25.5 mW/mm^3. The total power in tantalum for the model was 858 W for a full target, approximately 2% low.

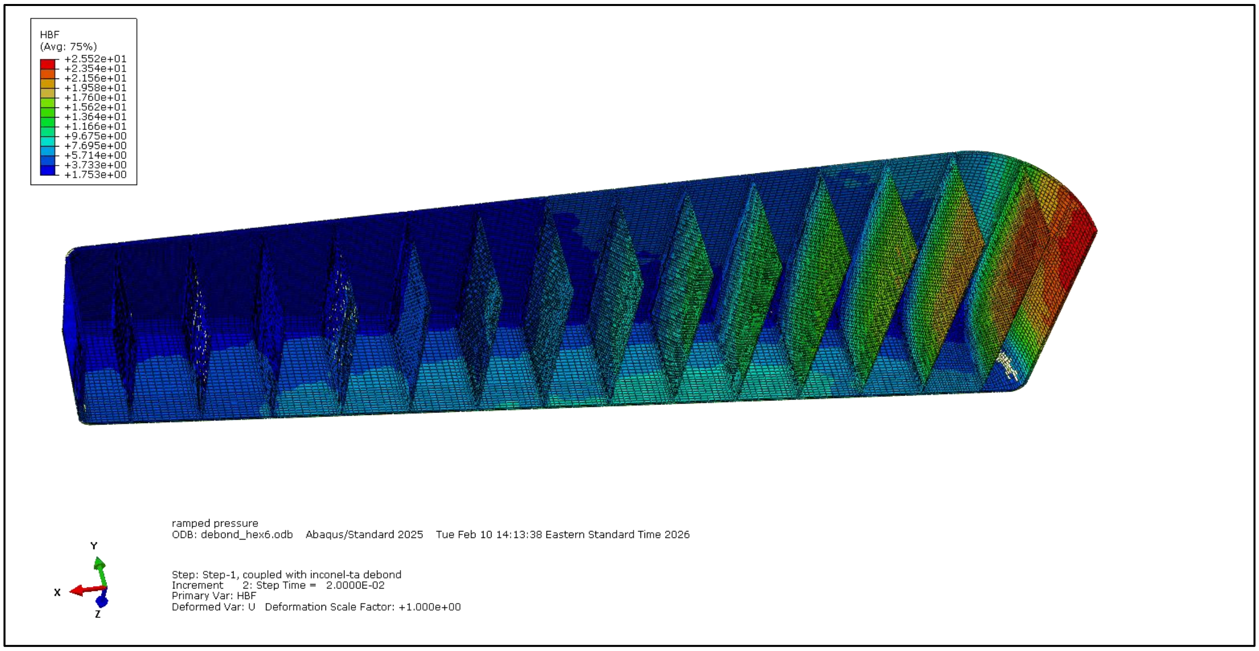

Figure 32 Tantalum Body Heat Flux

The heating for the Inconel mesh part is shown in Figure 33 and with a view of the outer side surface in Figure 34. The rear Inconel thickness was increased after the neutronic heating analysis, and the added region did not have any heating mapped. This was a low heating region and not considered to be significant for evaluating changes from debonding. Peak heating was 14.6 mW/mm^3 in the front region. Total power in the model for Inconel in a full target was 16.5 kW. approximately 13% low. Overall, the total power for tungsten, tantalum and Inconel was approximately 5 % lower than the CFD FDR values but this was not expected to significantly affect the results.

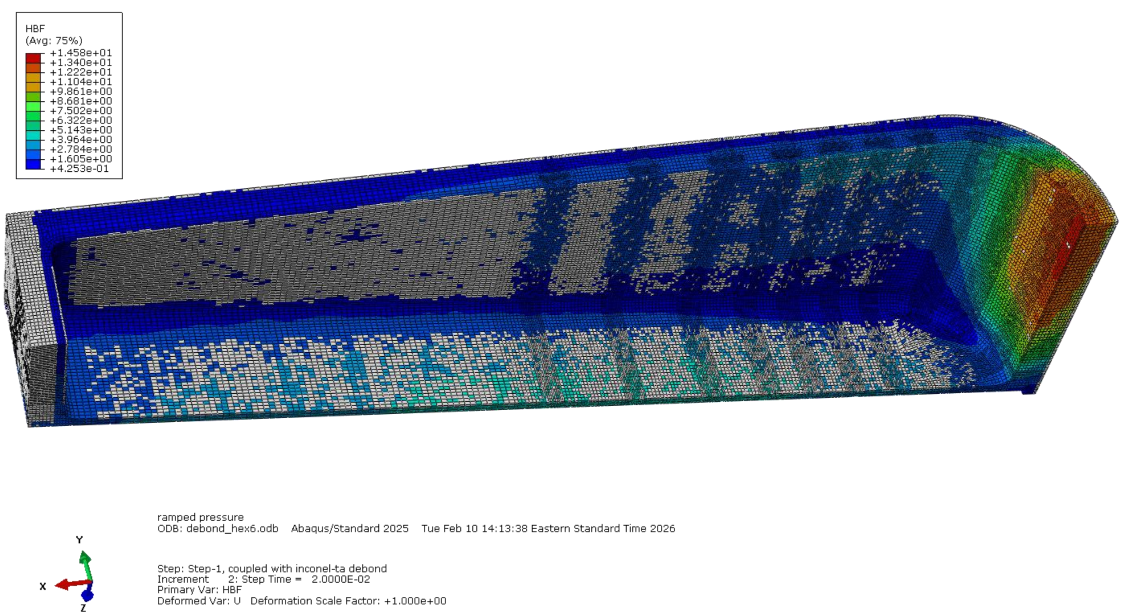

Figure 33 Inconel Body Heat Flux inside view

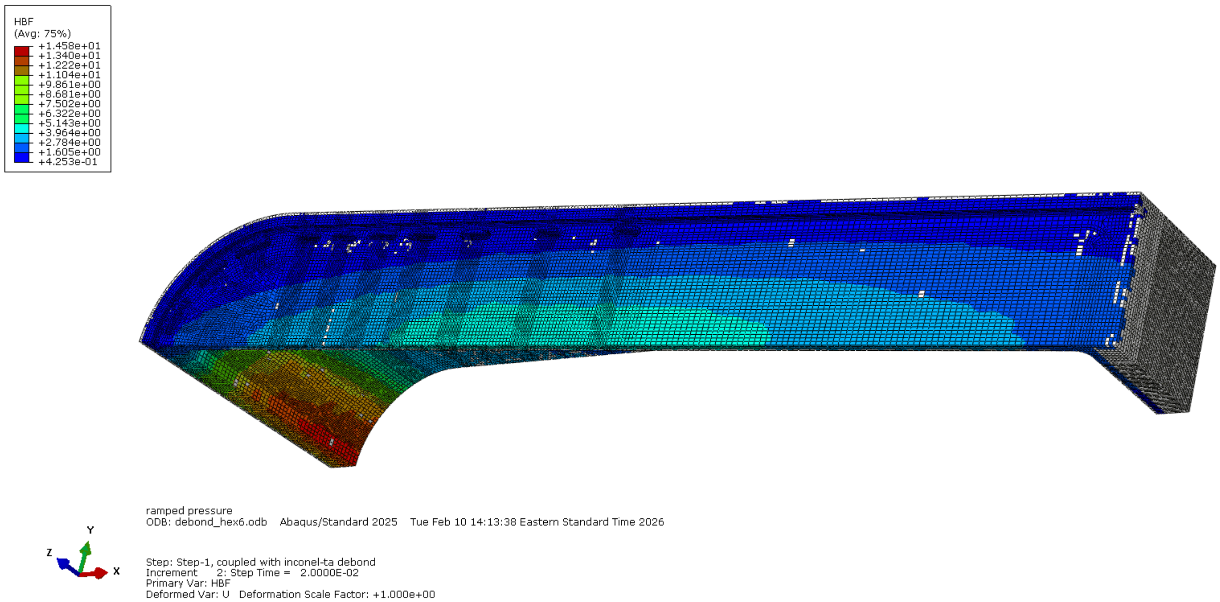

Figure 34 Inconel Body Heat Flux side view

4.8 SIMULATION METHODOLOGY

4.8.1 Analysis with Pressure and Steady State Heating

The effect of not having a bond between the tantalum and Inconel was estimated by first finding a steady state solution using the steady state heating rates and then using that solution as an initial condition for a transient analysis with the energy deposition from a single pulse. Initial attempts to do a true steady state Abaqus solution failed, possibly because of the very large memory requirements. A decision was made to do an Abaqus Standard coupled temperature-displacement transient analysis and to allow it to run long enough to reach near steady state conditions starting from an initial temperature of 40 °C for all material. The analysis was restarted twice from restart files for a total of approximately 14 minutes of heating. The temperatures were nearly at steady state after this period. Figure 35 shows the input file names, step names, loads, step times, analysis increments used and total time at the end of each step. The initial step (named Step 3) for the first run was with only the pressure load. This assumed water cooling pressure was applied before heating started. The pressure and heating were maintained for all following steps.

Input file (.inp)	Step #	Loads	Step time (s)	Increments	Total time (s)
debond_hex6	3	Pressure	10	16	10
	1	Pressure & Heating	0.4	8	10.4
	2	Pressure & Heating	99	600	109.443
debond_hex6_restart	4	Pressure & Heating	161.2	1000	270.671
debonde_hex6_restart22	5	Pressure & Heating	600	1424	870.671

Figure 35 Initial transient analysis input files and step times completed

The BERNIE cluster was used for all three runs with 2 nodes and 128 CPUs used for each analysis. The runs took clock times of 3.1, 3.9 and 5.2 days.

4.8.2 Pulse Heating Analysis

The last results from the steady state heating analysis were imported as an initial condition into an Explicit Abaqus transient coupled temperature and displacement analysis. The pulse energy profile was assumed to be deposited over 1 μs to give an equivalent volumetric heating rate. Details of the model and pulse heating results will be discussed in Section 6.3.

4.8.3 Fatigue Simulations

The cyclic fatigue life calculations are performed with fe-safe commercial software [3]. FTS has previously pursued an equivalent fatigue analysis method using commercial software for an elastic-plastic analysis that models the full transient response [8]. The same methodology was applied to the “Target Segment Thermostructural Analysis” DAC [2] and will also be applied here. Figure 36 provides a conceptual flowchart of the fe-safe fatigue analysis algorithm. An Abaqus ODB output file is provided as input. The fe-safe software pre-scans the ODB to load the stress tensor for every node over each timestep. For a fatigue analysis, the software loops through each nodal stress history. For each node, it rotates through possible stress planes. For every stress plane, it analyzes the time-stress history using a "rainflow" cycle counting algorithm to count stress cycles with their mean stress and amplitudes. The actual fatigue analysis requires material properties (modulus of elasticity, ultimate strength), a S-N curve for the material, and a failure model (i.e. brittle, ductile).

The tungsten plates are modeled according to brittle normal stress theory. The Inconel shroud and flow cover are modeled according to ductile Brown-Miller stress theory. The stainless steel heel structure is also modeled according to ductile Brown-Miller stress theory. These are all documented in the "Target Systems Materials Library" [1]. Best available fatigue curves are used but do not incorporate the "2 and 20" margins that are built into ASME/BPVC curves. The Goodman method is used to account for mean stress effects on fatigue life. Finally, the accumulated fatigue damage for the cycles and a FOS are calculated for that node at that stress plane. This is repeated until all stress planes are considered for each node. The worst stress plane (i.e. the critical plane that yields the lowest fatigue life) is exported for each node. In addition, fe-safe exports an ODB with variables for the worst stress amplitude, mean stress, and FOS at each node. As the fe-safe User Manual describes [3]:

> *The factor of strength (FOS) is the factor which, when applied to either the loading, or to the elastic stresses in the finite element model, will produce the required target life at the node. The FOS is calculated at each node, and the results written as an additional value to the output file. The FOS values can be plotted as contour plots.*

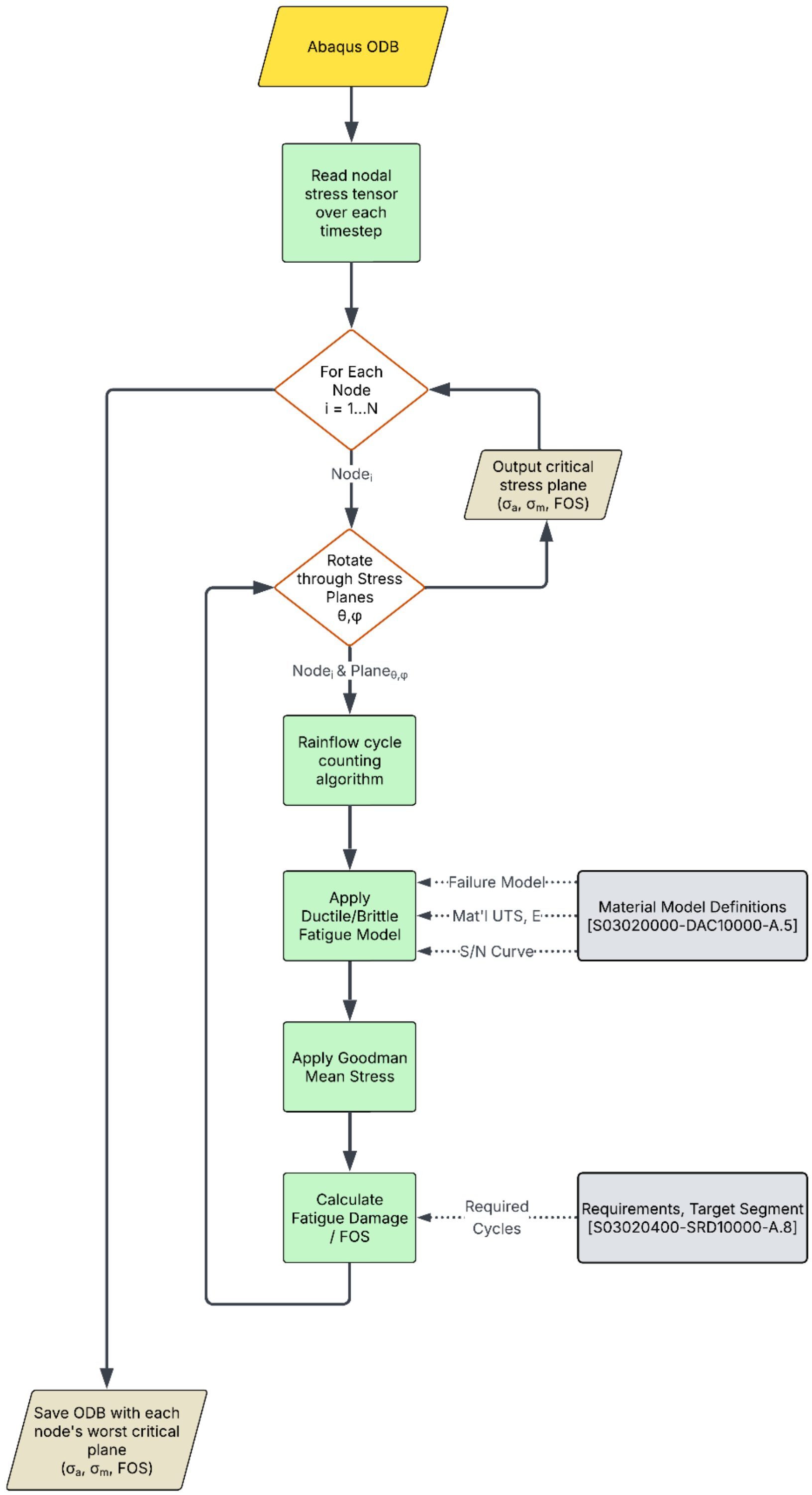

Figure 36: Conceptual flowchart of fe-safe fatigue analysis algorithm.

5. RESULTS FOR PRESSURE AND STEADY STATE HEATING

5.1 PRESSURE ONLY RESULTS

The 3 bar pressure applied prior to heating causes the Inconel to lift off the tantalum on the top surface away from the edge and away from the front curved surface up to approximately 10^{-3} mm. The cover is also displaced. Figure 37 shows the vertical displacements with all displacements magnified by a factor of 200. Horizontal displacements are shown in Figure 38 with a peak of approximately 0.021 mm.

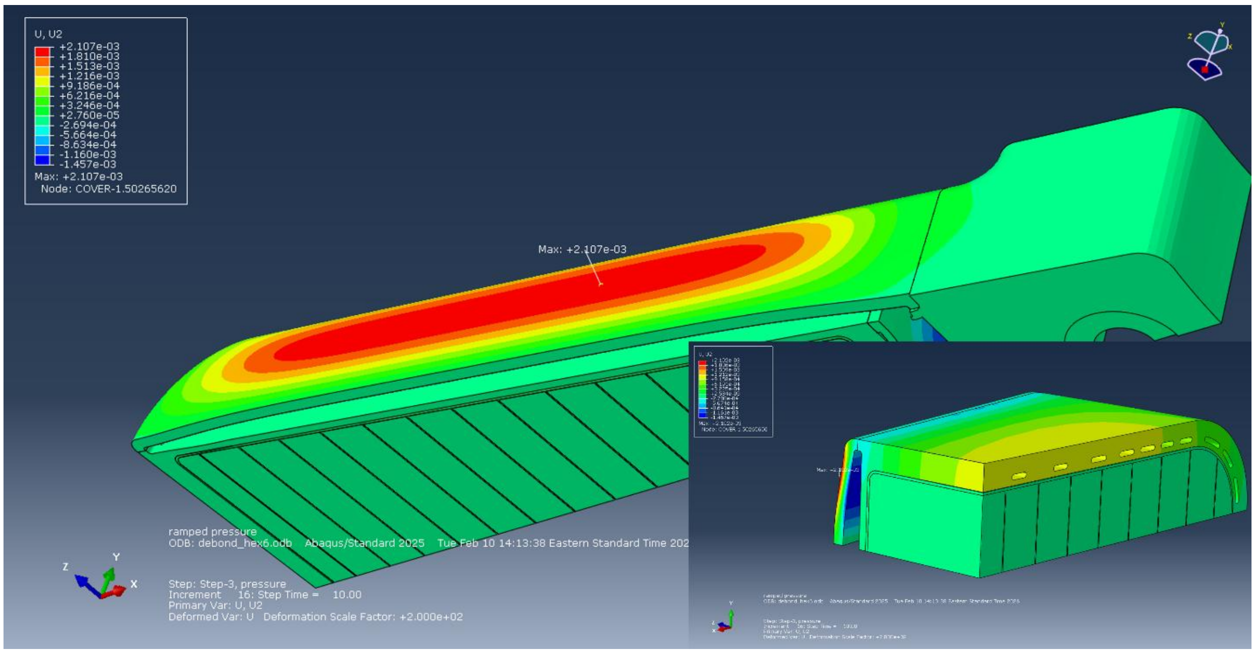

Figure 37 Vertical displacements with only pressure

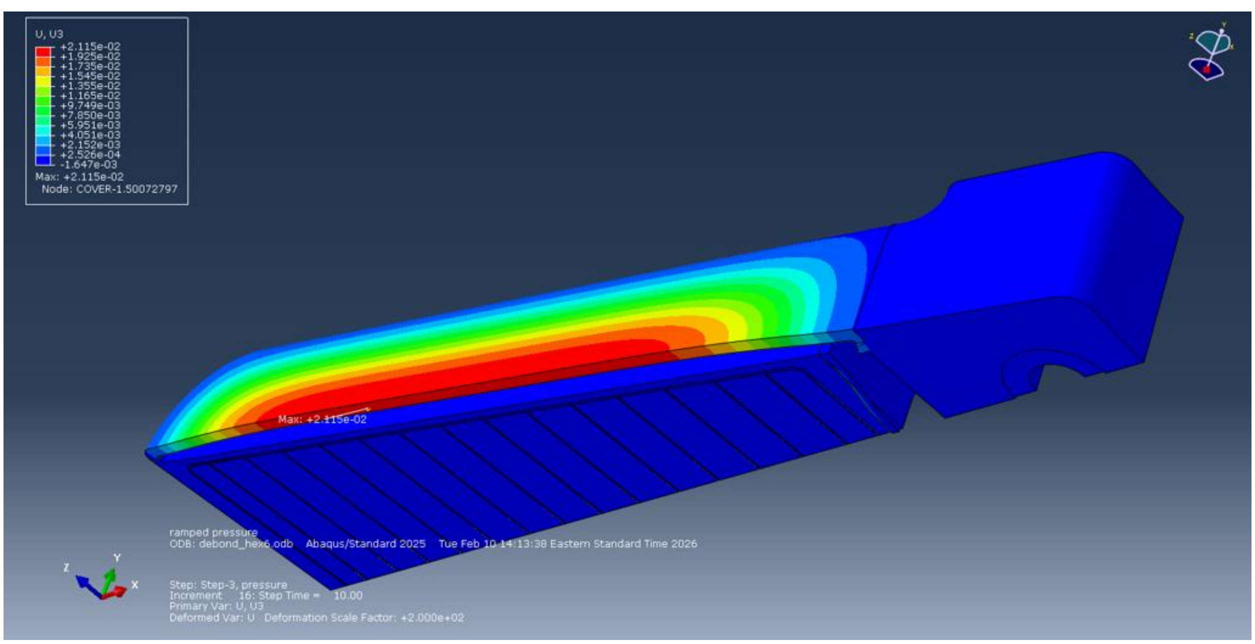

Figure 38 Horizontal displacements with only pressure

5.2 RESULTS FOR PRESSURE AND STEADY STATE HEATING

The peak temperature which occurs in the tungsten and the rate of change of the peak temperature for the steps given in Figure 35 are shown in Figure 39. During the heating the location of the peak moved towards the rear, so different nodes had to be tracked. After 870 seconds the peak temperature was 664 °C and the rate of change was only approximately 0.03 °C/s. This was considered close enough to be used as the steady state result. Results below will be for the last frame of Step 5 at approximately 870 seconds.

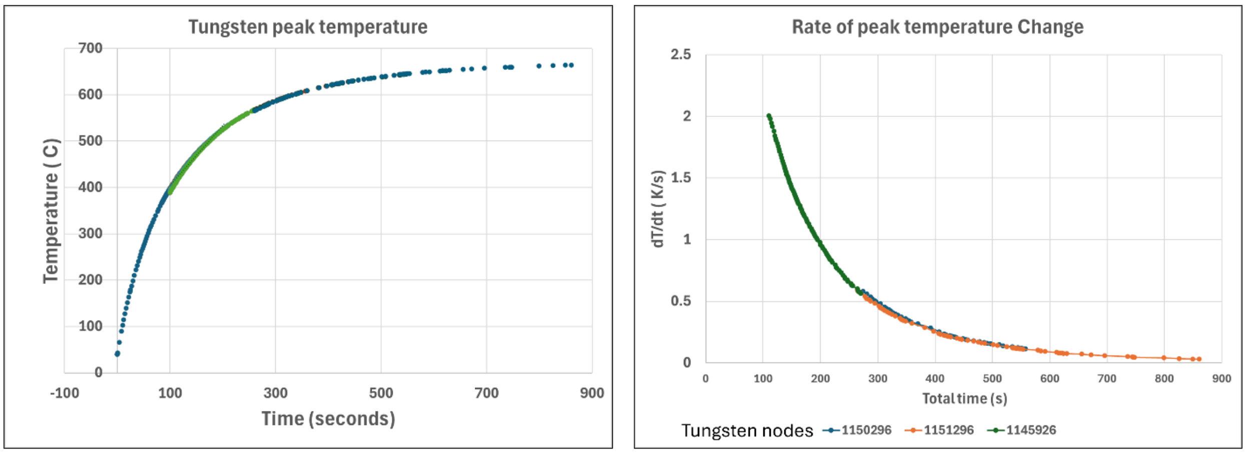

Figure 39 Steady State Heating Peak Temperature and Rate of change vs. time

The assembly temperature is shown in Figure 40 with a displacement scale factor of 30. The peak was 664 °C in the tungsten. This was well below the threshold temperature of 800 °C for tungsten vaporization in steam.

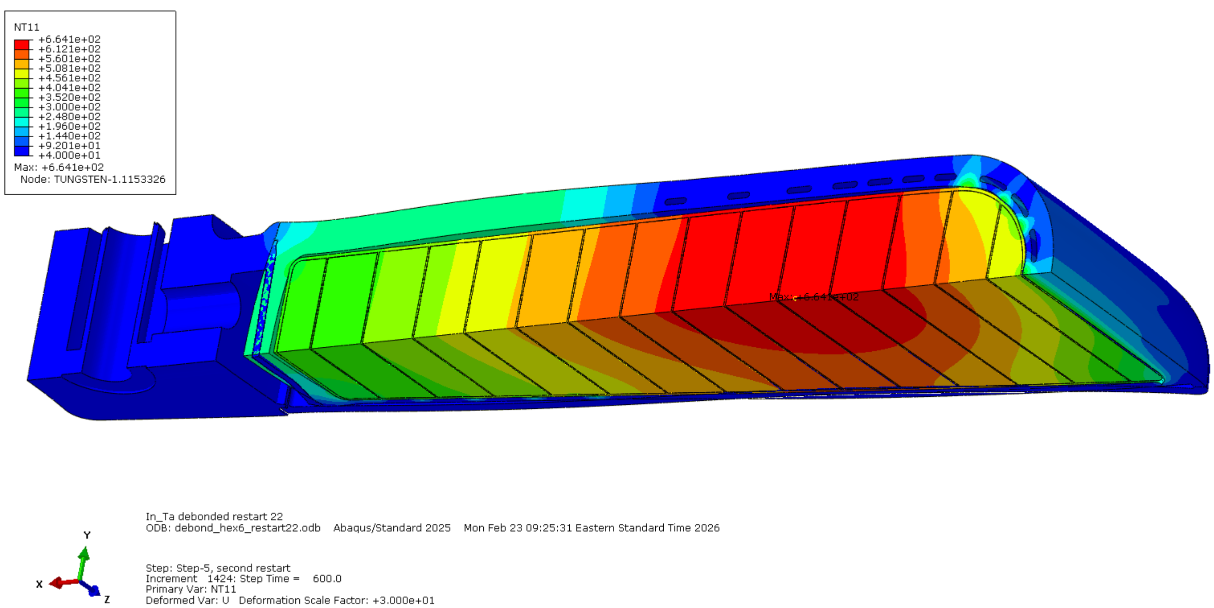

Figure 40 Assembly NT11 temperature with a peak of 664 °C

Inconel temperatures are shown in Figure 80 with a peak of 477 °C and a rear top surface temperature of approximately 300 °C.

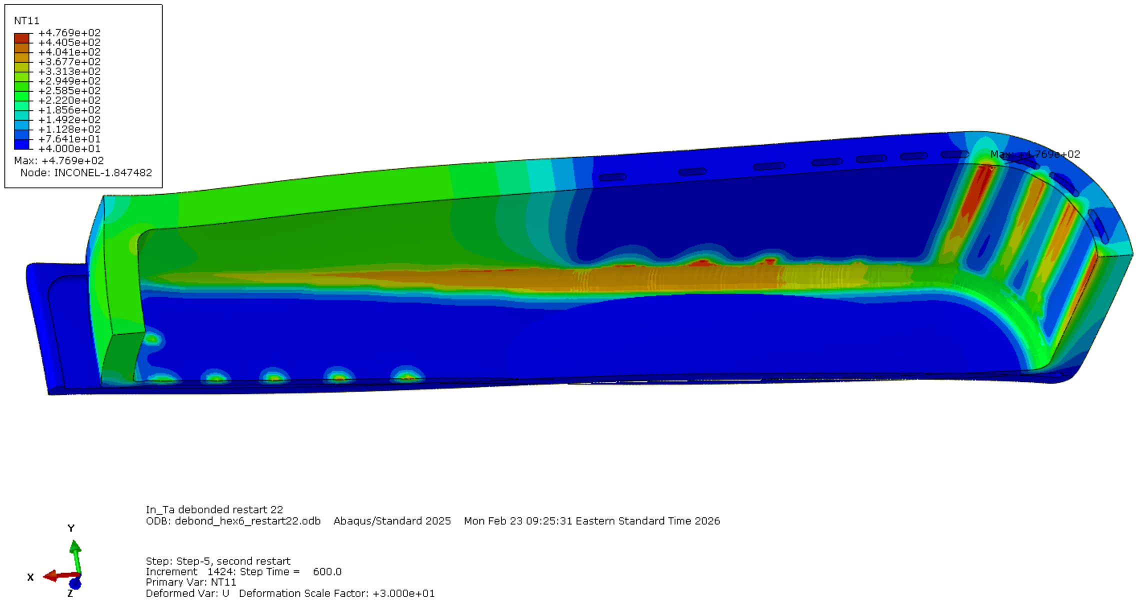

Figure 41 Inconel NT11 Temperature with a peak of 477 °C

Figure 42 shows an axial cut view of the assembly with side U3 displacements. This shows that most of the top surface is not in contact with the tantalum and most of the side Inconel wall also pulls away from the tantalum. The result is that most of the heat transfer and contact stresses are in the corner region. Figure 43 shows the Mises stress at this location. Tungsten stresses are high compared to a tensile limit of 356 MPa, but as a brittle material Maximum Principal stress as shown in Figure 51 should be used to evaluate failure. The stress versus fatigue limits including pulse heating is evaluated in section 7.

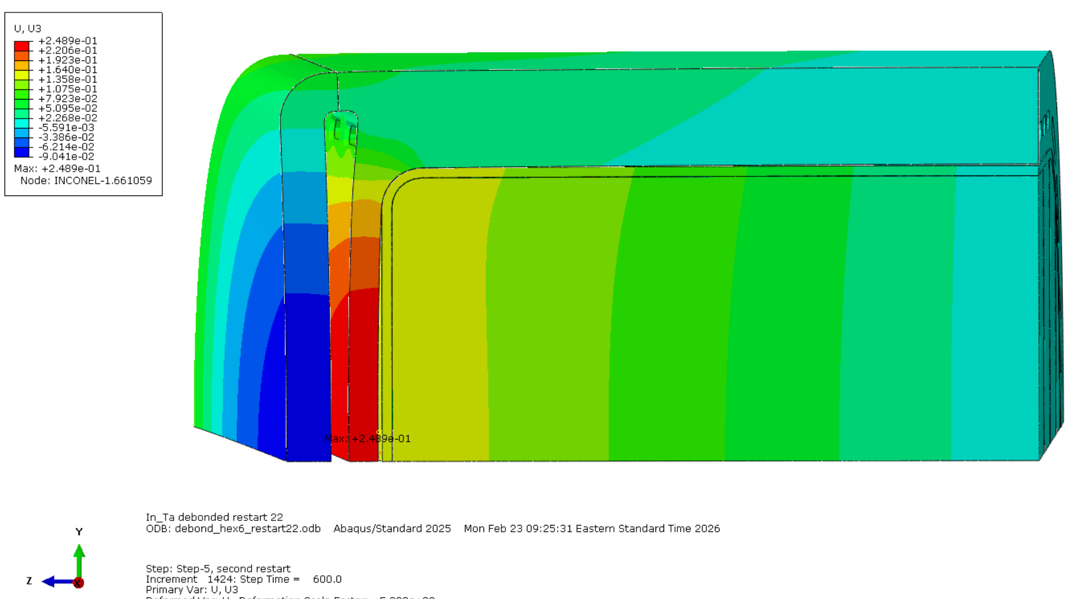

Figure 42 Assembly U3 with axial x cut

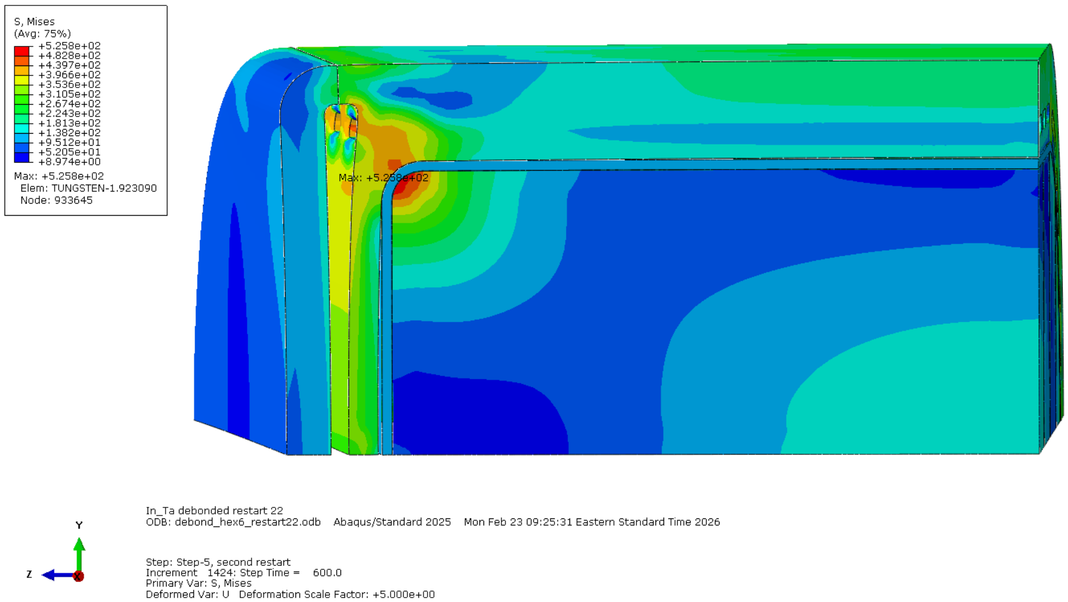

Figure 43 Assembly Mises Stress around axial cut

Figure 44 shows a plot of COPEN for the tantalum which shows the areas not in contact for heat or load transfer with peak separations of approximately 0.09 mm between the tantalum and Inconel.

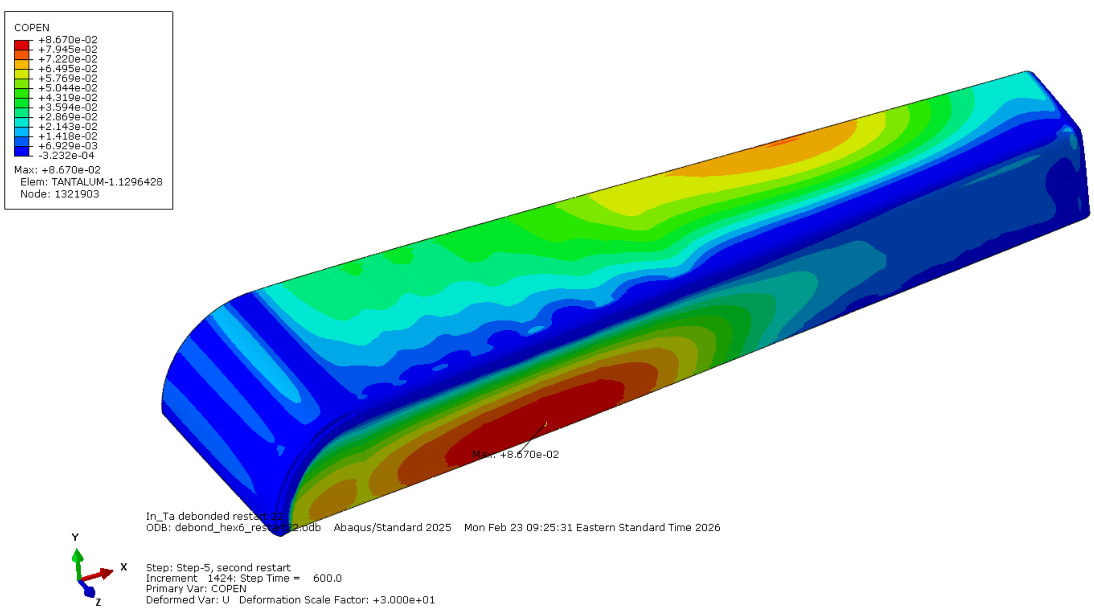

Figure 44 Tantalum COPEN

The contact pressure is shown in Figure 45 with a 500 MPa scale and also with a 93 MPa scale. All areas with CPRESS above 93 MPa have a conductance of 94 kW/m^2.

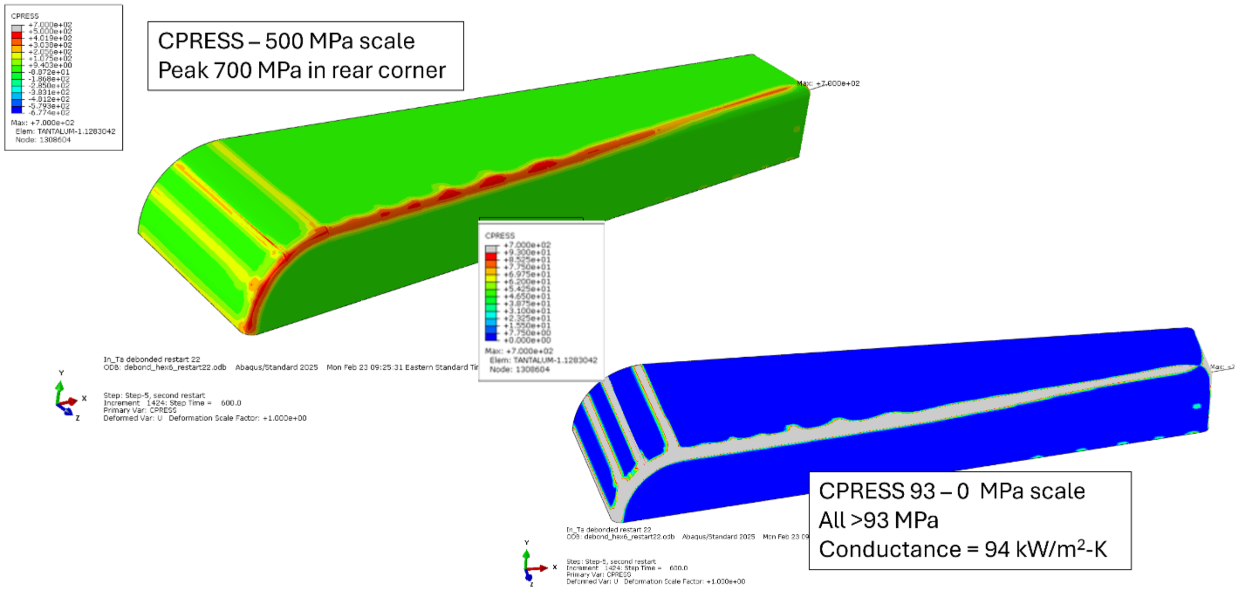

Figure 45 Contact Pressure CPRESS

Heat flux through the contact area to the Inconel is shown in Figure 46 with most near the front flow channels and side corner. In the front the heat flux is higher due to the stiffer areas between cooling channels which have higher contact pressures.

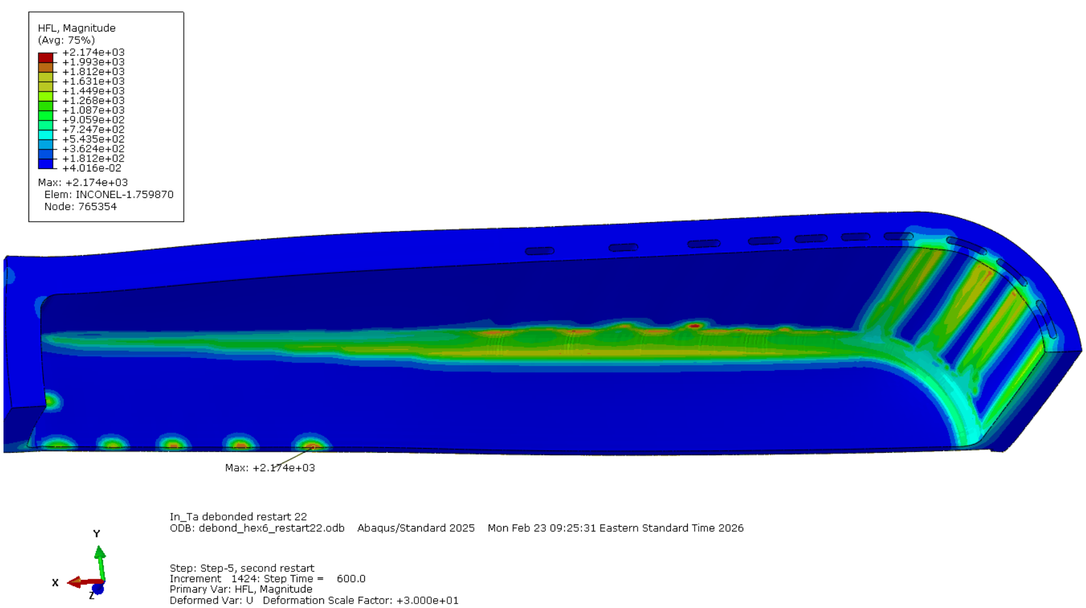

Figure 46 Inconel Heat Flux

The Inconel mesh part Mises stress is shown in Figure 47 and Figure 48 with a peak of 479.6 MPa. At 400 °C the Inconel yield strength is 283 MPa. As shown in Figure 41 there are zones on the inside corner area with temperatures above 400 °C and stresses above 400 MPa, which have yielded. Figure 50 will show this.

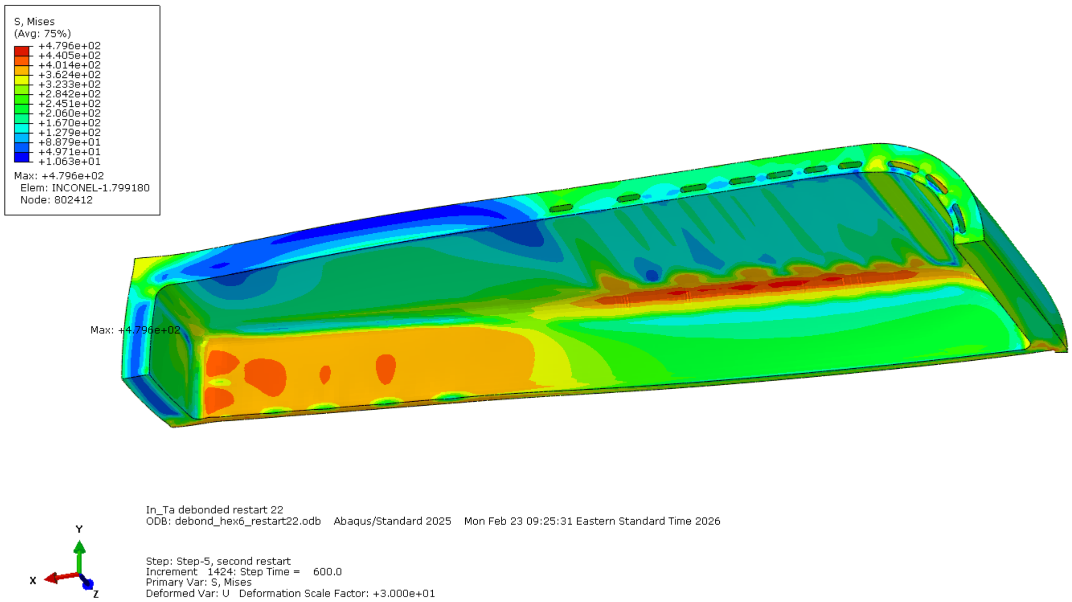

Figure 47 Inconel Stress (inner region)

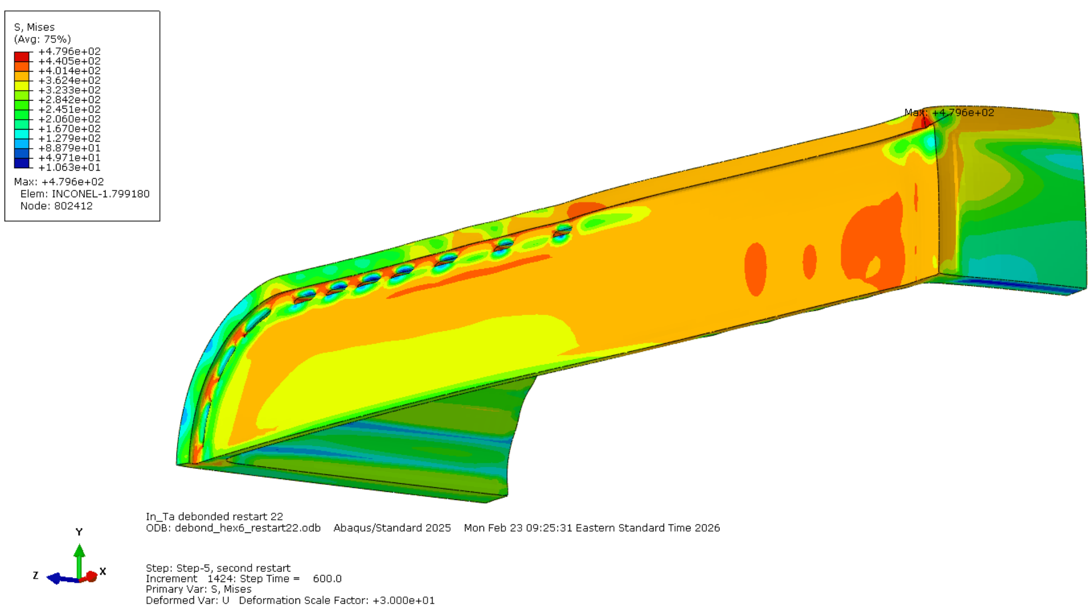

Figure 48 Inconel mesh part Stress side view

Figure 49 shows the Inconel Mises stress including the cover.

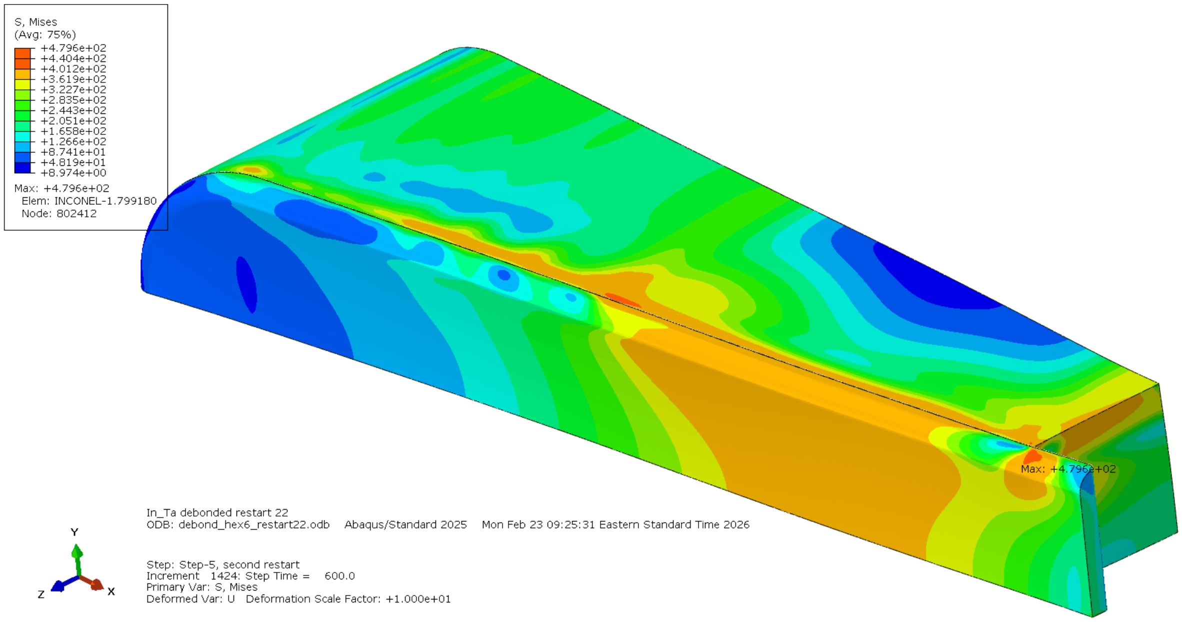

Figure 49 Inconel stress including the cover

Regions of the Inconel are beyond yield and the Inconel plastic PEEQ strain is shown in Figure 50 with a peak of .025. Fatigue analysis showed that a 10 year life can still be met with a Factor of Safety of 1.4 as shown later in Figure 74.

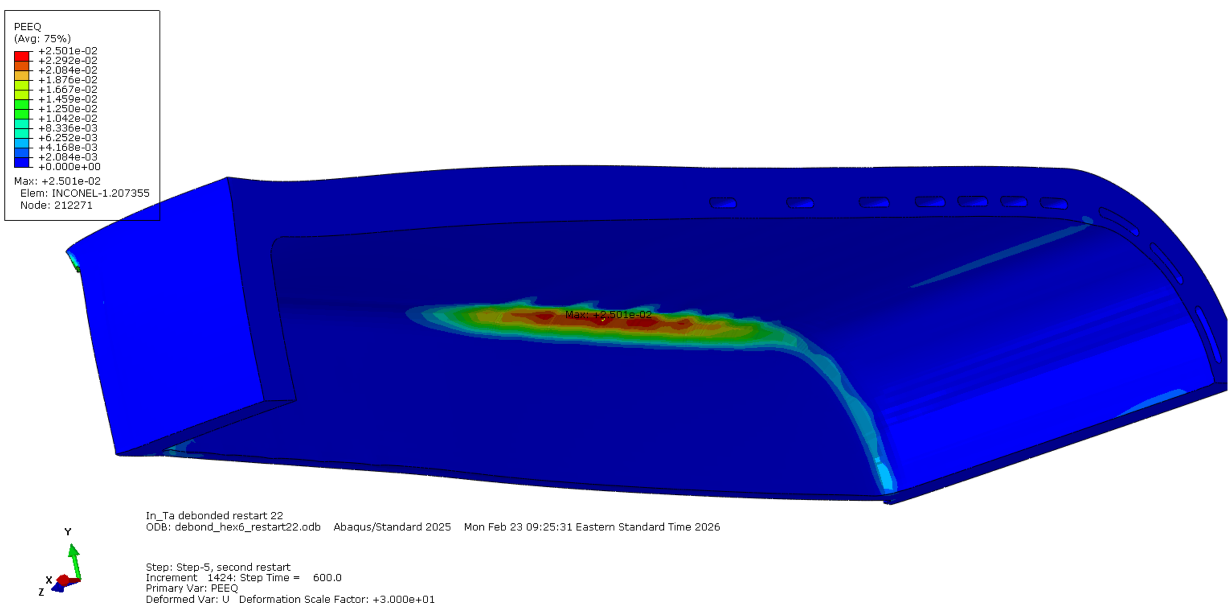

Figure 50 Inconel PEEQ

The peak Max Principal (Abs) stress in the tungsten was approximately 240 MPa excluding a small, isolated region in the middle of a plate which appears to be a singularity, and not physical. This is shown in Figure 51. The peak Von Mises stress excluding the singularity is approximately 600 MPa by the side corner area.

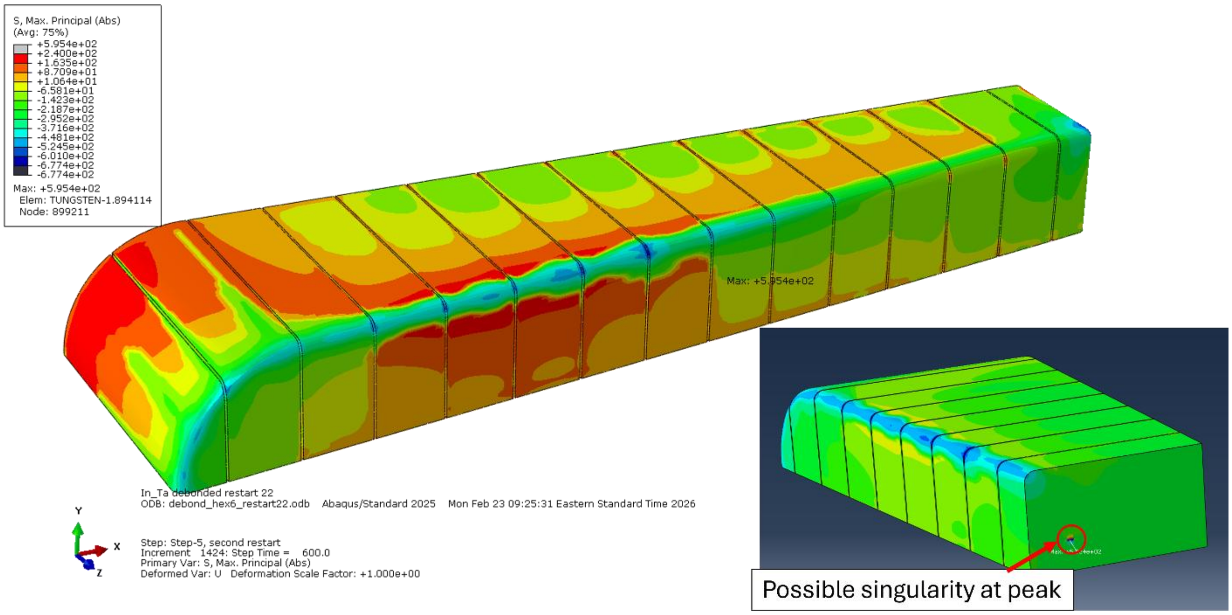

Figure 51 Tungsten Max Principal (Abs) Stress with 240 MPa scale

The tantalum peak Mises stress is approximately 150 MPa with nearly all the material in yield as shown in Figure 52. The yield strength varies between approximately 100 MPa at 600 °C to 150 MPa at 100 °C as shown in Figure 12. The tantalum is basically strain controlled by ties to tungsten.

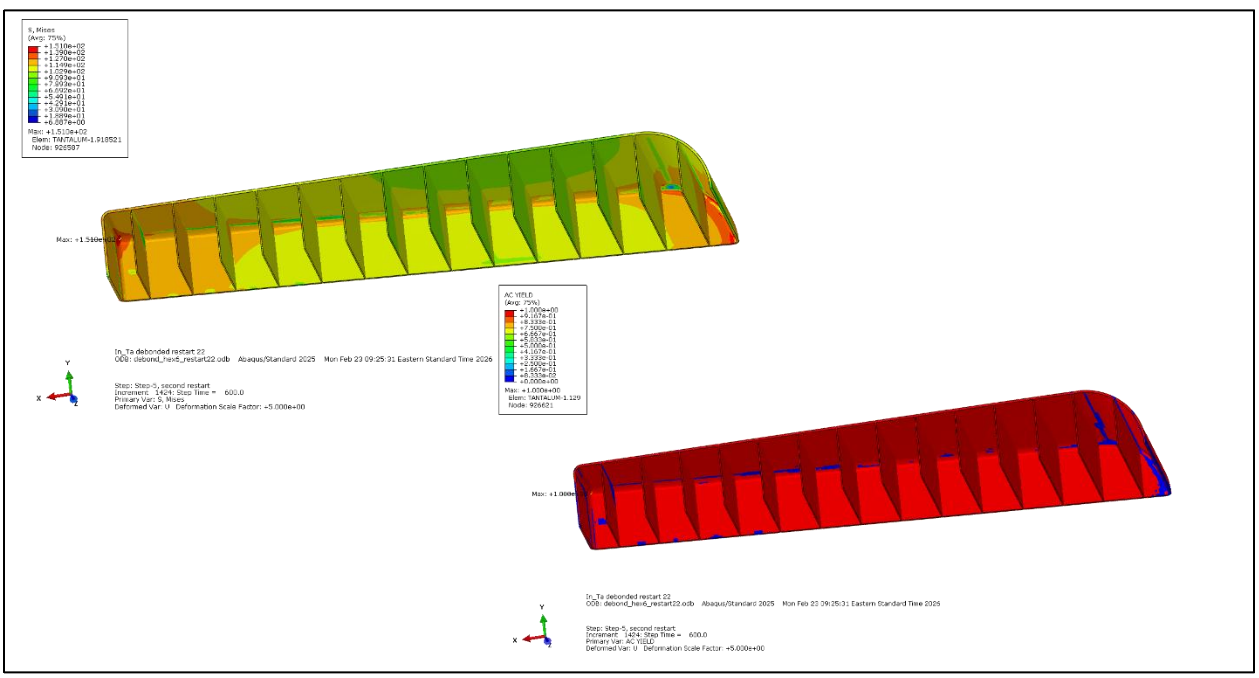

Figure 52 Tantalum Stress and AC YIELD

The Mises stress in the 316L heel is shown in Figure 53 with a peak of 279 MPa. The high stress was localized around the inside edge of the tie to the Inconel where the meshes between the materials did not match well with unrealistic deformations. Most of the material was below the yield strength of 131 MPa at 150 °C and well below the room temperature ultimate strength of 485 MPa [1]. There were small regions of plastic deformation.

Figure 53

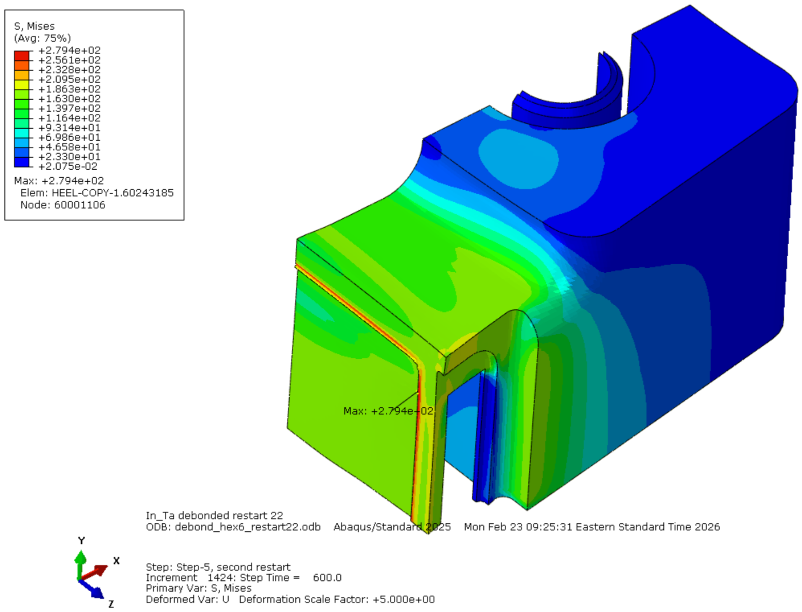

Figure 53 Heel Mises Stress

The surface temperatures of the wetted channels are shown in Figure 54 with a peak of 185 °C and a scale maximum of 133 °C. The effect of possible boiling in regions above saturation is not evaluated. Most of the channel surfaces however are well below the saturation temperature of approximately 133 °C at 3 Bar. The surfaces above saturation are very localized and no significant bulk boiling is expected and the overall effect is not expected to be significant.

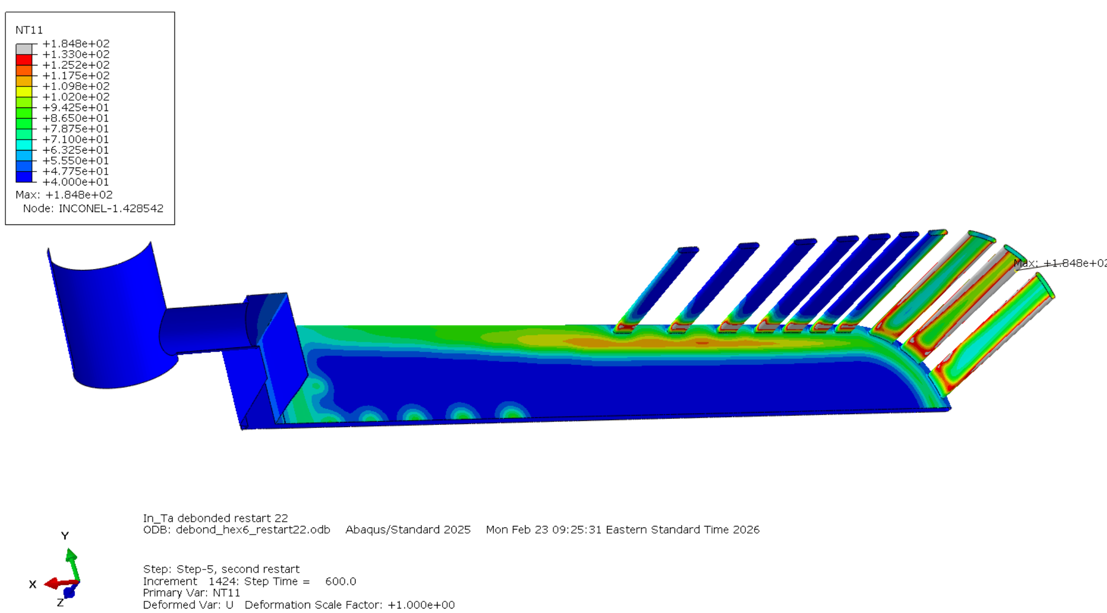

Figure 54 Wetted Surface NT11 Temperatures

6. DYNAMIC EXPLICIT PULSE ANALYSIS

6.1 ABAQUS MODEL

6.1.1 Predefined Fields and Interactions

A separate dynamic explicit coupled displacement – temperature model for the pulse analysis (debond_hex6_pulse7.cae) was developed. The model and results from the last frame of the analysis with steady state heating described above was imported as a predefined field for the initial configuration. This kept the same mesh model with C3D8RT elements and the same boundary conditions on displacements and symmetry. The input for this is shown in Figure 55.

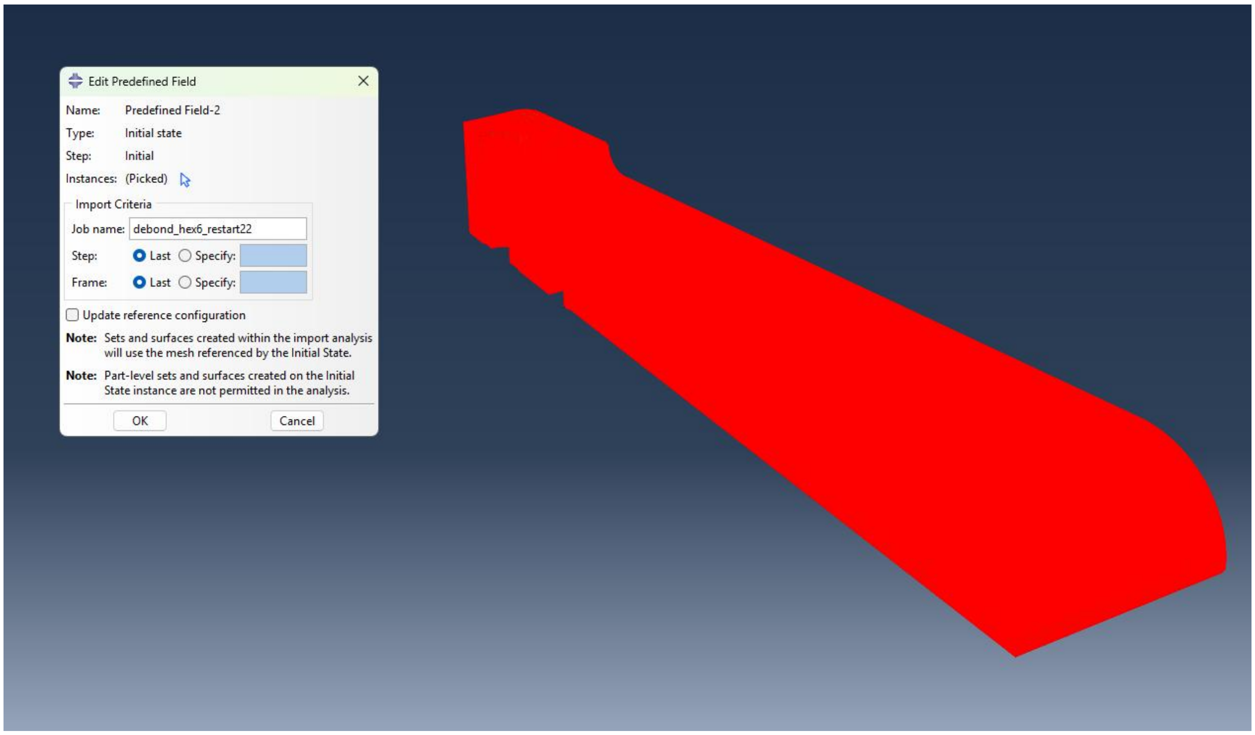

Figure 55 Predefined Field for Initial Configuration

Figure 56 shows a view of the assembly temperature and stress as imported into the pulse analysis with a scale factor of 30 on displacements.

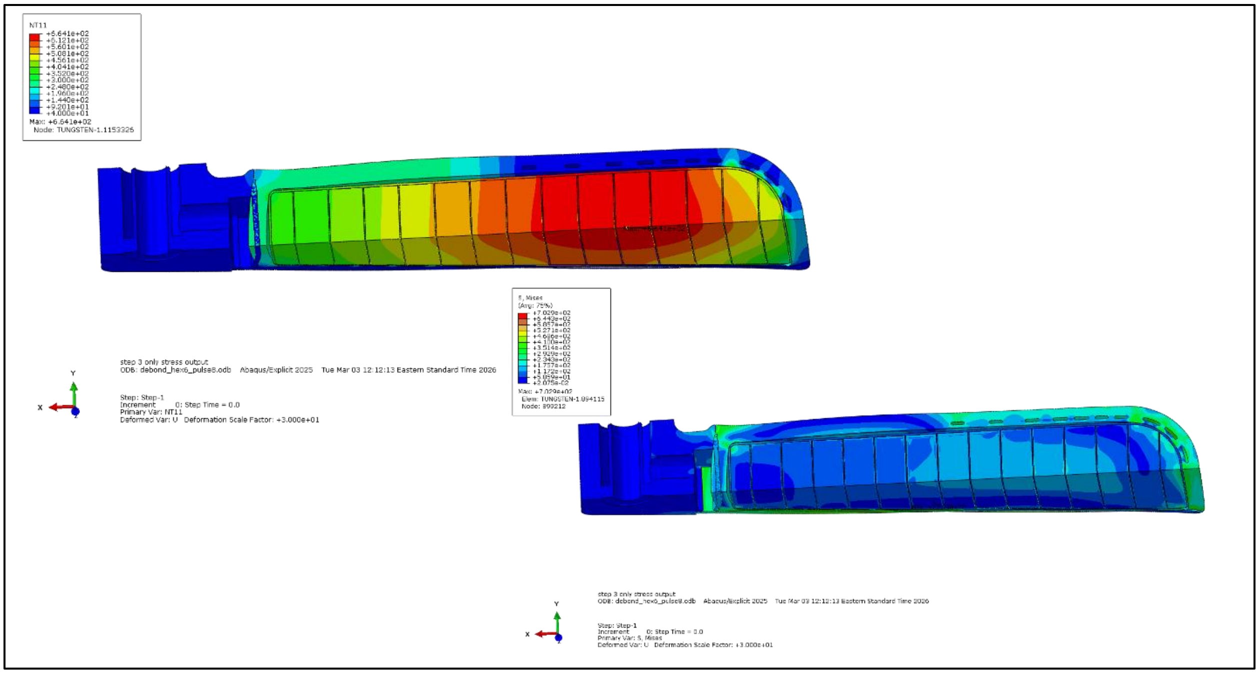

Figure 56 Pulse analysis initial configuration imported from debond_hex6_restart22.odb

The interaction between tantalum and Inconel was redefined for the explicit analysis with a Kinematic contact method with small sliding as shown below. The same interaction property from the steady state heating analysis was used.

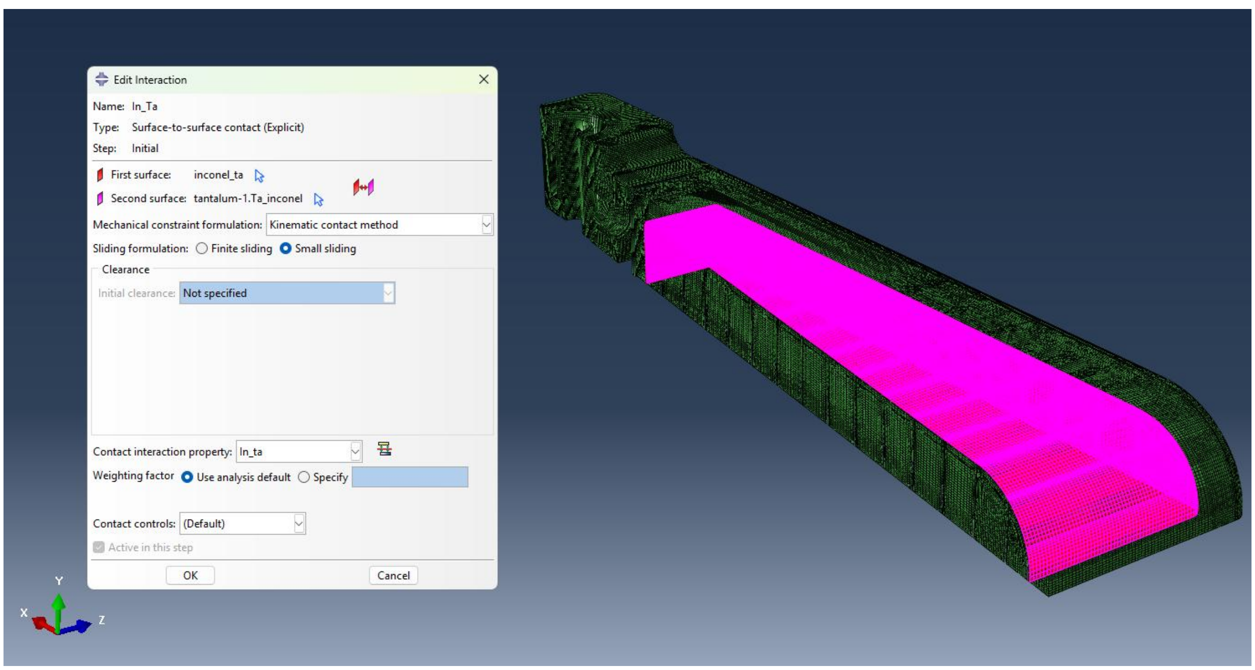

Figure 57 Inconel to Tantalum explicit surface to surface interaction

Heat transfer coefficient interactions were not included because the pulse analysis objective was to evaluate the transient stresses and fatigue life. Also, the analysis was only over 700 µs seconds and any temperature changes from water cooling would not be significant over such a short time.

6.1.2 Constraints

The same four tie constraints described previously were used for the pulse analysis, but the surface names were redefined with a "2" added to the surface names used for the steady state analysis. Prior to renaming the surfaces the input file did not recognize the constraints. The constraints with modified surface names are shown in Figure 58.

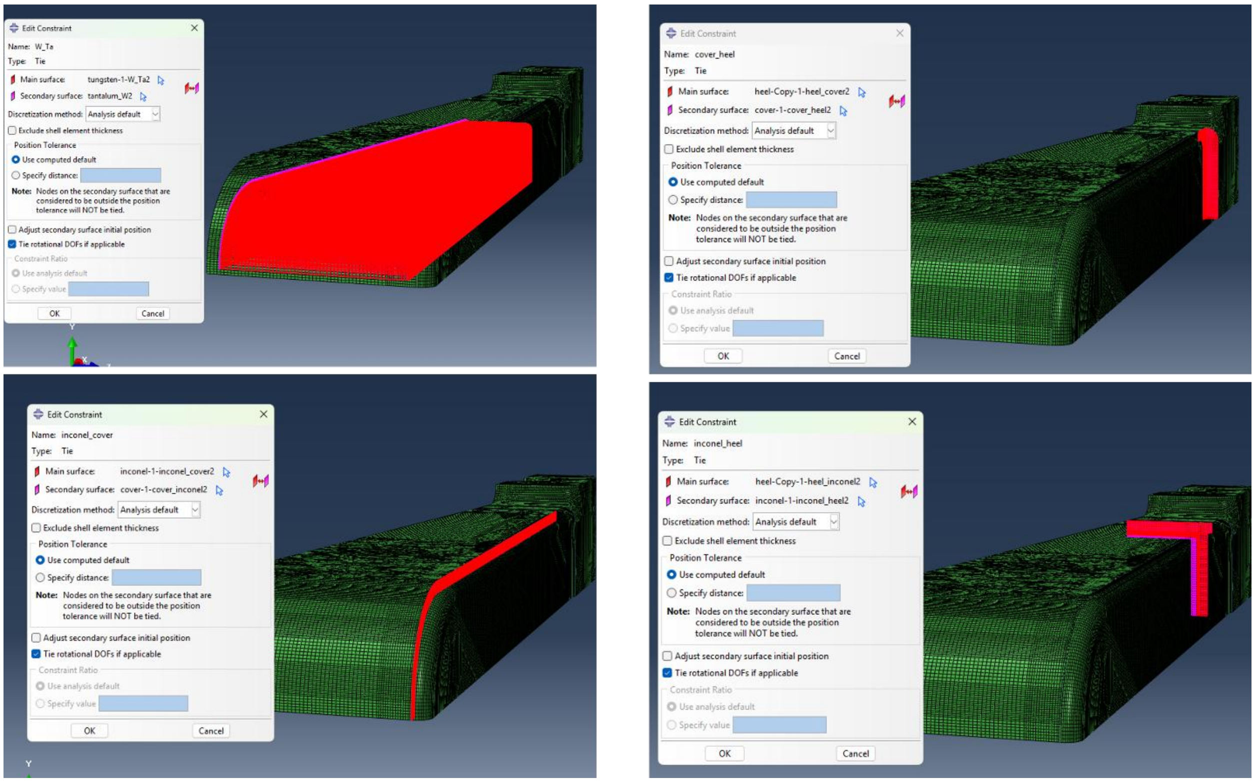

Figure 58 Pulse Tie Constraints with modified surface names

6.1.3 Pulse heating loads

Single pulse energy deposition in J/mm^3 were provided as described in Section 3.3 for the tungsten, tantalum and Inconel. These were imported as fields in Abaqus, and a plot is shown in Figure 59.

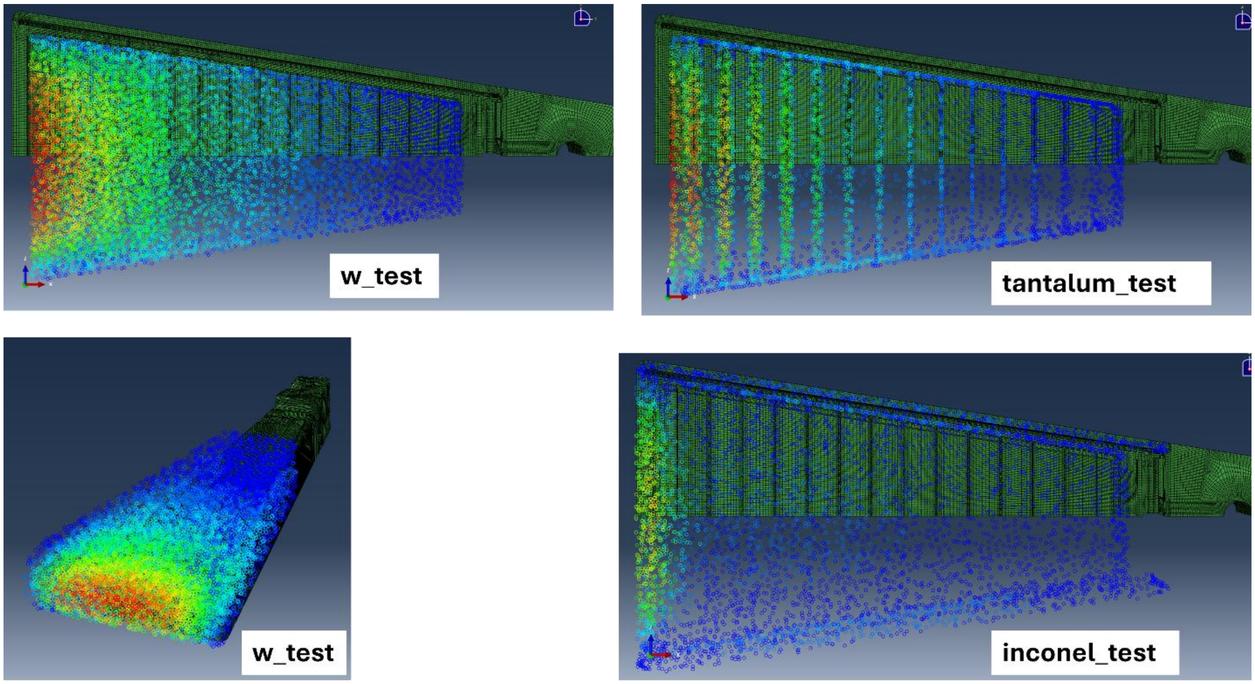

Figure 59 Pulse energy deposition plots

For the pulse analysis the energy was assumed to deposited over 1µs as a uniform heating rate. The volumetric heating rates were taken as the energy deposition divided by a 1e-6 s (step 1 time period). The consistent unit for energy in the mm system is mJ so the heating rates used a factor 1e9 on the J/mm^3 data ((1e3 mJ/J)/1e-6s) when importing into Abaqus for Step 1. The heating loads were disabled for the following steps. The tungsten, tantalum and Inconel loads for Step1 are shown in Figure 60. The lower pulse heating loads for the cover and heel were not included. Pulse heating effects in the water were also not included.

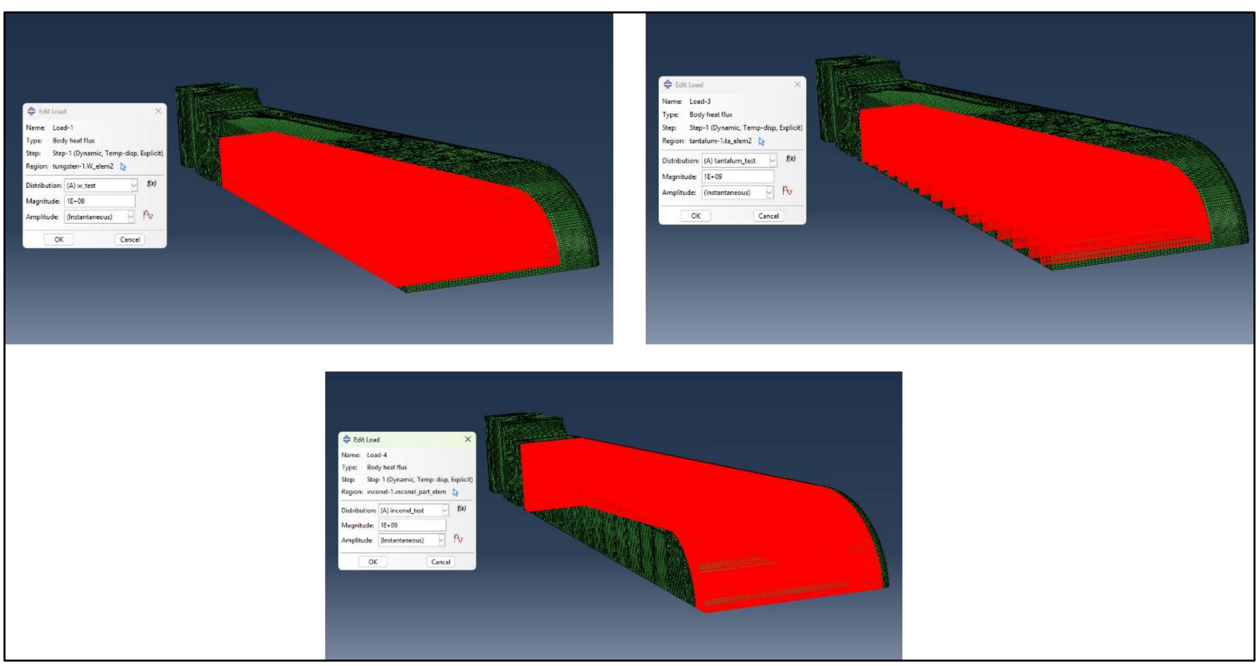

Figure 60 Pulse Volumetric heating loads for tungsten, tantalum and the Inconel mesh part

6.2 ANALYSIS STEPS

The pulse analysis was done with three steps. The Step 1 duration was 1 μs with three volumetric heat loads with temperature, displacements, contact conditions and stresses requested. Step 2 was for 10 μs without any loads with and with temperature, displacements, contact conditions and stresses also requested. Step 3 duration was 690 μs with no heating and only stress requested at 1 μs intervals to minimize the size of the output files. Figure 61shows the steps, loads, step time, number of increments to solve, number of output data frames, output data and total time.

Input file (.inp)	Step #	Loads	Step time (s)	Increments	Frames	Data	Total time (s)
debond_hex6_pulse8	1	Pulse heating	1.00E-06	77	11	NT11,S,U_C	1.00E-06
	2	none	1.00E-05	736	11	NT11,S,U_C	1.10E-05
	3	none	6.90E-04	50913	691	S	7.01E-04

Figure 61 Pulse Analysis Steps

The analysis was done on the BERNIE cluster with 2 nodes and 128 CPUs and took a clock time of 0.8 hours.

6.3 PULSE ANALYSIS ABAQUS RESULTS

The assembly temperature after the 1 μs of step 1 heating is shown in Figure 62 Assembly temperature after pulse peak was 671.9 °C.

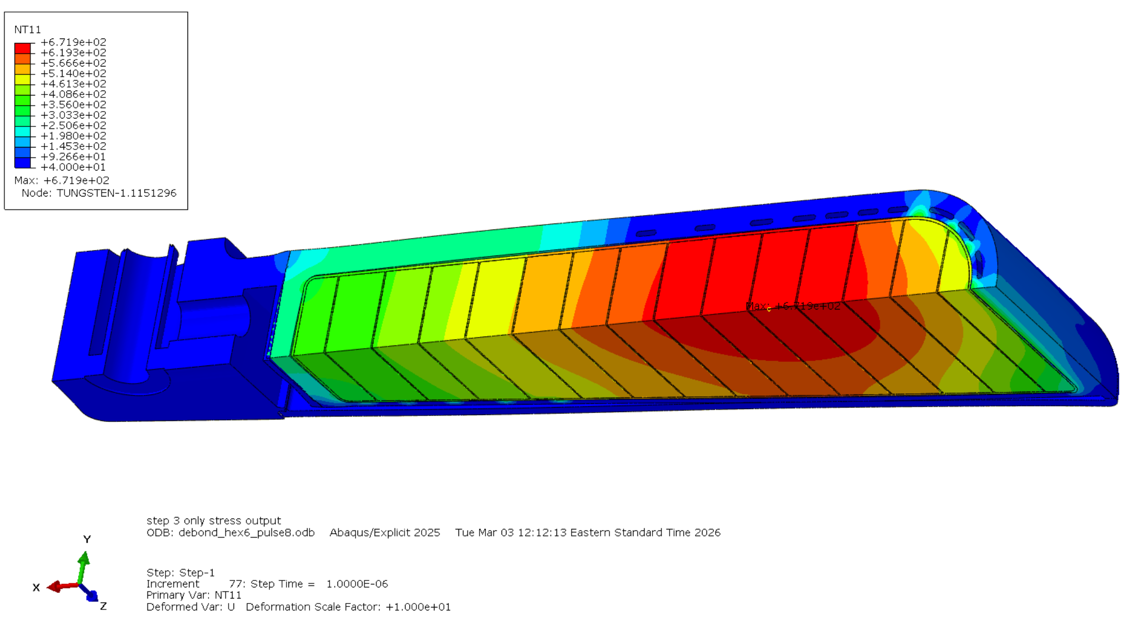

Figure 62 Assembly temperature after pulse with a peak of 671.9 °C

The pulse temperature increase is shown in Figure 63 with a peak of 14.5°C in the tungsten. This was calculated as the difference between the temperature for Step 1 at frame 10 minus the initial temperature.

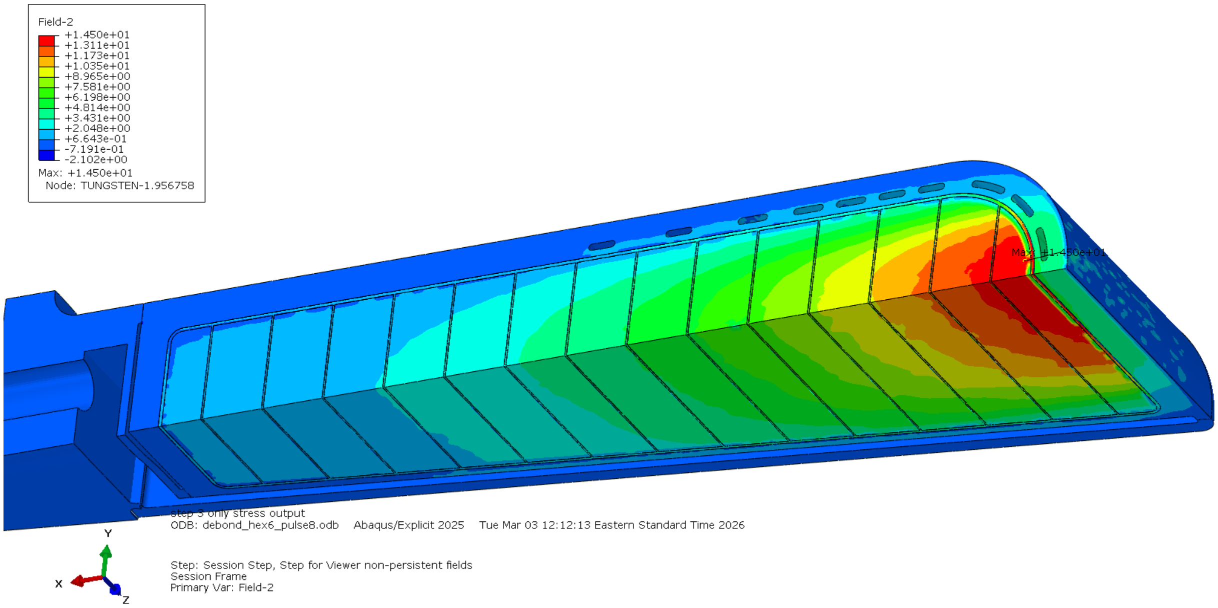

Figure 63 Pulse Temperature Increase with a peak of 14.5 °C

The temperature rise in the tungsten, tantalum and Inconel are shown separately in Figure 64.

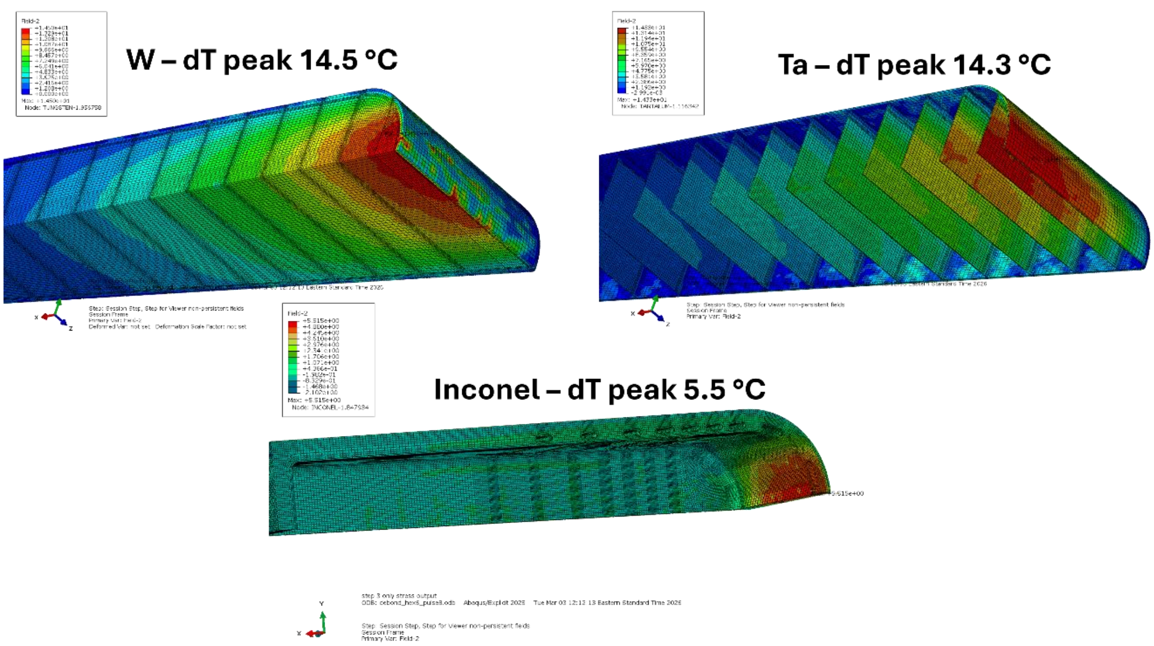

Figure 64 Pulse temperature rise in parts with peaks

The pulse temperature rise in 1 μs creates transient stress through the assembly. As an example, one tungsten node near a corner was selected to show stress versus time. Figure 65 shows the node used with stress at 11 μs and Figure 66 is a plot of Mises stress over 700 μs.

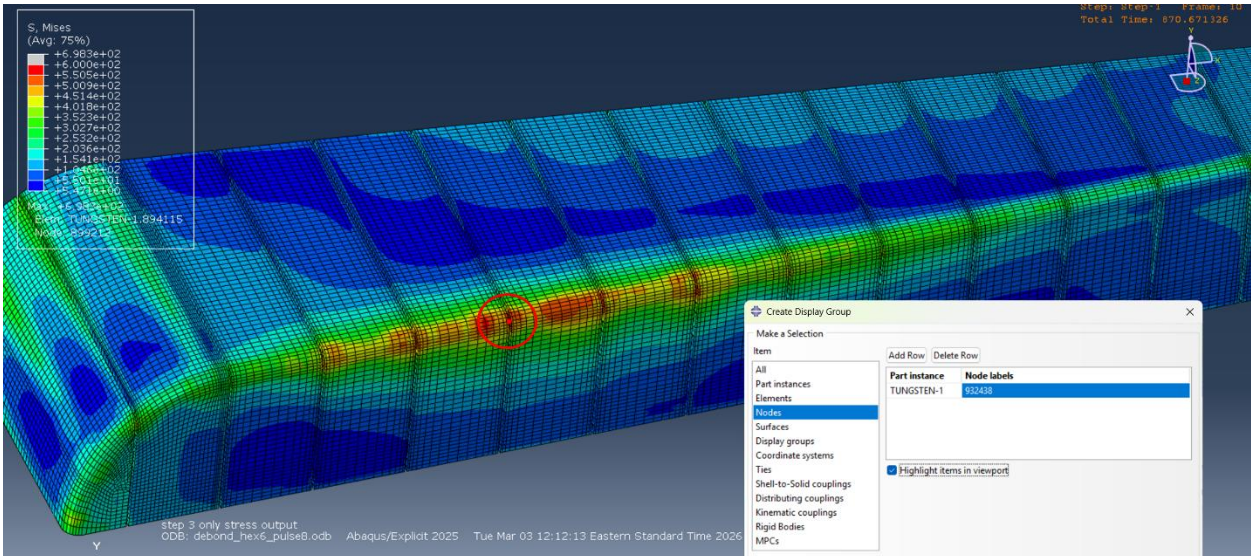

Figure 65 Tungsten node 932438

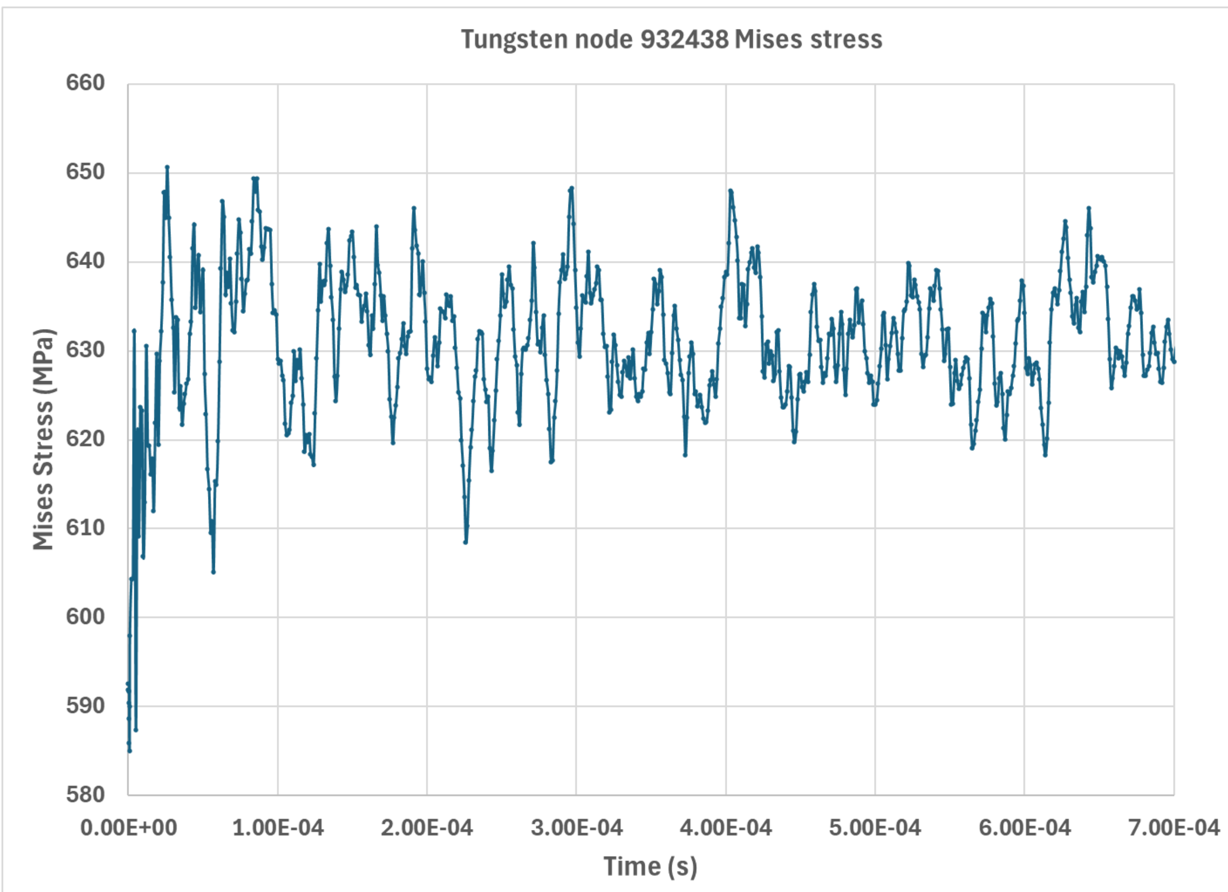

Figure 66 Example of tungsten node transient stress

The contact pressure on the Inconel and tantalum at the end of Step 2 are shown in Figure 67 and Figure 68.

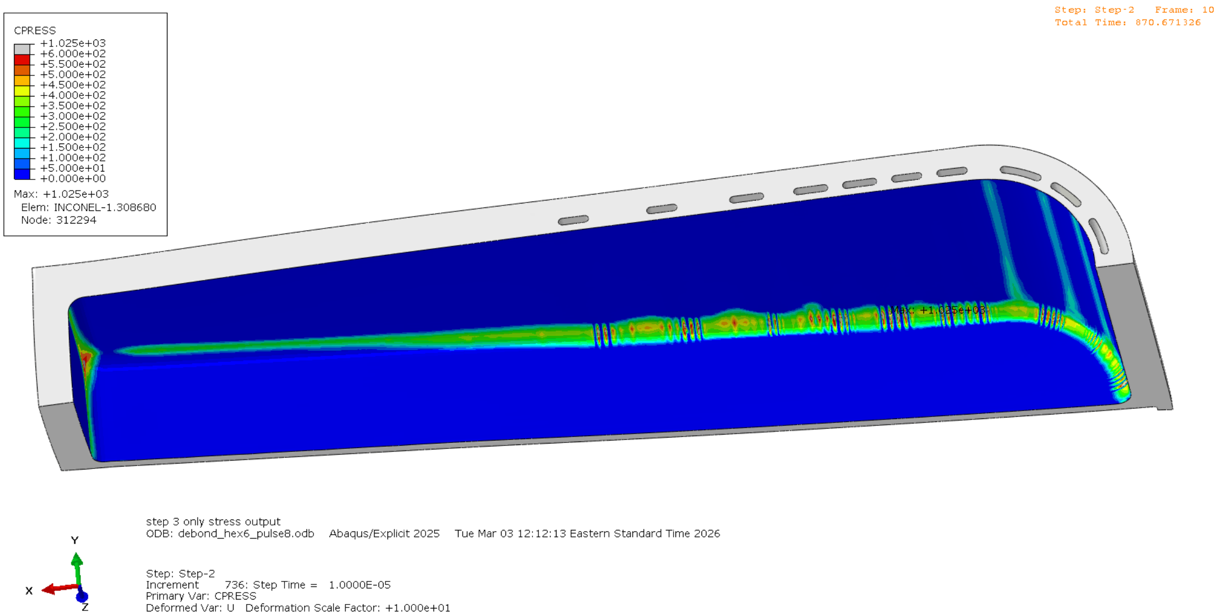

Figure 67 Inconel CPRESS at 11 µs

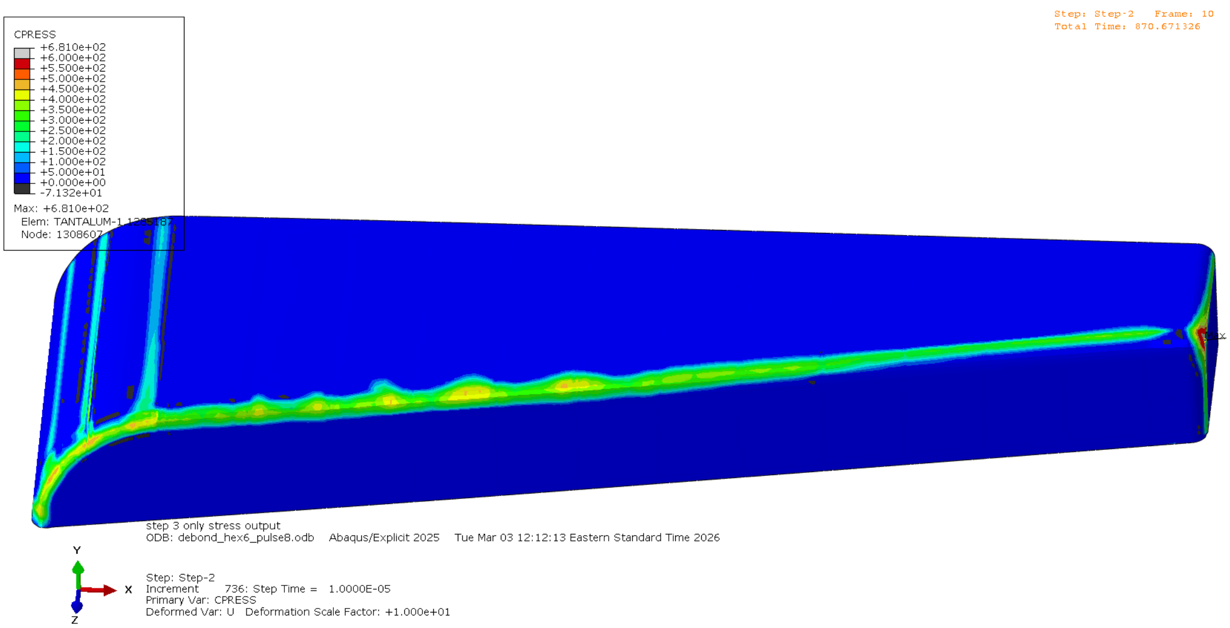

Figure 68 Tantalum CPRESS at 11 µs

The Inconel stress at 11 µs is shown in Figure 69.

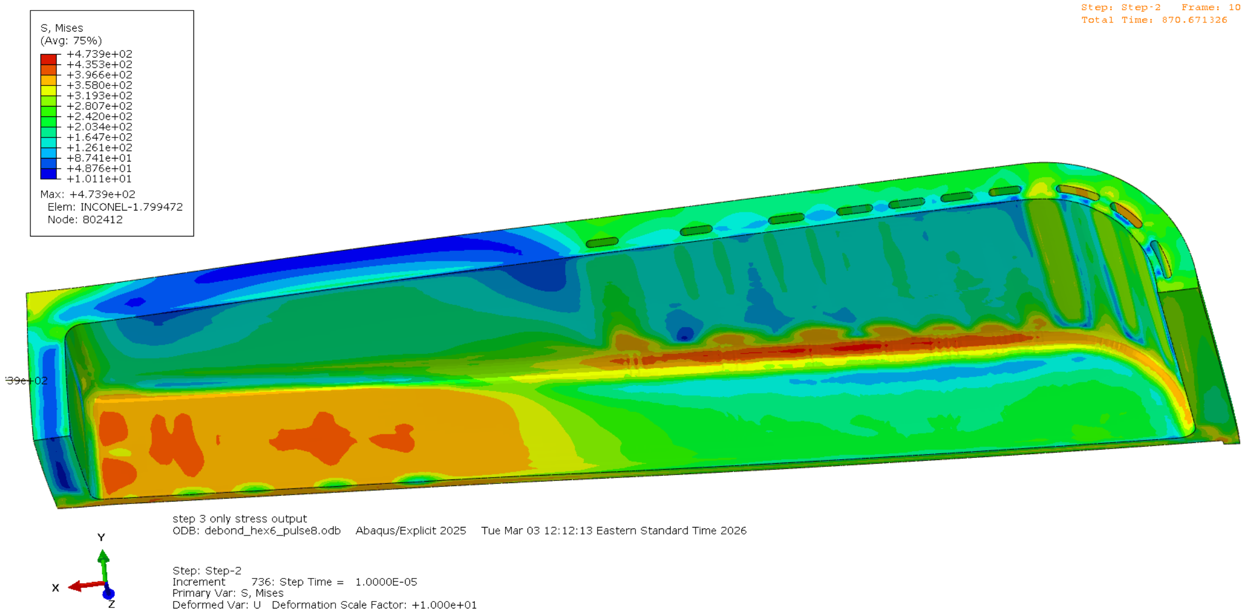

Figure 69 Inconel Stress at 11 μs

As an example, one node was selected on the surface in the corner as shown in Figure 70 and the transient Mises stress plotted in Figure 71.

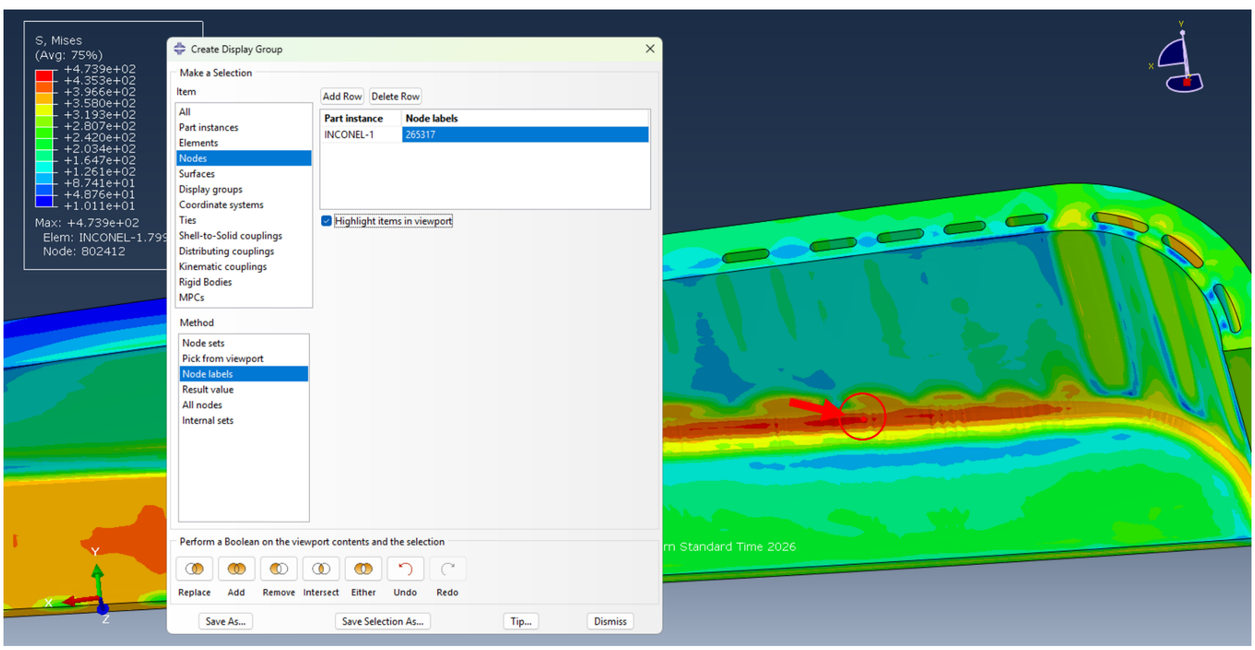

Figure 70 Inconel example node 265317

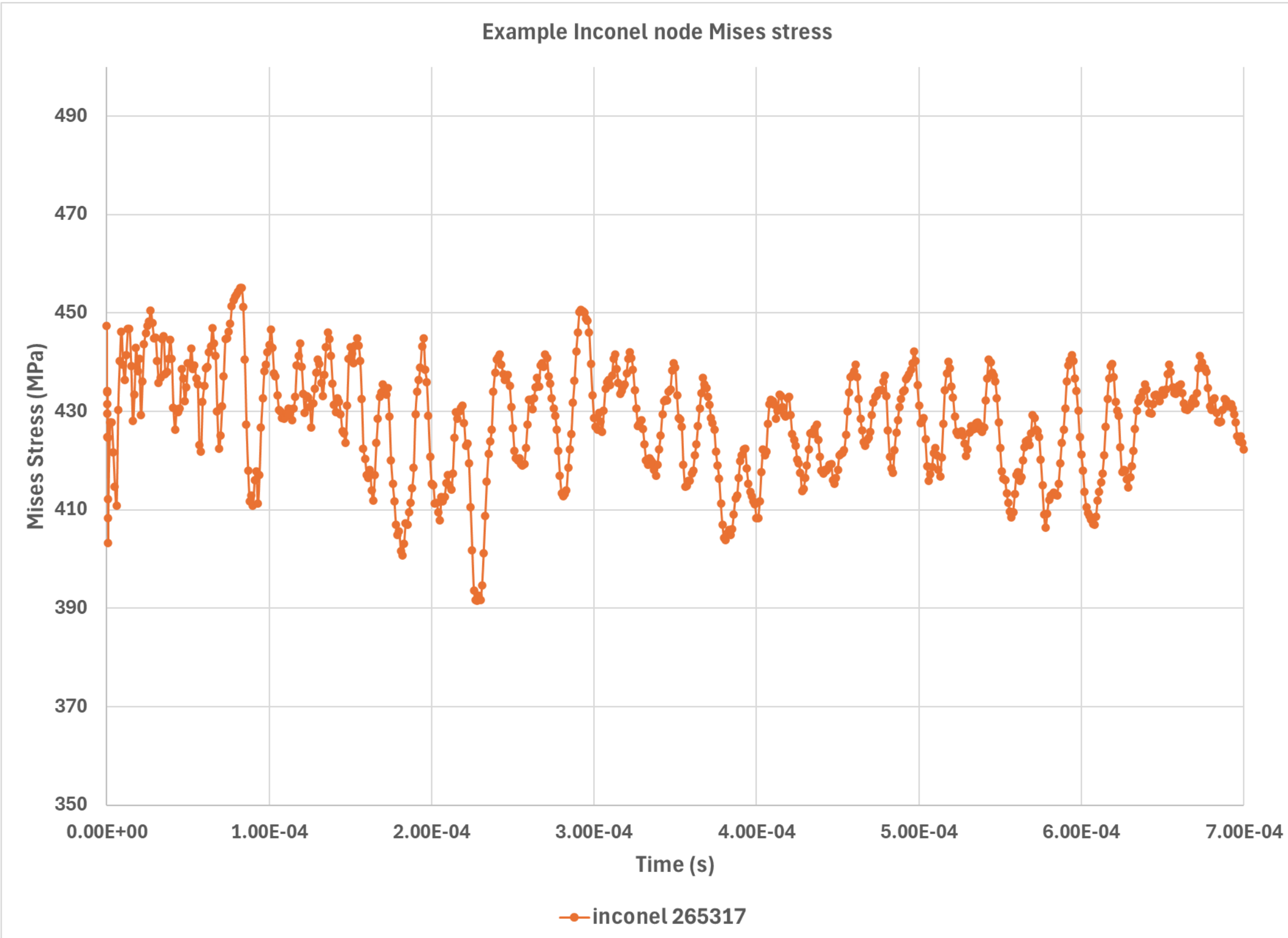

Figure 71 Inconel example node stress

7. FE-SAFE FATIGUE ANALYSIS

The fatigue analysis is driven by the quasi-steady temperature (which controls the mean stress of the beam pulse fatigue) and by the instantaneous pulse temperature rise (which controls the amplitude of the beam pulse).

7.1 GOODMAN DIAGRAMS

Figure 72 summarizes the fatigue analyses on a Goodman diagram for each of the material models (Inconel, tungsten, stainless steel) for a 10-year lifetime of beam pulses. The tungsten fatigue model uses the brittle normal stress failure theory. Fe-safe outputs worst-case mean stress and stress amplitudes for each node in the stress analysis. This data can be plotted directly on the Goodman diagram to visualize the FOS in relation to the design envelope. The Inconel and stainless-steel models use the stress-based Brown-Miller ductile fatigue theory. Fe-safe outputs worst-case mean stress along with the (Kandil) Brown-Miller strain parameter ($\Delta\epsilon_{BM}$) for each node. Before this can be plotted on the Goodman diagram, it must first be converted into an equivalent stress amplitude. Equation 7 shows the full Brown-Miller strain-life equation used by fe-safe [4]. The combined left-hand side ($(\Delta\gamma + \Delta\epsilon_n)/2$) is the (Kandil) Brown-Miller strain parameter ($\Delta\epsilon_{BM}$). The right-hand side combines the low-cycle fatigue life relationship (i.e. plastic deformation) with the high-cycle fatigue life relationship (i.e. elastic deformation). If only high-cycle fatigue is assumed, then the relationship simplifies to Equation 8. This can be re-expressed in Equation 9 to show how the (Kandil) Brown-Miller strain parameter can be converted into an equivalent fully reversing stress amplitude ($\sigma_{a,eq}$) for plotting.

$$\frac{\Delta\gamma}{2} + \frac{\Delta\epsilon_n}{2} = 1.75\epsilon_f'\left(2N_f\right)^c + 1.665\frac{\sigma_f'}{E}\left(2N_f\right)^b \tag{7}$$

$$\Delta\epsilon_{BM} \approx 1.665\frac{\sigma_f'}{E}\left(2N_f\right)^b \tag{8}$$

$$\sigma_{a,eq} = \frac{\Delta\epsilon_{BM} \cdot E}{1.665} \approx \sigma_f'\left(2N_f\right)^b \tag{9}$$

As Figure 72 shows, every FEA node of the Inconel and stainless-steel components has fatigue stresses that are below the 10-year lifetime envelope (i.e. FOS > 1). The tungsten, however, shows several FEA nodes with combinations of mean stress and stress amplitude that exceed the 10-year lifetime fatigue limit (i.e. FOS < 1). Fatigue contour plots can be used to explore this further.

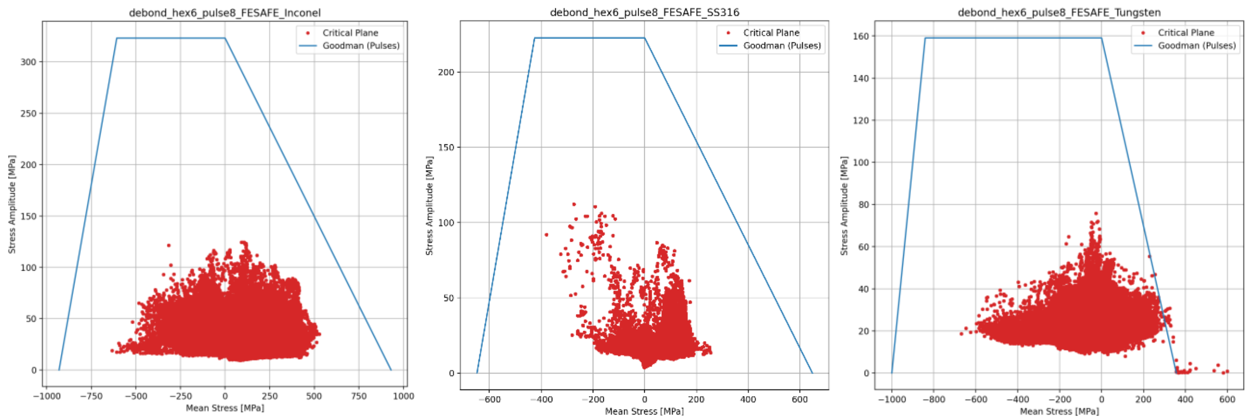

Figure 72: Goodman fatigue diagrams for L-R: Inconel, stainless steel, and tungsten. Each point is a FEA nodal stress with worst-case fatigue stress amplitude and mean stress coordinates.

7.2 FATIGUE CONTOUR PLOTS

Fe-safe also outputs contour plot solution data of the FOS, worst-case mean stress field, worst-case amplitude field, and worst stress at any point in the cycle. It should be noted that fe-safe uses the same "Cycle-Amp" field to represent both stress amplitude (for normal stress fatigue models) and (Kandil) Brown-Miller strain parameter (for ductile Brown-Miller fatigue models).

Figure 73 and Figure 74 show fatigue contour plots for the Inconel flow cover and Inconel shroud. The minimum FOS is 1.4 and is located on the fillet of the flow cover. This corresponds to the region of maximum bending as the flow cover bows outward. Peak fatigue stresses on the shroud are on the side wall region.

Figure 75 shows fatigue contour plots for the stainless-steel heel. The minimum FOS is 1.8 and is located at the interface with the target foot. This region is artificially weak due to the inadvertent omission of the interior flow manifold mesh. Nevertheless, there is sufficient fatigue margin.

Figure 76 shows fatigue contour plots of the tungsten plates. The contact regions with the Inconel cause regions of compressive stress surrounded by regions of tensile “bulging-out” as a result. Figure 78 shows the steady-state stresses in the tungsten with 1500x magnification to illustrate this effect. Figure 77 identifies elements with FOS < 1 that fail the fatigue analysis. These elements appear to be located at the “bulging-out” areas on the edge of the plates. The rearmost elements appear to be a spurious numerical result as was identified in Figure 51. Even if the tungsten were to fail in these regions, the surrounding contact area with the Inconel would continue to apply a compressive stress and would continue to provide a pathway for heat transfer.

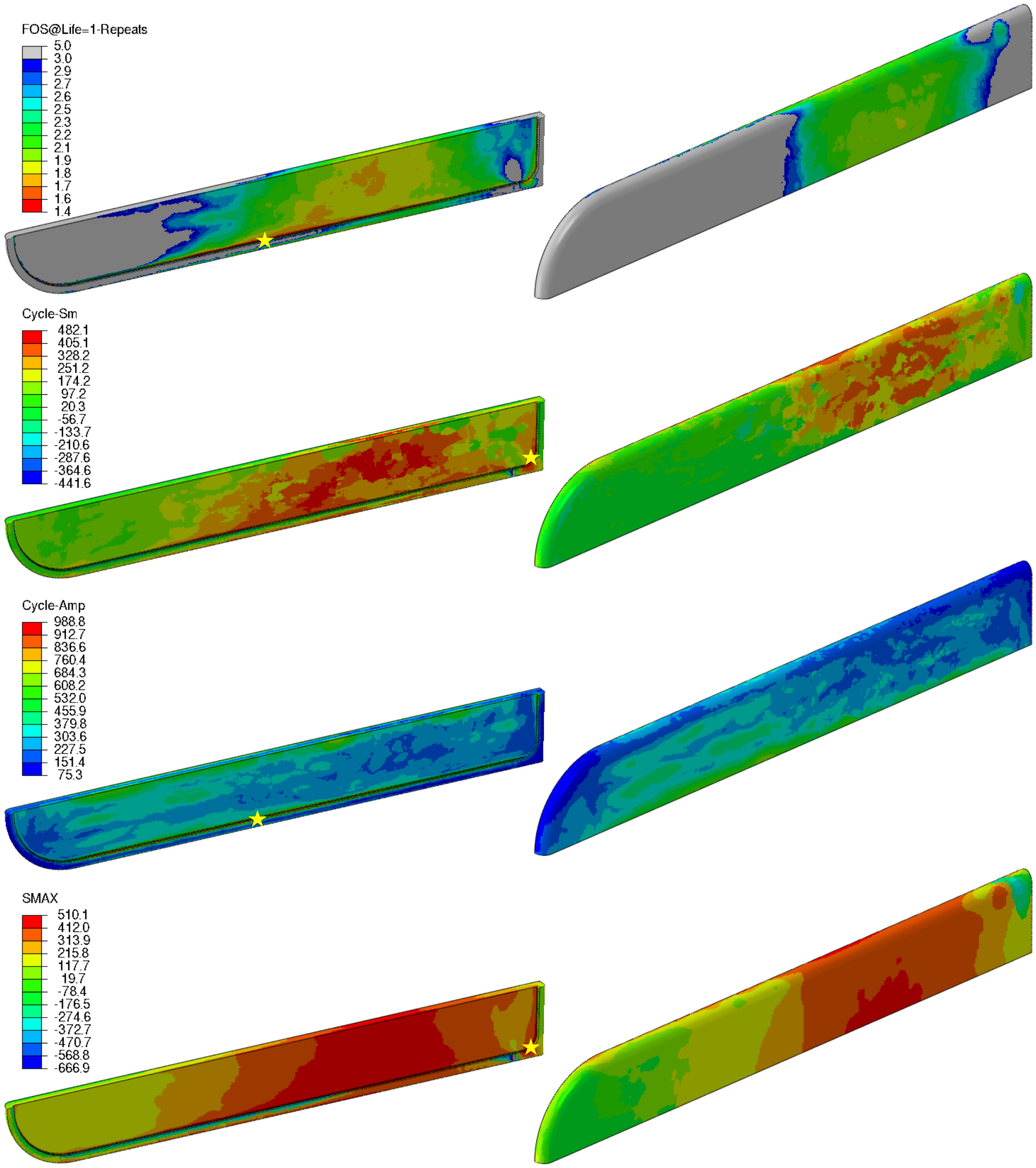

Figure 73: Fatigue contour plots for Inconel flow cover under beam pulses (top to bottom): FOS, worst plane stress amplitude, worst plane mean stress, maximum stress at any timepoint. Location of peak values (minimum for FOS and maximum for stresses) are indicated with a yellow star.

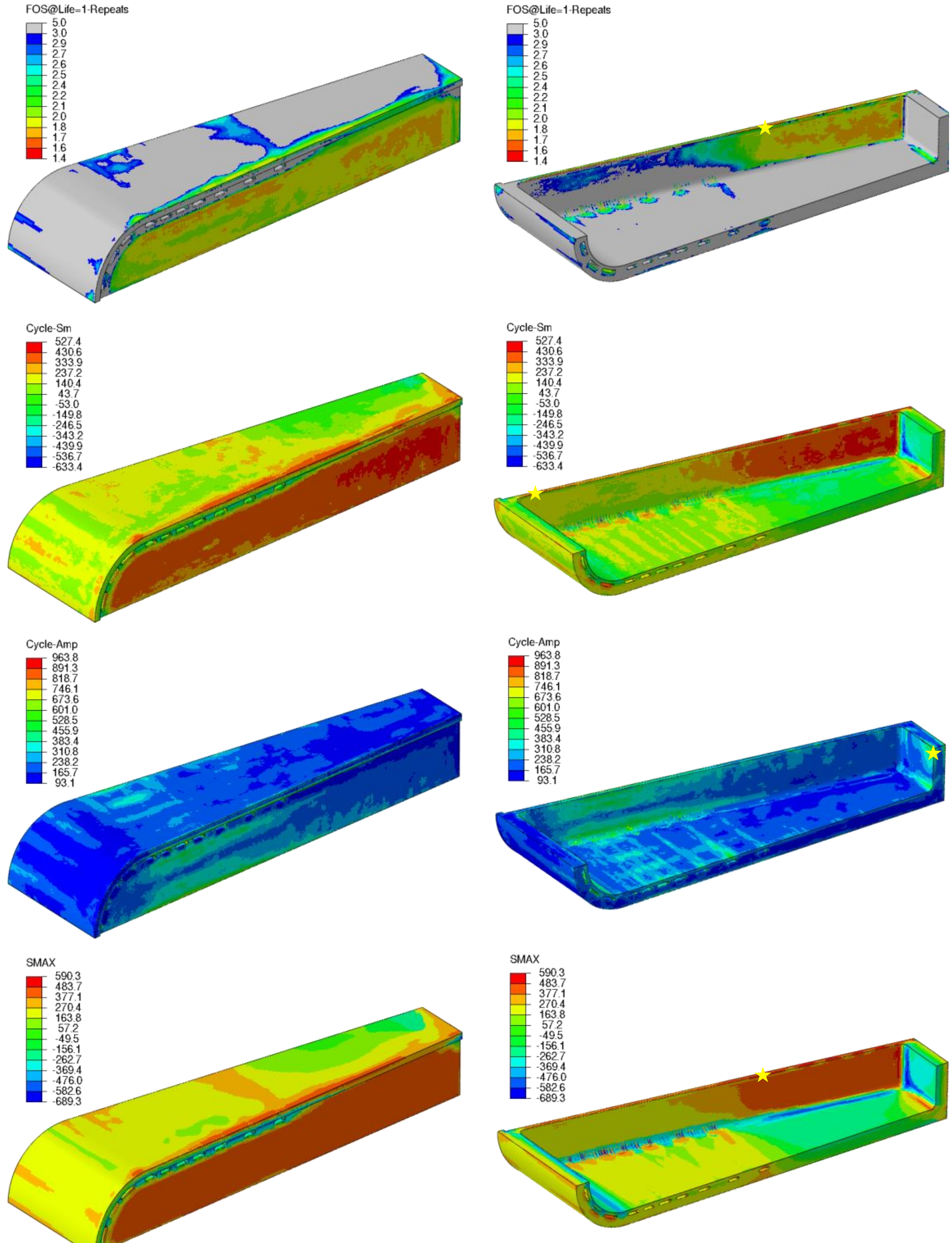

Figure 74: Fatigue contour plots for Inconel shroud under beam pulses (top to bottom): FOS, worst plane stress amplitude, worst plane mean stress, maximum stress at any timepoint. Location of peak values (minimum for FOS and maximum for stresses) are indicated with a yellow star.

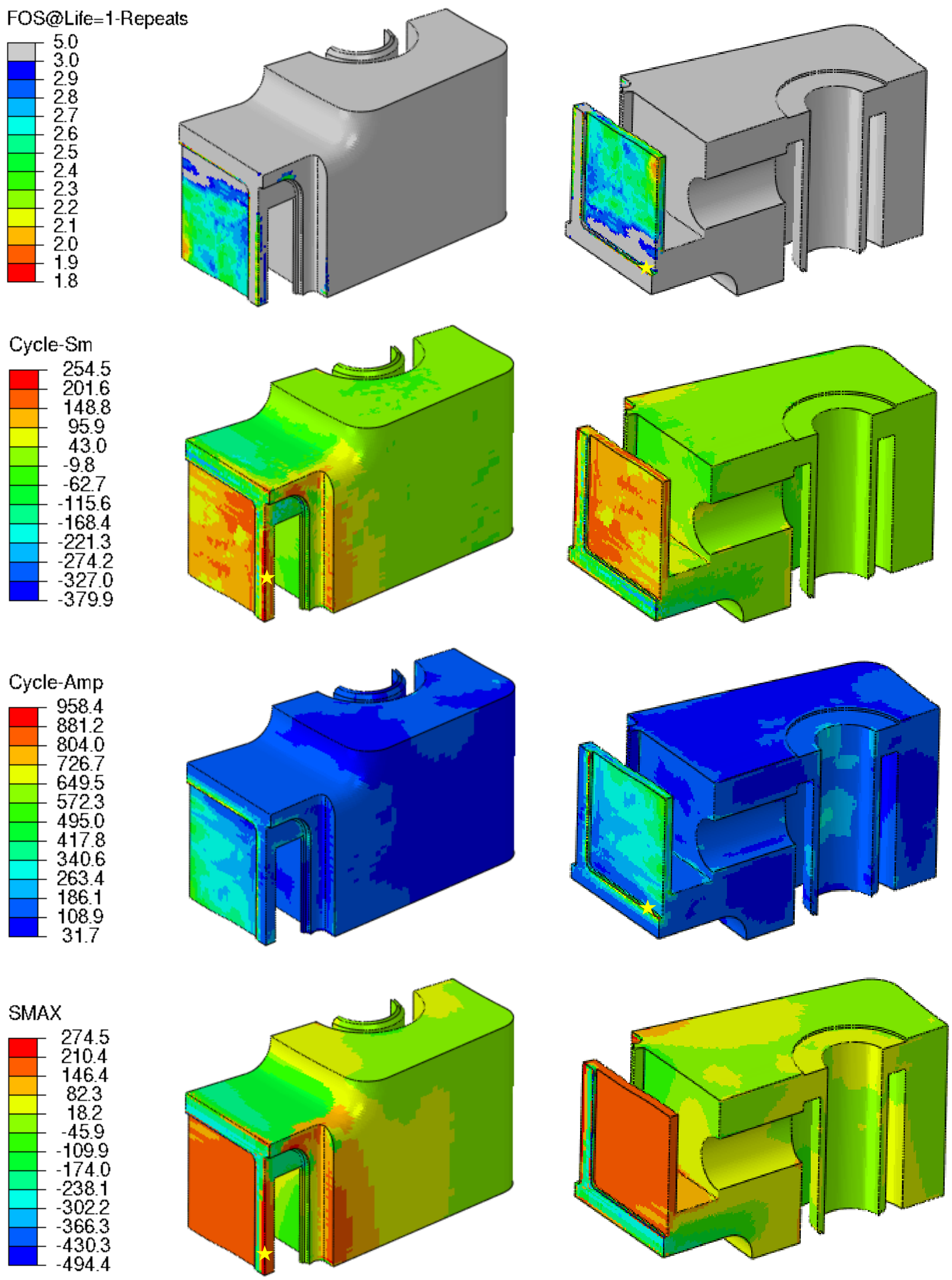

.

Figure 75: Fatigue contour plots for stainless steel heel under beam pulses (top to bottom): FOS, worst plane stress amplitude, worst plane mean stress, maximum stress at any timepoint. Location of peak values (minimum for FOS and maximum for stresses) are indicated with a yellow star.

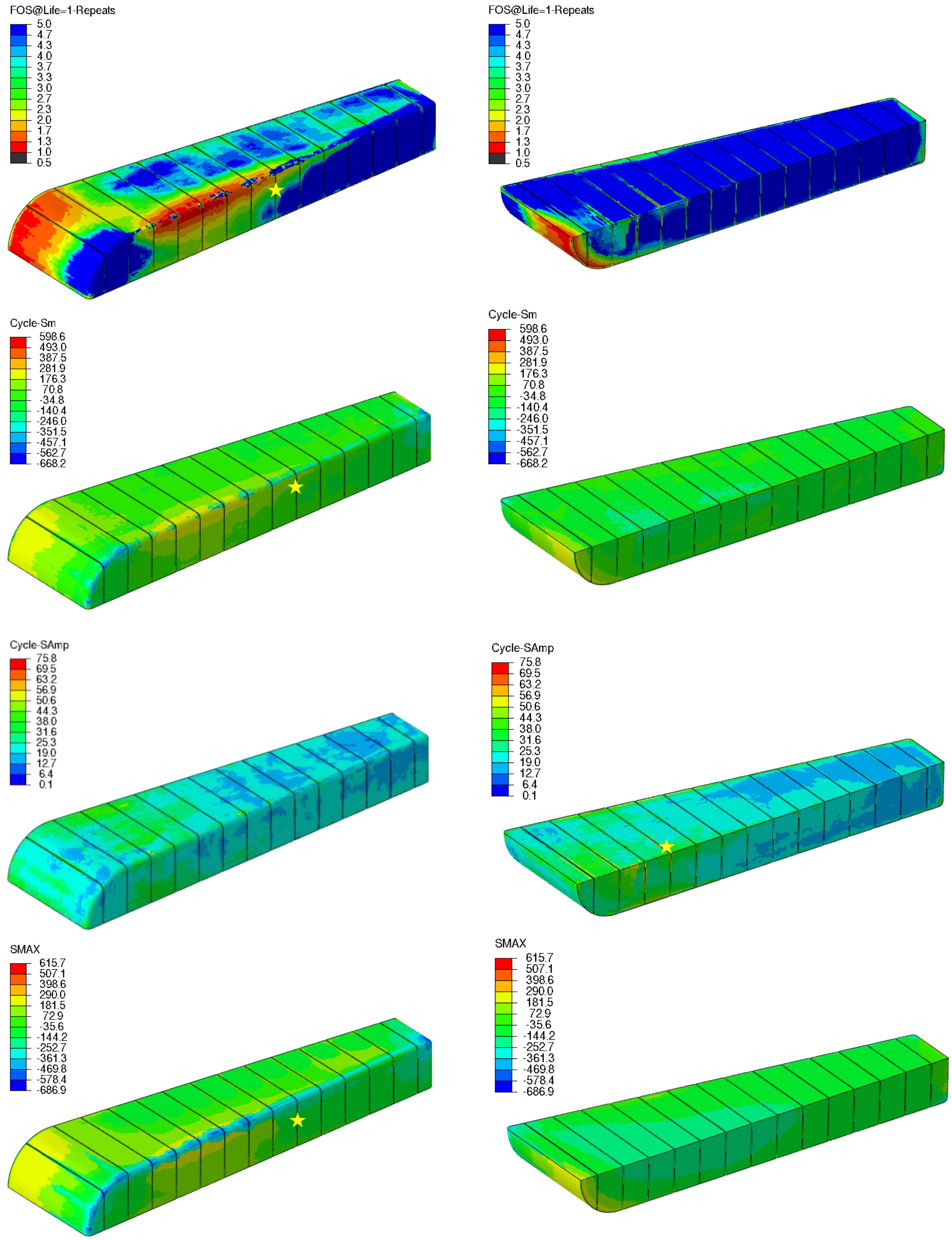

Figure 76: Fatigue contour plots for tungsten plates under beam pulses (top to bottom): FOS, worst plane stress amplitude, worst plane mean stress, maximum stress at any timepoint. Location of peak values (minimum for FOS and maximum for stresses) are indicated with a yellow star.

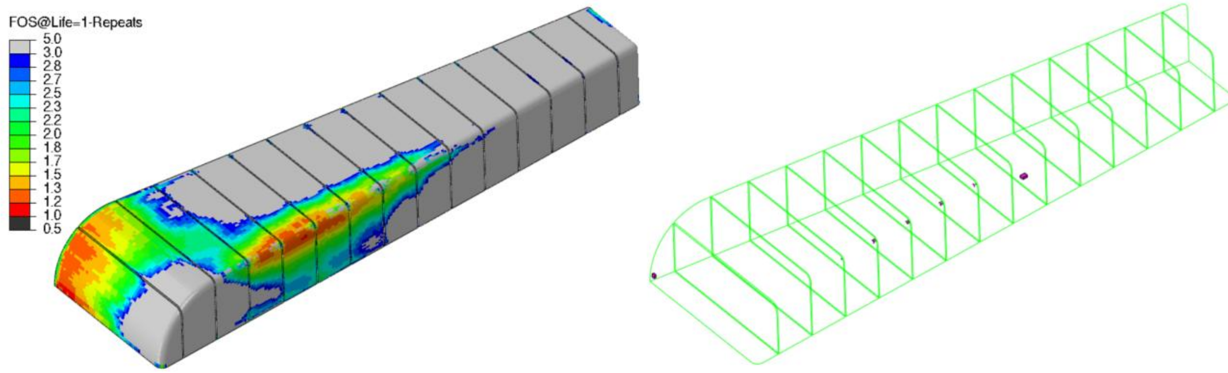

Figure 77: Locations of elements with FOS < 1 on tungsten plates.

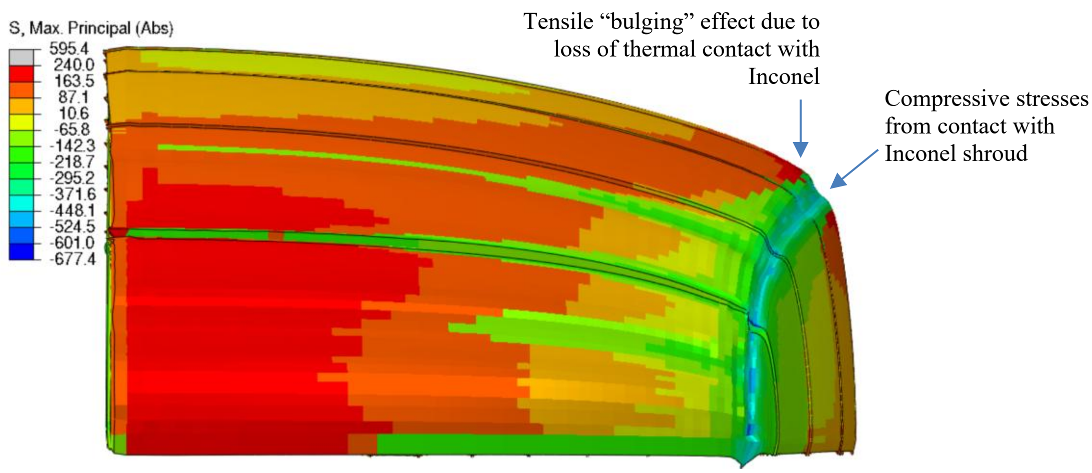

Figure 78: Steady-state stresses in tungsten plates with 1500x magnification to show tensile bulging outside the corner edge contact region.

7.3 COMPARISON AGAINST NORMAL OPERATION

The "Target Segment Thermostructural Analysis" DAC [2] analyzes the lower target segment against normal beam fatigue in the as-designed bonded configuration. The HIP manufacturing steps are simulated as well as the final machining of cooling passages to ascertain the residual stresses in the fully-bonded target. These stresses are then used as initial conditions for a 10-year operation fatigue analysis under normal beam conditions. Figure 79 overlays the Goodman diagrams for comparisons against the analyses in this DAC.

For the Inconel shroud and flow cover, the debonded scenario appears to reduce the fatigue stress amplitude and increase the mean stress. Since the tungsten absorbs most of the proton beam pulse, it stands to reason that the Inconel could experience less fatigue amplitude as the interface with the tungsten is debonded. The increase in mean stress is most likely due to the Inconel now having to constrain the hotter tungsten over a reduced contact surface area.

The fatigue comparison for the stainless-steel shows little difference in terms of stress amplitude range and mean stress range. This makes sense as the heel is not part of the Inconel-to-tantalum bond change. (The nodes with highest stress amplitude in the bonded fatigue analysis were identified in that DAC as numerical effects at the pin/slot contact point, and this feature was not included in the present analysis.)

Finally, the tungsten experiences roughly the same fatigue stress amplitudes while the mean stress shifts significantly higher (around 100 MPa) in the debonded configuration. It is seen that the residual stresses from HIP manufacturing serve to place a largely compressive residual stress on the tungsten as the Inconel shroud has a higher CTE and shrinks around the W/Ta laminate. In the present analysis, residual stresses are assumed to be fully relaxed due to radiation effects and the Inconel/Ta contact surfaces are debonded. This explains the increase in tungsten mean stresses.

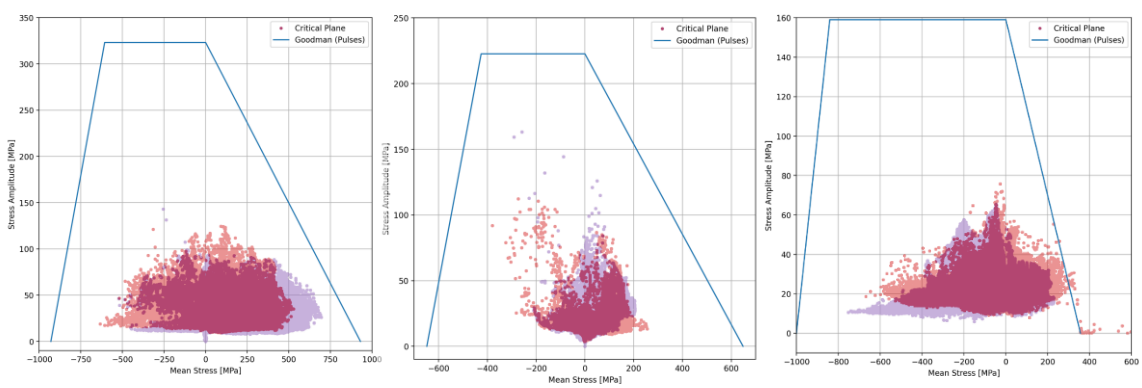

Figure 79: Goodman fatigue diagrams for L-R: Inconel, stainless steel, and tungsten. Results are overlayed against another analysis [2] that was performed for the as-designed target segment including a complete Inconel/Ta bond with manufacturing residual stresses. The present debonded analysis is presented in red while the as-designed analysis is presented in purple.

8. CONCLUSIONS

- The steady state analysis assuming no bonding between tantalum and Inconel showed a peak temperature of 664 °C in tungsten which is below the threshold of tungsten vaporization in steam.

- Fatigue analysis for the structural materials of Inconel and SS316L showed a Factor of Safety greater than 1 for a 10 year lifetime of pulse beam operation.

- Tungsten fatigue analysis showed a Factor of Safety below 1 for a 10 year lifetime of pulse beam operation. Several elements fail in contact regions where the high compression of contact creates surrounding tensile “bulges”. The tungsten is not a structural material, however, and should continue to remain in compression at the regions of heat transfer contact.

- The analysis used a frictionless surface-to-surface contact between tantalum and Inconel which allowed separation with an assumed thermal conductance that was a function of the contact pressure.

- The assumed contact conductance was based on a functional relation from literature as described in Appendix A and compared with literature references for nickel on nickel as a function of pressure. No experimental conductance data for tantalum on Inconel or for broken HIP bonds between Inconel and tantalum was available. The model used for this analysis should be considered as a first order of magnitude estimate.

- The deformed shape of the Inconel resulted in very limited contact areas for heat removal from the tungsten and is considered to likely have resulted in a conservative maximum temperature.

- Analyses show the target segment should be able to operate even if the tantalum-to-Inconel surfaces debond.

9. REFERENCES

[1] Windchill Doc. No. S03020000-DAC10000-A.5, "Target Systems Analysis - Material Model Definitions," ORNL STS Second Target Station, February 2026. [Online]. Available: https://windchill-prod.ornl.gov:8443/Windchill/app/#ptc1/tcomp/infoPage?ContainerOid=OR:wt.pdmlink.PDMLinkProduct:1228746141&oid=VR:wt.doc.WTDocument:844237287&u8=1.

[2] Windchill Doc. No. S03020400-DAC10000-A.19, "Target Segment Thermostructural Analysis," ORNL STS Second Target Station, [Online]. Available: https://windchill-prod.ornl.gov:8443/Windchill/app/#ptc1/tcomp/infoPage?ContainerOid=OR%3Awt.pdmlink.PDMLinkProduct%3A1228746141&oid=VR%3Awt.doc.WTDocument%3A455757856&u8=1.

[3] "fe-safe 2025 fe-safe User Guide," Dassault Systemes Americas Corp., Vol. 1, Issue 25.2, 2024.

[4] "fe-safe 2025 Fatigue Theory Reference," Dassault Systemes Americas Corp., Vol. 2, Issue 1, 2024.

[5] Windchill Doc. No. S00000000-CAC10001-A.6, "Neutronics Energy Deposition and DPA Data," ORNL STS Second Target Station, January 2026. [Online]. Available: https://windchill-prod.ornl.gov:8443/Windchill/app/#ptc1/tcomp/infoPage?ContainerOid=OR:wt.pdmlink.PDMLinkProduct:1228746141&oid=VR:wt.doc.WTDocument:810253597&u8=1.

[6] Windchill Doc. No. S03020000-DAC10003-A.7, "Target Assembly Thermo-Fluid Analysis," ORNL STS Second Target Station, January 2026. [Online]. Available: https://windchill-prod.ornl.gov:8443/Windchill/app/#ptc1/tcomp/infoPage?ContainerOid=OR:wt.pdmlink.PDMLinkProduct:1228746141&oid=VR:wt.doc.WTDocument:850350792&u8=1.

[7] Windchill Doc. No. S03020400-SRD10000-A.8, "Requirements, Target Segment," ORNL STS Second Target Station, February 2026. [Online]. Available: https://windchill-prod.ornl.gov:8443/Windchill/app/#ptc1/tcomp/infoPage?ContainerOid=OR%3Awt.pdmlink.PDMLinkProduct%3A1228746141&oid=VR%3Awt.doc.WTDocument%3A714656499&u8=1.

[8] C. Barbier, K. Johns and J. Mach, "Structural Design Criteria for Mercury Target Module," Design Criteria Document, Spallation Neutron Source, Oak Ridge National Laboratory, 106010101-DC0001-R03, 2020.

[9] A. Tariq and M. Asif, "Experimental Investigation of Thermal Conductance for Nominally Flat Metallic Contact," *Heat and Mass Transfer,* vol. 52, pp. 291-307, 2016.

[10] R. Dou, T. Ge, X. Liu and Z. Wen, "Effects of contact pressure, interface temperature, and surface roughness on thermal contact conductance between stainless steel surfaces under atmosphere condition," *International Journal of Heat and Mass Transfer,* vol. 94, pp. 156-163, 2016.

[11] "Thermal Contact Conductance Metal Surfaces Air," Engineers Edge, LLC, [Online]. Available: https://www.engineersedge.com/heat_transfer/thermal_contact_conductance_13849.htm. [Accessed 27 March 2026].

APPENDIX A. MATERIAL PROPERTIES

A consistent set of units needs to be used with the Abaqus model defined in mm. The table below shows the units for SI in m and SI in mm

Parameter	**SI (mm)**	**SI**
Length	mm	m
Mass	tonne	kg
Temperature	°C	°C
Area	mm^2	m^2
Volume	mm^3	m^3
Density	tonne/mm^3	kg/m^3
Force	N	N
Pressure	MPa	Pa
Velocity	mm/s	m/2
Acceleration	mm/sec^2	m/sec^2
Moment	N-mm	N-m
Stress	MPa	Pa
Young's Modulus	MPa	Pa
Energy	mJ	J
Power	mW	W
Thermal Expansion	/°C	/°C
Thermal Conductivity	mW/mm °C	W/m °C
Specific Heat	mJ/tonne °C	J/kg °C
Heat Flux	mW/mm^2	W/m^2

The material properties used are given below using the consistent units for SI in mm.

*Material, name=Inconel

```
*Conductivity
12.,
*Density
 8.19e-09,
*Elastic
210000., 0.3
*Expansion, zero=20.
 1.41e-05, 25.
 1.41e-05,100.
 1.43e-05,200.
 1.45e-05,300.
 1.48e-05,400.
 1.52e-05,500.
*Plastic
 400.,         0.,        20.
 407.,      0.001,        20.
 409., 0.00143845,        20.
 414., 0.00206914,        20.
 419., 0.00297635,        20.
 428., 0.00428133,        20.
 440., 0.00615848,        20.
 457., 0.00885867,        20.
 481.,  0.0127428,        20.
 514.,  0.0183298,        20.
 561.,  0.0263665,        20.
 626.,  0.0379269,        20.
 713.,  0.0545559,        20.
 827.,   0.078476,        20.
 969.,   0.112884,        20.
1140.,   0.162378,        20.
1320.,   0.233572,        20.
1500.,   0.335982,        20.
1640.,   0.483293,        20.
1730.,   0.695193,        20.
1770.,         1.,        20.
 341.,         0.,       200.
 347.,      0.001,       200.
 350., 0.00143845,       200.
 354., 0.00206914,       200.
 360., 0.00297635,       200.
 368., 0.00428133,       200.
 380., 0.00615848,       200.
 397., 0.00885867,       200.
 421.,  0.0127428,       200.
 454.,  0.0183298,       200.
 501.,  0.0263665,       200.
 565.,  0.0379269,       200.
 650.,  0.0545559,       200.
 760.,   0.078476,       200.
 898.,   0.112884,       200.
1060.,   0.162378,       200.
1230.,   0.233572,       200.
1380.,   0.335982,       200.
1500.,   0.483293,       200.
1570.,   0.695193,       200.
1600.,         1.,       200.
 283.,         0.,       400.
 289.,      0.001,       400.
 292., 0.00143845,       400.
```

```
 296., 0.00206914,       400.
 302., 0.00297635,       400.
 310., 0.00428133,       400.
 322., 0.00615848,       400.
 339., 0.00885867,       400.
 363.,  0.0127428,       400.
 396.,  0.0183298,       400.
 442.,  0.0263665,       400.
 504.,  0.0379269,       400.
 587.,  0.0545559,       400.
 694.,   0.078476,       400.
 823.,   0.112884,       400.
 970.,   0.162378,       400.
1120.,   0.233572,       400.
1250.,   0.335982,       400.
1350.,   0.483293,       400.
1400.,   0.695193,       400.
1420.,         1.,       400.
 234.,         0.,       600.
 241.,      0.001,       600.
 244., 0.00143845,       600.
 248., 0.00206914,       600.
 254., 0.00297635,       600.
 262., 0.00428133,       600.
 274., 0.00615848,       600.
 290., 0.00885867,       600.
 314.,  0.0127428,       600.
 347.,  0.0183298,       600.
 392.,  0.0263665,       600.
 453.,  0.0379269,       600.
 533.,  0.0545559,       600.
 634.,   0.078476,       600.
 754.,   0.112884,       600.
 886.,   0.162378,       600.
1010.,   0.233572,       600.
1120.,   0.335982,       600.
1190.,   0.483293,       600.
1220.,   0.695193,       600.
1230.,         1.,       600.
*Specific Heat
 4.35e+08,
```

*Material, name=SS316L

```
*Conductivity
 16.2,
*Density
 8.03e-09,
*Elastic
195000., 0.31
*Expansion, zero=20.
 1.53e-05, 20.
 1.54e-05, 25.
  1.6e-05, 50.
 1.65e-05, 75.
  1.7e-05,100.
 1.74e-05,125.
 1.78e-05,150.
 1.81e-05,175.
 1.84e-05,200.
 1.86e-05,225.
```

```
 1.88e-05,250.
 1.89e-05,275.
 1.91e-05,300.
 1.92e-05,325.
 1.93e-05,350.
 1.94e-05,375.
 1.95e-05,400.
 1.96e-05,425.
 1.98e-05,450.
    2e-05,475.
 2.02e-05,500.
*Plastic
 172.,         0.,         40.
 174.,      0.001,         40.
 175., 0.00143845,         40.
 176., 0.00206914,         40.
 178., 0.00297635,         40.
 180., 0.00428133,         40.
 184., 0.00615848,         40.
 189., 0.00885867,         40.
 196.,  0.0127428,         40.
 206.,  0.0183298,         40.
 221.,  0.0263665,         40.
 243.,  0.0379269,         40.
 274.,  0.0545559,         40.
 319.,   0.078476,         40.
 383.,   0.112884,         40.
 476.,   0.162378,         40.
 609.,   0.233572,         40.
 801.,   0.335982,         40.
1080.,   0.483293,         40.
1470.,   0.695193,         40.
2050.,         1.,         40.
 157.,         0.,         65.
 159.,      0.001,         65.
 160., 0.00143845,         65.
 161., 0.00206914,         65.
 163., 0.00297635,         65.
 165., 0.00428133,         65.
 169., 0.00615848,         65.
 174., 0.00885867,         65.
 181.,  0.0127428,         65.
 191.,  0.0183298,         65.
 206.,  0.0263665,         65.
 228.,  0.0379269,         65.
 259.,  0.0545559,         65.
 304.,   0.078476,         65.
 368.,   0.112884,         65.
 461.,   0.162378,         65.
 594.,   0.233572,         65.
 786.,   0.335982,         65.
1060.,   0.483293,         65.
1460.,   0.695193,         65.
2030.,         1.,         65.
 145.,         0.,        100.
 147.,      0.001,        100.
 148., 0.00143845,        100.
 149., 0.00206914,        100.
 151., 0.00297635,        100.
 153., 0.00428133,        100.
 157., 0.00615848,        100.
 162., 0.00885867,        100.
```

```
 169.,  0.0127428,       100.
 179.,  0.0183298,       100.
 194.,  0.0263665,       100.
 216.,  0.0379269,       100.
 247.,  0.0545559,       100.
 292.,   0.078476,       100.
 356.,   0.112884,       100.
 449.,   0.162378,       100.
 582.,   0.233572,       100.
 774.,   0.335982,       100.
1050.,   0.483293,       100.
1450.,   0.695193,       100.
2020.,         1.,       100.
 137.,         0.,       125.
 139.,      0.001,       125.
 140., 0.00143845,       125.
 141., 0.00206914,       125.
 143., 0.00297635,       125.
 145., 0.00428133,       125.
 149., 0.00615848,       125.
 154., 0.00885867,       125.
 161.,  0.0127428,       125.
 171.,  0.0183298,       125.
 186.,  0.0263665,       125.
 208.,  0.0379269,       125.
 239.,  0.0545559,       125.
 284.,   0.078476,       125.
 348.,   0.112884,       125.
 441.,   0.162378,       125.
 574.,   0.233572,       125.
 766.,   0.335982,       125.
1040.,   0.483293,       125.
1440.,   0.695193,       125.
2010.,         1.,       125.
 131.,         0.,       150.
 133.,      0.001,       150.
 134., 0.00143845,       150.
 135., 0.00206914,       150.
 137., 0.00297635,       150.
 139., 0.00428133,       150.
 143., 0.00615848,       150.
 148., 0.00885867,       150.
 155.,  0.0127428,       150.
 165.,  0.0183298,       150.
 180.,  0.0263665,       150.
 202.,  0.0379269,       150.
 233.,  0.0545559,       150.
 278.,   0.078476,       150.
 342.,   0.112884,       150.
 435.,   0.162378,       150.
 568.,   0.233572,       150.
 760.,   0.335982,       150.
1040.,   0.483293,       150.
1430.,   0.695193,       150.
2000.,         1.,       150.
 125.,         0.,       175.
 127.,      0.001,       175.
 128., 0.00143845,       175.
 129., 0.00206914,       175.
 131., 0.00297635,       175.
 133., 0.00428133,       175.
 137., 0.00615848,       175.
```

```
 142., 0.00885867,       175.
 149.,  0.0127428,       175.
 159.,  0.0183298,       175.
 174.,  0.0263665,       175.
 196.,  0.0379269,       175.
 227.,  0.0545559,       175.
 272.,   0.078476,       175.
 336.,   0.112884,       175.
 429.,   0.162378,       175.
 562.,   0.233572,       175.
 754.,   0.335982,       175.
1030.,   0.483293,       175.
1430.,   0.695193,       175.
2000.,         1.,       175.
 121.,         0.,       200.
 123.,      0.001,       200.
 124., 0.00143845,       200.
 125., 0.00206914,       200.
 127., 0.00297635,       200.
 129., 0.00428133,       200.
 133., 0.00615848,       200.
 138., 0.00885867,       200.
 145.,  0.0127428,       200.
 155.,  0.0183298,       200.
 170.,  0.0263665,       200.
 192.,  0.0379269,       200.
 223.,  0.0545559,       200.
 268.,   0.078476,       200.
 332.,   0.112884,       200.
 425.,   0.162378,       200.
 558.,   0.233572,       200.
 750.,   0.335982,       200.
1030.,   0.483293,       200.
1420.,   0.695193,       200.
1990.,         1.,       200.
 118.,         0.,       225.
 120.,      0.001,       225.
 121., 0.00143845,       225.
 122., 0.00206914,       225.
 124., 0.00297635,       225.
 126., 0.00428133,       225.
 130., 0.00615848,       225.
 135., 0.00885867,       225.
 142.,  0.0127428,       225.
 152.,  0.0183298,       225.
 167.,  0.0263665,       225.
 189.,  0.0379269,       225.
 220.,  0.0545559,       225.
 265.,   0.078476,       225.
 329.,   0.112884,       225.
 422.,   0.162378,       225.
 555.,   0.233572,       225.
 747.,   0.335982,       225.
1020.,   0.483293,       225.
1420.,   0.695193,       225.
1990.,         1.,       225.
 114.,         0.,       250.
 116.,      0.001,       250.
 117., 0.00143845,       250.
 118., 0.00206914,       250.
 120., 0.00297635,       250.
 122., 0.00428133,       250.
```

126.,	0.00615848,	250.
131.,	0.00885867,	250.
138.,	0.0127428,	250.
148.,	0.0183298,	250.
163.,	0.0263665,	250.
185.,	0.0379269,	250.
216.,	0.0545559,	250.
261.,	0.078476,	250.
325.,	0.112884,	250.
418.,	0.162378,	250.
551.,	0.233572,	250.
743.,	0.335982,	250.
1020.,	0.483293,	250.
1420.,	0.695193,	250.
1990.,	1.,	250.
111.,	0.,	275.
113.,	0.001,	275.
114.,	0.00143845,	275.
115.,	0.00206914,	275.
117.,	0.00297635,	275.
119.,	0.00428133,	275.
123.,	0.00615848,	275.
128.,	0.00885867,	275.
135.,	0.0127428,	275.
145.,	0.0183298,	275.
160.,	0.0263665,	275.
182.,	0.0379269,	275.
213.,	0.0545559,	275.
258.,	0.078476,	275.
322.,	0.112884,	275.
415.,	0.162378,	275.
548.,	0.233572,	275.
740.,	0.335982,	275.
1020.,	0.483293,	275.
1410.,	0.695193,	275.
1980.,	1.,	275.
109.,	0.,	300.
111.,	0.001,	300.
112.,	0.00143845,	300.
113.,	0.00206914,	300.
115.,	0.00297635,	300.
117.,	0.00428133,	300.
121.,	0.00615848,	300.
126.,	0.00885867,	300.
133.,	0.0127428,	300.
143.,	0.0183298,	300.
158.,	0.0263665,	300.
180.,	0.0379269,	300.
211.,	0.0545559,	300.
256.,	0.078476,	300.
320.,	0.112884,	300.
413.,	0.162378,	300.
546.,	0.233572,	300.
738.,	0.335982,	300.
1010.,	0.483293,	300.
1410.,	0.695193,	300.
1980.,	1.,	300.
107.,	0.,	325.
109.,	0.001,	325.
110.,	0.00143845,	325.
111.,	0.00206914,	325.
113.,	0.00297635,	325.

```
 115., 0.00428133,       325.
 119., 0.00615848,       325.
 124., 0.00885867,       325.
 131.,  0.0127428,       325.
 141.,  0.0183298,       325.
 156.,  0.0263665,       325.
 178.,  0.0379269,       325.
 209.,  0.0545559,       325.
 254.,   0.078476,       325.
 318.,   0.112884,       325.
 411.,   0.162378,       325.
 544.,   0.233572,       325.
 736.,   0.335982,       325.
1010.,   0.483293,       325.
1410.,   0.695193,       325.
1980.,         1.,       325.
 105.,         0.,       350.
 107.,      0.001,       350.
 108., 0.00143845,       350.
 109., 0.00206914,       350.
 111., 0.00297635,       350.
 113., 0.00428133,       350.
 117., 0.00615848,       350.
 122., 0.00885867,       350.
 129.,  0.0127428,       350.
 139.,  0.0183298,       350.
 154.,  0.0263665,       350.
 176.,  0.0379269,       350.
 207.,  0.0545559,       350.
 252.,   0.078476,       350.
 316.,   0.112884,       350.
 409.,   0.162378,       350.
 542.,   0.233572,       350.
 734.,   0.335982,       350.
1010.,   0.483293,       350.
1410.,   0.695193,       350.
1980.,         1.,       350.
 103.,         0.,       375.
 105.,      0.001,       375.
 106., 0.00143845,       375.
 107., 0.00206914,       375.
 109., 0.00297635,       375.
 111., 0.00428133,       375.
 115., 0.00615848,       375.
 120., 0.00885867,       375.
 127.,  0.0127428,       375.
 137.,  0.0183298,       375.
 152.,  0.0263665,       375.
 174.,  0.0379269,       375.
 205.,  0.0545559,       375.
 250.,   0.078476,       375.
 314.,   0.112884,       375.
 407.,   0.162378,       375.
 540.,   0.233572,       375.
 732.,   0.335982,       375.
1010.,   0.483293,       375.
1410.,   0.695193,       375.
1980.,         1.,       375.
 101.,         0.,       400.
 103.,      0.001,       400.
 104., 0.00143845,       400.
 105., 0.00206914,       400.
```

```
 107., 0.00297635,       400.
 109., 0.00428133,       400.
 113., 0.00615848,       400.
 118., 0.00885867,       400.
 125.,  0.0127428,       400.
 135.,  0.0183298,       400.
 150.,  0.0263665,       400.
 172.,  0.0379269,       400.
 203.,  0.0545559,       400.
 248.,   0.078476,       400.
 312.,   0.112884,       400.
 405.,   0.162378,       400.
 538.,   0.233572,       400.
 730.,   0.335982,       400.
1010.,   0.483293,       400.
1400.,   0.695193,       400.
1970.,         1.,       400.
*Specific Heat
 5e+08,
```

***Material, name=W**

```
*Conductivity
87.,
*Density
 1.925e-08,
*Elastic
398000., 0.28
*Expansion, zero=20.
 4.5e-06,
*Specific Heat
 1.34e+08,
```

***Material, name=tantalum**

```
*Conductivity
 54.4,
*Density
 1.66e-08,
*Elastic
184000.,    0.35,     25.
183000.,    0.35, 89.7548
182000.,    0.35, 119.514
181000.,    0.35, 185.469
180000.,    0.35, 201.558
179000.,    0.35, 237.752
179000.,    0.35, 264.295
178000.,    0.35, 287.624
177000.,    0.35, 318.191
177000.,    0.35, 354.373
175000.,    0.35, 409.878
175000.,    0.35, 429.997
173000.,    0.35, 475.037
173000.,    0.35, 496.754
170000.,    0.35,    600.
168000.,    0.35,    700.
166000.,    0.35,    800.
163000.,    0.35,    900.
161000.,    0.35,   1000.
*Expansion, zero=20.
  6.356e-06,     25.
 6.4761e-06, 89.7548
```

```
 6.5291e-06, 119.514
 6.6418e-06, 185.469
 6.6683e-06, 201.558
 6.7264e-06, 237.752
 6.7677e-06, 264.295
 6.8032e-06, 287.624
 6.8484e-06, 318.191
    6.9e-06, 354.373
 6.9754e-06, 409.878
 7.0015e-06, 429.997
 7.0578e-06, 475.037
 7.0839e-06, 496.754
 7.1979e-06,    600.
 7.2927e-06,    700.
 7.3723e-06,    800.
 7.4367e-06,    900.
 7.4857e-06,   1000.
*Plastic
  204.,          0.,         25.
 207.6,       0.001,         25.
 208.6, 0.00143845,          25.
 209.9, 0.00206914,          25.
 211.7, 0.00297635,          25.
 213.9, 0.00428133,          25.
 216.8, 0.00615848,          25.
 220.5, 0.00885867,          25.
 225.2,  0.0127428,          25.
 231.4,  0.0183298,          25.
 239.3,  0.0263665,          25.
 249.5,  0.0379269,          25.
 262.7,  0.0545559,          25.
 279.8,   0.078476,          25.
 301.7,   0.112884,          25.
 330.1,   0.162378,          25.
 366.6,   0.233572,          25.
 413.7,   0.335982,          25.
 474.5,   0.483293,          25.
 552.9,   0.695193,          25.
  654.,         1.,          25.
 157.1,         0.,         100.
 159.8,      0.001,         100.
 160.6, 0.00143845,         100.
 161.6, 0.00206914,         100.
  163., 0.00297635,         100.
 164.7, 0.00428133,         100.
 166.9, 0.00615848,         100.
 169.7, 0.00885867,         100.
 173.4,  0.0127428,         100.
 178.1,  0.0183298,         100.
 184.2,  0.0263665,         100.
 192.1,  0.0379269,         100.
 202.3,  0.0545559,         100.
 215.4,   0.078476,         100.
 232.3,   0.112884,         100.
 254.1,   0.162378,         100.
 282.2,   0.233572,         100.
 318.5,   0.335982,         100.
 365.3,   0.483293,         100.
 425.6,   0.695193,         100.
 503.5,         1.,         100.
 138.1,         0.,         200.
 140.5,      0.001,         200.
```

```
141.2, 0.00143845,        200.
142.1, 0.00206914,        200.
143.3, 0.00297635,        200.
144.8, 0.00428133,        200.
146.8, 0.00615848,        200.
149.3, 0.00885867,        200.
152.5,  0.0127428,        200.
156.6,  0.0183298,        200.
 162.,  0.0263665,        200.
168.9,  0.0379269,        200.
177.9,  0.0545559,        200.
189.4,   0.078476,        200.
204.3,   0.112884,        200.
223.5,   0.162378,        200.
248.2,   0.233572,        200.
280.1,   0.335982,        200.
321.2,   0.483293,        200.
374.3,   0.695193,        200.
442.8,         1.,        200.
125.1,         0.,        300.
127.2,      0.001,        300.
127.9, 0.00143845,        300.
128.7, 0.00206914,        300.
129.8, 0.00297635,        300.
131.1, 0.00428133,        300.
132.9, 0.00615848,        300.
135.1, 0.00885867,        300.
138.1,  0.0127428,        300.
141.8,  0.0183298,        300.
146.7,  0.0263665,        300.
 153.,  0.0379269,        300.
161.1,  0.0545559,        300.
171.5,   0.078476,        300.
 185.,   0.112884,        300.
202.3,   0.162378,        300.
224.7,   0.233572,        300.
253.6,   0.335982,        300.
290.9,   0.483293,        300.
338.9,   0.695193,        300.
400.9,         1.,        300.
114.6,         0.,        400.
116.6,      0.001,        400.
117.2, 0.00143845,        400.
 118., 0.00206914,        400.
118.9, 0.00297635,        400.
120.2, 0.00428133,        400.
121.8, 0.00615848,        400.
123.9, 0.00885867,        400.
126.6,  0.0127428,        400.
 130.,  0.0183298,        400.
134.5,  0.0263665,        400.
140.2,  0.0379269,        400.
147.6,  0.0545559,        400.
157.2,   0.078476,        400.
169.5,   0.112884,        400.
185.5,   0.162378,        400.
 206.,   0.233572,        400.
232.5,   0.335982,        400.
266.6,   0.483293,        400.
310.7,   0.695193,        400.
367.5,         1.,        400.
105.8,         0.,        500.
```

```
107.6,      0.001,       500.
108.2, 0.00143845,       500.
108.8, 0.00206914,       500.
109.7, 0.00297635,       500.
110.9, 0.00428133,       500.
112.4, 0.00615848,       500.
114.3, 0.00885867,       500.
116.8,  0.0127428,       500.
 120.,  0.0183298,       500.
124.1,  0.0263665,       500.
129.4,  0.0379269,       500.
136.2,  0.0545559,       500.
145.1,   0.078476,       500.
156.4,   0.112884,       500.
171.1,   0.162378,       500.
190.1,   0.233572,       500.
214.5,   0.335982,       500.
 246.,   0.483293,       500.
286.6,   0.695193,       500.
339.1,         1.,       500.
97.96,         0.,       600.
99.68,      0.001,       600.
100.2, 0.00143845,       600.
100.8, 0.00206914,       600.
101.6, 0.00297635,       600.
102.7, 0.00428133,       600.
104.1, 0.00615848,       600.
105.9, 0.00885867,       600.
108.2,  0.0127428,       600.
111.1,  0.0183298,       600.
114.9,  0.0263665,       600.
119.8,  0.0379269,       600.
126.2,  0.0545559,       600.
134.4,   0.078476,       600.
144.9,   0.112884,       600.
158.5,   0.162378,       600.
 176.,   0.233572,       600.
198.7,   0.335982,       600.
227.9,   0.483293,       600.
265.5,   0.695193,       600.
314.1,         1.,       600.
90.94,         0.,       700.
92.53,      0.001,       700.
92.99, 0.00143845,       700.
93.59, 0.00206914,       700.
94.36, 0.00297635,       700.
95.35, 0.00428133,       700.
96.63, 0.00615848,       700.
98.28, 0.00885867,       700.
100.4,  0.0127428,       700.
103.1,  0.0183298,       700.
106.7,  0.0263665,       700.
111.2,  0.0379269,       700.
117.1,  0.0545559,       700.
124.7,   0.078476,       700.
134.5,   0.112884,       700.
147.1,   0.162378,       700.
163.4,   0.233572,       700.
184.4,   0.335982,       700.
211.5,   0.483293,       700.
246.5,   0.695193,       700.
291.5,         1.,       700.
```

```
84.52,         0.,        800.
  86.,      0.001,        800.
86.43, 0.00143845,        800.
86.98, 0.00206914,        800.
87.69, 0.00297635,        800.
88.61, 0.00428133,        800.
 89.8, 0.00615848,        800.
91.33, 0.00885867,        800.
93.31,  0.0127428,        800.
95.86,  0.0183298,        800.
99.15,  0.0263665,        800.
103.4,  0.0379269,        800.
108.9,  0.0545559,        800.
115.9,   0.078476,        800.
 125.,   0.112884,        800.
136.7,   0.162378,        800.
151.9,   0.233572,        800.
171.4,   0.335982,        800.
196.6,   0.483293,        800.
229.1,   0.695193,        800.
270.9,         1.,        800.
78.57,         0.,        900.
79.95,      0.001,        900.
80.35, 0.00143845,        900.
80.86, 0.00206914,        900.
81.53, 0.00297635,        900.
82.38, 0.00428133,        900.
83.49, 0.00615848,        900.
84.91, 0.00885867,        900.
86.75,  0.0127428,        900.
89.12,  0.0183298,        900.
92.17,  0.0263665,        900.
96.12,  0.0379269,        900.
101.2,  0.0545559,        900.
107.8,   0.078476,        900.
116.2,   0.112884,        900.
127.1,   0.162378,        900.
141.2,   0.233572,        900.
159.3,   0.335982,        900.
182.8,   0.483293,        900.
212.9,   0.695193,        900.
251.9,         1.,        900.
73.02,         0.,       1000.
 74.3,      0.001,       1000.
74.67, 0.00143845,       1000.
75.15, 0.00206914,       1000.
75.77, 0.00297635,       1000.
76.56, 0.00428133,       1000.
77.59, 0.00615848,       1000.
78.91, 0.00885867,       1000.
80.62,  0.0127428,       1000.
82.82,  0.0183298,       1000.
85.66,  0.0263665,       1000.
89.33,  0.0379269,       1000.
94.05,  0.0545559,       1000.
100.1,   0.078476,       1000.
 108.,   0.112884,       1000.
118.1,   0.162378,       1000.
131.2,   0.233572,       1000.
148.1,   0.335982,       1000.
169.8,   0.483293,       1000.
197.9,   0.695193,       1000.
```

```
 234.1,         1.,      1000.
 67.81,         0.,      1100.
 68.99,      0.001,      1100.
 69.34, 0.00143845,      1100.
 69.78, 0.00206914,      1100.
 70.36, 0.00297635,      1100.
 71.09, 0.00428133,      1100.
 72.05, 0.00615848,      1100.
 73.28, 0.00885867,      1100.
 74.86,  0.0127428,      1100.
 76.91,  0.0183298,      1100.
 79.54,  0.0263665,      1100.
 82.95,  0.0379269,      1100.
 87.33,  0.0545559,      1100.
 92.99,   0.078476,      1100.
 100.3,   0.112884,      1100.
 109.7,   0.162378,      1100.
 121.9,   0.233572,      1100.
 137.5,   0.335982,      1100.
 157.7,   0.483293,      1100.
 183.8,   0.695193,      1100.
 217.4,         1.,      1100.
 62.87,         0.,      1200.
 63.98,      0.001,      1200.
 64.29, 0.00143845,      1200.
 64.71, 0.00206914,      1200.
 65.24, 0.00297635,      1200.
 65.92, 0.00428133,      1200.
 66.81, 0.00615848,      1200.
 67.95, 0.00885867,      1200.
 69.42,  0.0127428,      1200.
 71.31,  0.0183298,      1200.
 73.76,  0.0263665,      1200.
 76.91,  0.0379269,      1200.
 80.98,  0.0545559,      1200.
 86.23,   0.078476,      1200.
   93.,   0.112884,      1200.
 101.7,   0.162378,      1200.
  113.,   0.233572,      1200.
 127.5,   0.335982,      1200.
 146.2,   0.483293,      1200.
 170.4,   0.695193,      1200.
 201.6,         1.,      1200.
*Specific Heat
 1.4e+08,
```

APPENDIX B. CONTACT CONDUCTANCE

To evaluate the de-bonded case an estimate of the thermal conductance between surfaces after de-bonding occurs is needed. This can be very complicated and depends on many factors including the surface roughness, pressure, and material properties. Tariq and Asif experimentally investigated conductance for nominal flat metallic contact [9]. Dou et al. also investigated thermal conductance with varying surface roughness and pressure [10]. Figure 80 shows the variables and model selected for this analysis from Tariq and Asif.

List of symbols

A	Nominal contact area
A_r	Real contact area
E	Modulus of elasticity
E'	Reduced modulus of elasticity, $E' = [((1-\nu_1^2)/E_1) + ((1-\nu_2^2)/E_2)]^{-1}$
h_c	Solid spot conductance
$\bar{h}_c$	Normalized solid spot contact conductance, $\bar{h}_c = (h_c R_q)/(mk)$
h_g	Gap conductance
h_j	Joint thermal contact conductance
h_r	Radiation heat transfer coefficient
ΔT	Temperature drop across the interface
H	Vickers hardness
k	Effective thermal conductivity, $k = 2k_1k_2/(k_1+k_2)$
m	Effective arithmetic average slope, $m = \sqrt{(m_1^2 + m_2^2)}$
$\bar{P}$	Normalized pressure, $\bar{P} = P/H$
P	Applied pressure
Q	Heat flow rate
R_q	Effective root mean square roughness, $R_q = \sqrt{(R_{q1}^2 + R_{q2}^2)}$
U_{Q_1}, U_{Q_2}	Uncertainties in the estimation of heat fluxes, Q_1 and Q_2

Mikic plastic model for conductance selected for de-bonded model

Table 3 Theoretical models with correlations

Model	Correlation
CMY plastic [12]	$\bar{h}_c = 1.45\,(\bar{P})^{0.985}$
Mikic plastic [14]	$\bar{h}_c = 1.13\,(\bar{P})^{0.94}$
Mikic elastic [14]	$\bar{h}_c = 1.55\,\left(P\sqrt{2}/E'm\right)^{0.94}$
Yovanovich plastic [15]	$\bar{h}_c = 1.25\,(\bar{P})^{0.95}$

Figure 80 Conductance models listed in Tariq and Asif [9].

The material properties and calculated conductance using the Mikic model are shown in Table 6 and Figure 81. Surface roughness for Copper from the Tariq and Asif experiments was assumed for the Tantalum and Inconel. The arithmetic slope was measured for several materials with varying surface roughness in that reference. Stainless steel values varied from 0.12 to 0.09 depending on roughness. For this analysis a value of 0.1 was assumed for both tantalum and Inconel.

Table 6 Assumed Tantalum and Inconel Properties for contact

	Units		Tantalum	Inconel 718
Assumed RMS surface roughness (M)	m	s	2.82E-06	2.82E-06
Thermal conductivity	W/m-K	k	54.4	12.1
Youngs Modulus	Pa	E	1.86E+11	2.05E+11
Poisson's ration		ν	0.35	0.3
Hardness	Pa	H	9.00E+08	
assumed arithmetic slope		m	0.1	0.1
calculated reduced Youngs modulus		E'	1.09209E+11	
RMS roughness	m	Rq	3.99E-06	

The calculated conductance as a function of pressure using the Mikic plastic relation is shown in Figure 81.

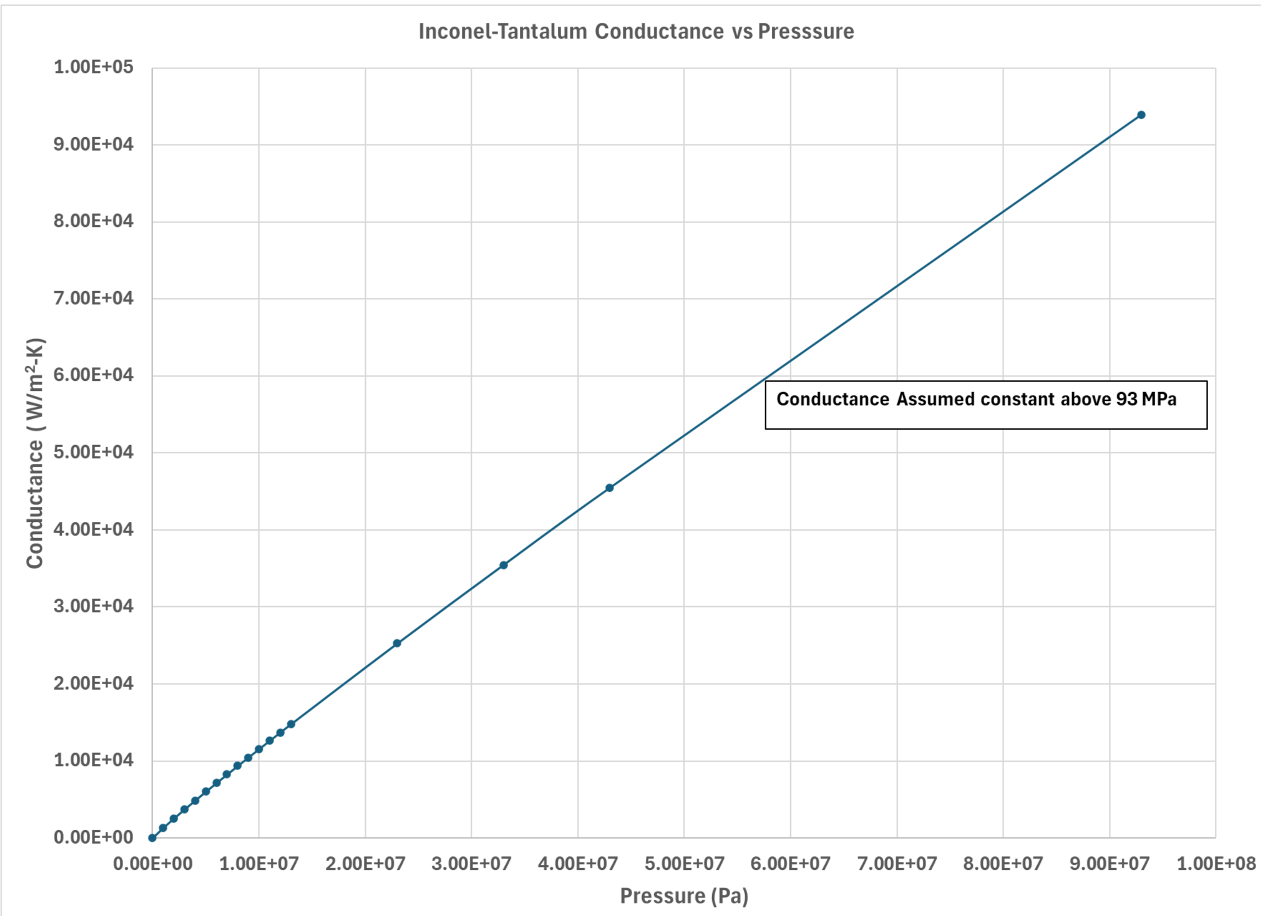

Figure 81 Conductance vs Pressure

A literature example of surface conductance vs. pressure [11] is shown in Figure 82.

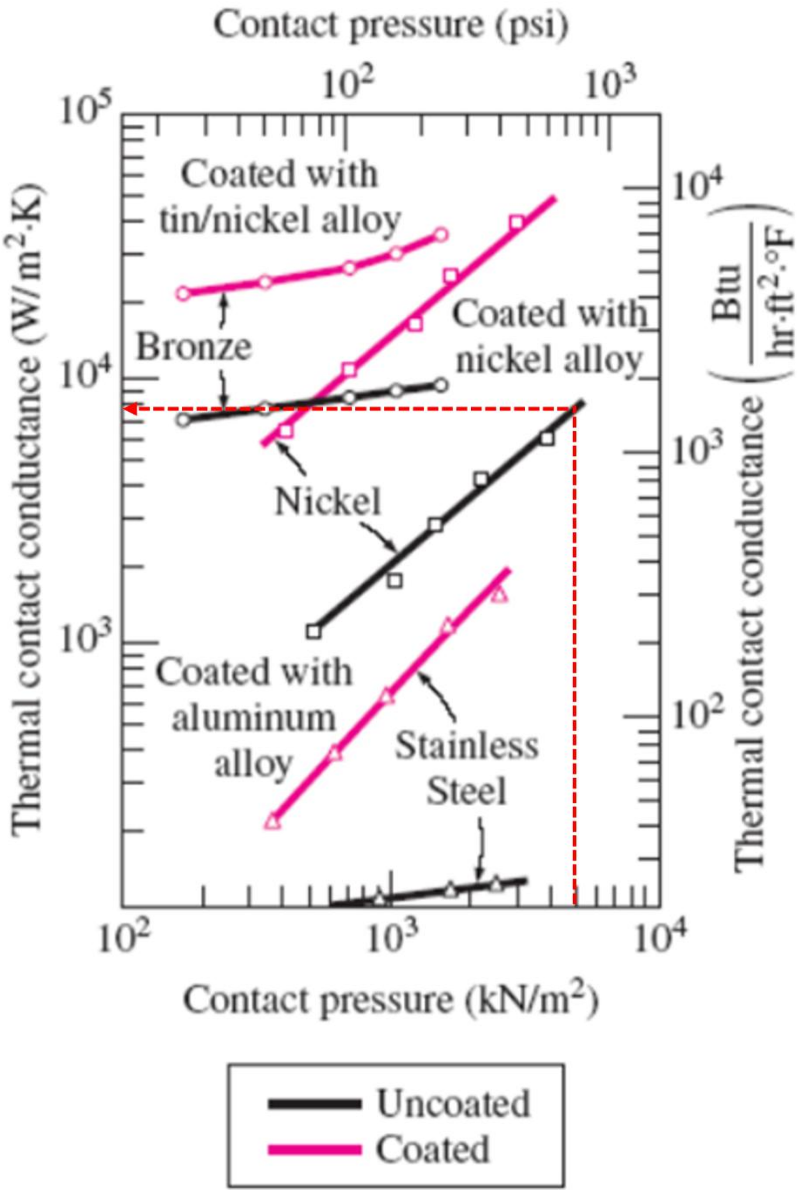

Figure 82 Literature example of Conductance with Pressure [11] with 5 MPa pressure reference lines added for Nickel.

The conductance from Figure 82 for uncoated nickel surfaces with approximately 5 MPa pressure is approximately 8 kW/m^2-K. The estimated value for the Inconel to Tantalum case from Figure 81 is approximately 6 kW/m^2-K at 5 MPa.

There is no R&D data available for the surface conditions after a bond breaks or the surface conditions after the Hipping process for bonds that are not made or any measured conductance without a bond. The estimate here should be considered as a first order of magnitude estimate.

APPENDIX C. CONVECTION HEAT TRANSFER COEFFICIENTS

The heat transfer convection coefficients used in this report originated from thermostructural analyses on an earlier target geometry. The flow channel dimensions and placement were the same. A Python script was created to calculate the flow balance between the cooling channels based on a 1-D flow network using the Hardy Cross Method for solving pipe network flow. The heat transfer solution was compared with a full CFD conjugate heat transfer study and found excellent agreement. The PowerPoint slides that summarized this comparison are included below, followed by a copy of the Python script that was used to generate the convection coefficients in this report.

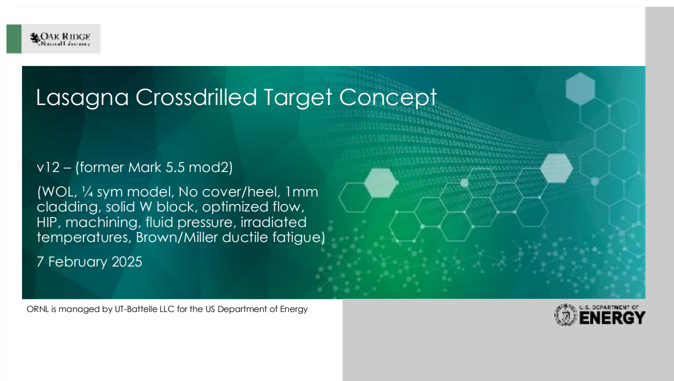

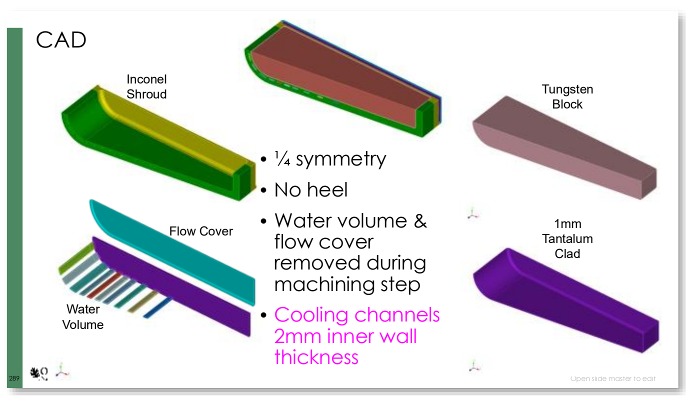

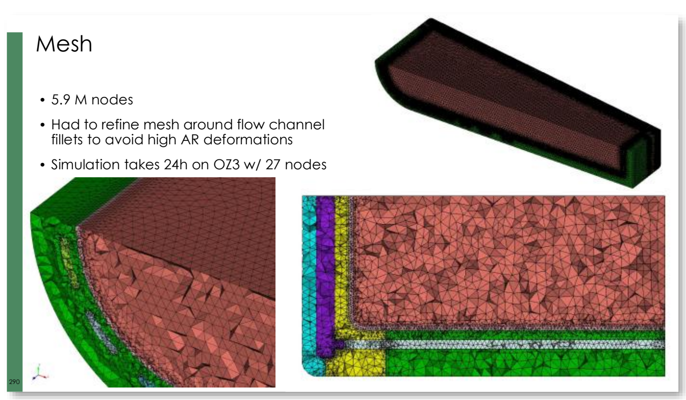

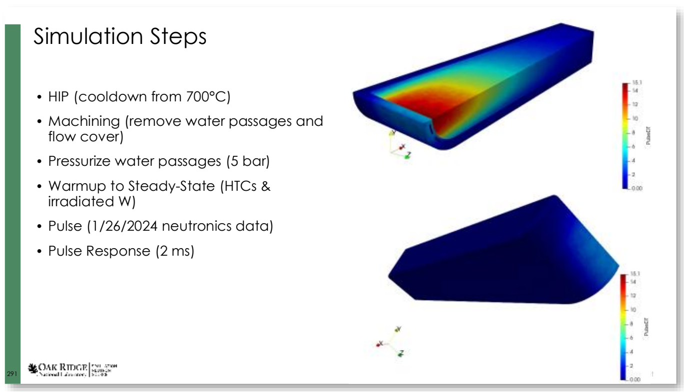
Simulation Steps
• HIP (cooldown from 700°C)
• Machining (remove water passages and flow cover)
• Pressurize water passages (5 bar)
• Warmup to Steady-State (HTCs & irradiated W)
• Pulse (1/26/2024 neutronics data)
• Pulse Response (2 ms)
291
OAK RIDGE National Laboratory

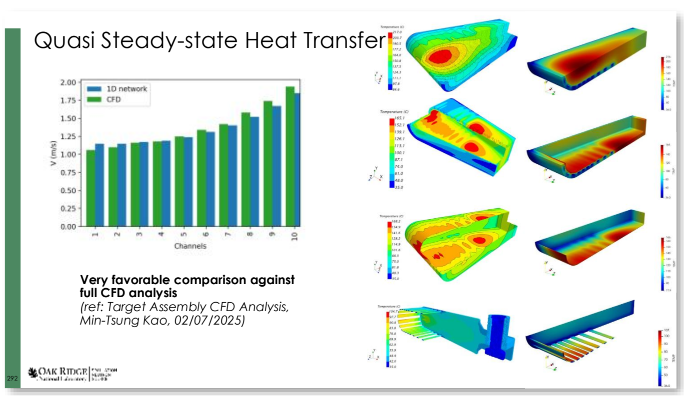
Quasi Steady-state Heat Transfer
1D network
CFD
V (m/s)
Channels
Very favorable comparison against full CFD analysis
(ref: Target Assembly CFD Analysis, Min-Tsung Kao, 02/07/2025)
292
OAK RIDGE National Laboratory

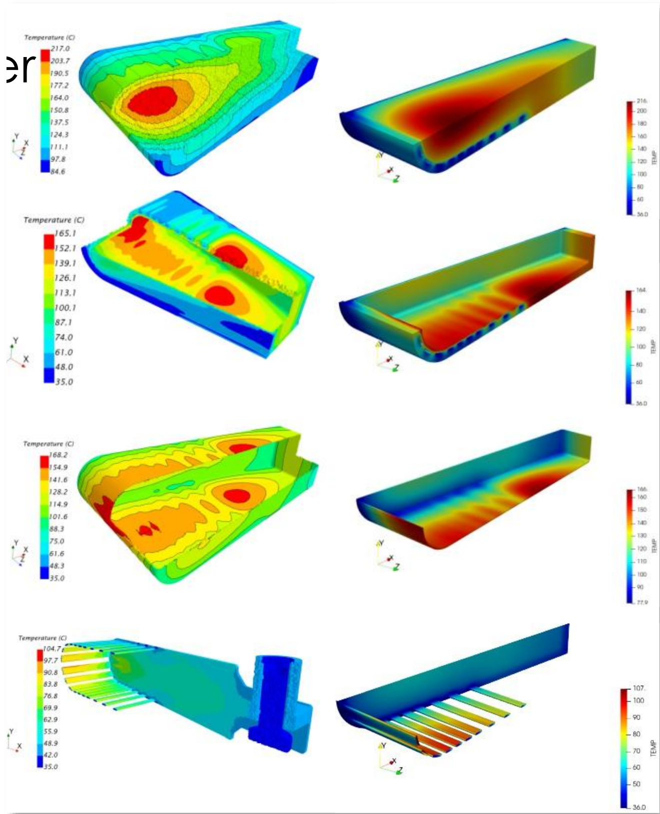

LasagnaOpt_Thermal_HTC_v1.py

```
"""
CROSSDRILLED LASAGNA SIDE FLOW COOLANT FLOW CALCS
@author: tvj

CHANGELOG:
2024-08-30
  --> added bar plot of channel V and HTC
2024-09-13
  --> changed to 8 channel version
"""

import numpy as np
import pandas as pd
import matplotlib.pyplot as plt

# =========== constants ===================================================
paToPsi = 0.00014504 # psi/Pa
m3ToGal = 264.172 # gal/m^3
inchTometer = 0.0254 # meter/inch
g = 9.81 # m/s^2


# =========== water props =================================================
Cp        =  4181.72          # J/(kg*K), specific heat of water
rho       =  997.561          # kg/m^3, density
mu        =  8.8871E-4        # Pa-s
k_thermal =  0.62170          # W/m-K, thermal conductivity
Pr        =  mu*Cp/k_thermal  # Prandtl number


# =========== geometry ====================================================
numSeg    = 20
#  , number target segments
```

```
n         = int(20/2)
#  , number channels per segment

L_sides   = np.array([15, 15, 15, 12, 12, 13, 18, 22, 25, 142])*0.001
# m, distance between channels


L_chan    = np.array([164, 163, 158, 154, 150, 146, 142, 136, 130, 122])*0.001
# m, channel lengths

P_chan    = np.array([24.4, 22.1, 24.4, 18.3, 18.3, 20.3, 20.3, 20.2, 20.3, 18.3])*0.001
# m, channel perimeters

A_chan    = np.array([21.3, 19.0, 21.3, 15.1, 15.1, 17.1, 17.1, 17.0, 17.1, 15.1])*1.0e-6
# m^2, channel areas

P_sides   = np.ones(n) * 0.0742
# m, side perimeters (with sym)

A_sides   = np.ones(n) * 143.3/1000./1000.
# m^2, side areas (with sym)

Dh_chan   = 4.0*A_chan/P_chan
# m, channel hydraulic diameters

Dh_sides  = 4.0*A_sides/P_sides
# m, side hydraulic diameters


# =========== flow conditions: chan============================================
Q_gpm = 150./numSeg          # gpm
Q_tot = Q_gpm/m3ToGal/60.    # m^3/s
m_dot = Q_tot * rho          # kg/s, water mass flow rate


# initialize flow guess
Q_chan    = np.ones(n)*Q_tot/n/2.            # flow through channels (with sym)
Q_sides   = np.zeros(n)                      # flow through sides between channels
for ii in range(n):
    Q_sides[ii] = Q_tot/n/2. * (ii+1)


# =========== Hardy Cross Method for solving pipe network flow ===============
Change = 1.0
LoopCount = 1

while np.max(np.abs(Change/Q_chan)) > 1.e-6:
  # Bulk fluid velocities (m/s)
  V_chan = Q_chan/A_chan
  V_sides = Q_sides/A_sides
  #
  # Reynolds number
  Re_chan = rho*np.abs(V_chan)*Dh_chan/mu
  Re_sides = rho*np.abs(V_sides)*Dh_sides/mu
  #
  # Moody friction factors
  # McAdams/Koo correlation for turbulent regime
  # High aspect ratio correlation for laminar regime
  #
  f_chan = 0.184/Re_chan**0.2
  #for ii in range(n):
  #    if Re_chan[ii] < 3000.:
  #        f_chan[ii] = 96.0 / Re_chan[ii] # Laminar flow
  #
  f_sides = 0.184/Re_sides**0.2
  #for ii in range(n):
  #    if Re_sides[ii] < 3000.:
  #        f_sides[ii] = 96.0 / Re_sides[ii] # Laminar flow
  #
```

```
  # Channel flow resistance between plates
  R_chan = f_chan * (L_chan / Dh_chan + 2.0*60.0) / A_chan**2.0 / (2.0*g)
  # the front channel has 2 90-deg bends instead of T-junctions
  #R_chan[0] = ((f_chan[0] * L_chan[0] / Dh_chan[0]) + 2.0*1.1) / A_chan[0]**2.0 / (2.0*g)
  #
  # Incoming side flow resistances
  R_sides_in = f_sides * (L_sides / Dh_sides + 20.0) / A_sides**2.0 / (2.0*g)
  # the back side leg does not have a T-junction resistance
  R_sides_in[-1] = f_sides[-1] * (L_sides[-1] / Dh_sides[-1]) / A_sides[-1]**2.0 / (2.0*g)
  #
  # Outgoing side flow resistances
  R_sides_out = f_sides * (L_sides / Dh_sides + 20.0) / A_sides**2.0 / (2.0*g)
  # the front side leg does not have a T-junction resistance
  R_sides_out[0] = f_sides[0] * (L_sides[0] / Dh_sides[0]) / A_sides[0]**2.0 / (2.0*g)
  #
  # Calculate sum of losses in each loop using clockwise direction as positive
  Loss_cw = R_sides_in*Q_sides**2.0 + R_chan*Q_chan**2.0 + R_sides_out*Q_sides**2.0
  #Loss_cw = R_chan*Q_chan**2.0
  Loss_ccw = np.roll(R_chan*Q_chan**2.0,-1)
  Loss_ccw[-1] = 0.0  # last leg has known flowrate and is not a loop
  Loss_cw_tot = Loss_cw - Loss_ccw
  #
  # Calculate derivative of losses using clockwise direction as positive
  Dloss_cw = 2.0*R_sides_in*Q_sides + 2.0*R_chan*Q_chan + 2.0*R_sides_out*Q_sides
  #Dloss_cw = 2.0*R_chan*Q_chan
  Dloss_ccw = np.roll(2.0*R_chan*Q_chan,-1)
  Dloss_ccw[-1] = 0.0  # last leg has known flowrate and is not a loop
  Dloss_tot = Dloss_cw + Dloss_ccw
  #
  # Calculate the correction (originates from a Taylor Series expansion of the pressure drop)
  Change = Loss_cw_tot / Dloss_tot
  Change[-1] = 0.0 # last leg has known flowrate and is not a loop
  #
  # Apply correction to side supply legs
  Q_sides = Q_sides - Change
  #
  # Apply correction to channels (interior channels have corrections from adjacent loops)
  func = np.eye(n, k=-1) + -1.0*np.identity(n)
  Q_chan = Q_chan + np.sum(Change*func,axis=1)
  #
  # Keep track of iterations
  LoopCount = LoopCount + 1


# Nusselt number for channels between plates using Gneilinski correlation
Nu_chan = (f_chan/8.)*(Re_chan-1000.)*Pr / (1. + 12.7*np.sqrt(f_chan/8)*(Pr**(2./3.)-1.))

for ii in range(n):
    if Re_chan[ii] < 3000.:
        Nu_chan[ii] = 5.0 # If flow is laminar, set to narrow channel Nu

# Convection coeff. for channels (W/m^2-K)
HTC_chan = Nu_chan * k_thermal / Dh_chan


# Summarize & Save
df = pd.DataFrame(V_chan, index=np.linspace(1,n,n).astype(int), columns=['V'])
df['HTC'] = HTC_chan

fig = plt.figure(figsize=(6,4), dpi=200) # Create matplotlib figure

ax = fig.add_subplot(111) # Create matplotlib axes
ax2 = ax.twinx() # Create another axes that shares the same x-axis as ax.

width = 0.4

df.V.plot(kind='bar', color='tab:blue', ax=ax, width=width, position=1)
df.HTC.plot(kind='bar', color='tab:orange', ax=ax2, width=width, position=0)

ax.set_ylabel('V (m/s)')
```

```
ax2.set_ylabel('HTC ($W/m^2 K$)')
ax.set_xlabel('Channels')

ax.yaxis.label.set_color('tab:blue')          #setting up Y-axis label color to blue
ax.tick_params(axis='y', colors='tab:blue')    #setting up X-axis tick color to red

ax2.yaxis.label.set_color('tab:orange')          #setting up Y-axis label color to blue
ax2.tick_params(axis='y', colors='tab:orange')    #setting up X-axis tick color to red

plt.subplots_adjust(right=0.85)
plt.subplots_adjust(bottom=0.15)
plt.savefig('LasagnaOpt_Thermal_HTC.png') #, bbox_inces = "tight")


for ii in range(n):
  file = open('LasagnaOpt_Thermal_HTC_C'+str(ii+1).zfill(2)+'.txt', "w")
  file.write(str(HTC_chan[ii]))
  file.close()


# =========== flow calculations: sides ======================================
# ASSUMES CONSTANT AREA
A_sides = A_sides[0]
Dh_sides = Dh_sides[0]

# Bulk fluid velocities (m/s)
V_sides = Q_tot/2./A_sides

# Reynolds number
Re_sides = rho*np.abs(V_sides)*Dh_sides/mu

# Moody friction factors
# McAdams/Koo correlation for turbulent regime
# High aspect ratio correlation for laminar regime

if Re_sides < 3000.:
  f_sides = 96./Re_sides
  Nu_sides = 8.0 # If flow is laminar, set to narrow channel Nu
else:
  f_sides = 0.184/Re_sides**0.2
  # Gneilinski correlation
  Nu_sides = (f_sides/8.)*(Re_sides-1000.)*Pr / (1. + 12.7*np.sqrt(f_sides/8)*(Pr**(2./3.)-1.))

# Convection coeff. for channels (W/m^2-K)
HTC_sides = Nu_sides * k_thermal / Dh_sides


# Summarize & Save
#ans = np.column_stack((W_chan*1000,V_chan,Re_chan,HTC_chan))

file = open("LasagnaOpt_Thermal_HTC_sides.txt", "w")
file.write(str(HTC_sides))
file.close()


# =========== flow calculations: heel =======================================
# JUST ASSUME IT IS THE SAME AS THE SIDES FOR NOW
file = open("LasagnaOpt_Thermal_HTC_heel.txt", "w")
file.write(str(HTC_sides))
file.close()
```

APPENDIX D. MAINTENANCE CASE TEMPERATURE ESTIMATES

This report focuses on analyzing the effect of a complete bond failure between the Inconel shroud and the W/Ta spallation package. A second avenue of analysis is to estimate the temperature at which bond failure would occur during a maintenance event. This was performed in parallel to the debonding simulation efforts using the simulation models documented in the "Target Segment Thermostructural Analysis" DAC [2]. This model incorporated thermoelastic-plastic material models for Inconel, tantalum, and stainless steel along with a thermoelastic material model for brittle tungsten. To mimic a maintenance scenario, dead loads were applied to the target segment structure while live loads (i.e. rotation) and pressure loads were omitted. To further mimic a maintenance scenario with decay heating (dominated by long-lived isotopes in the tantalum cladding), the target segment was started at a uniform 20°C and was then uniformly ramped to 100°C and 200°C. Bond strengths were assumed to be equal to the parent materials of the bond. (Note that the stress state of the bond after manufacturing operations has already been discussed in [2].) Two initial stress states at 20°C were considered:

- Worst of Life (WOL) – Incorporates a manufacturing simulation that captures residual stresses in the target foot (tungsten plates, tantalum cladding, and Inconel shroud) as it goes through HIP with creep followed by machining of cooling passages in the shroud. This places the tantalum and Inconel into the plastic regime with significant stress and strain hardening. The tungsten is placed in a state of surface compression as the shroud is deformed around it due to the CTE mismatch.
- End of Life (EOL) – Assumes all residual manufacturing stresses have been relieved through radiation induced stress relaxation. The entire target segment structure is at a stress-free state.

Table 7 summarizes the results for each of the 4 analysis cases. The images that follow capture the stress state of the components for each of the 4 analysis cases. The stainless-steel heel structure experiences some plastic deformation in the bond region to the foot but overall is not of concern. The Inconel shroud and tantalum cladding are both in a state of plastic deformation, however, they remain well within the range of ultimate. The largest stresses on the shroud occur at the side flow cover. With no water cooling, the flow cover wants to expand and places bending loads on the weld area to the shroud.

For irradiated tungsten, the estimated mean tensile strength is 350 MPa [1]. Since the material is brittle, a large amount of statistical scatter around this mean is expected. The EOL condition places the tungsten in the most challenging stress state as the compressive surface residual stress is removed. The tungsten would be expected to fail between 100°C and 200°C (or 150 ± 50°C). Stress contour plots show the failure location would be in the rear of the target. The tungsten would be expected to crack at the W/Ta interface. R&D experience at STS has shown that tantalum is a good crack inhibitor and stops tungsten cracks from propagating. Thus, the best engineering judgement is that the rear tungsten block would crack and completely debond from the tantalum interface but not propagate to adjacent blocks.

The lack of test data on bond strengths introduces a large amount of uncertainty to these analyses. The IN718/Ta bond or W/Ta bond could also fail before the tungsten were to reach ultimate. Hence, this larger document attempts to perform a bounding estimate of the behavior of a fully debonded target. It would be beneficial to pursue additional cooling schemes if maintenance scenarios are determined to produce large temperature increases in the target segments.

Finally, the analysis presented in this appendix do not address what happens after water coolant flow is reestablished to the target segment. Transient effects such as flash cooling could further damage the material bonds. Cool down rates should be considered pending operational decisions with target segments that have gone through maintenance thermal excursions.

Table 7: Material peak stresses during each maintenance simulation case of uniform temperature rise from 20°C initial. Tungsten stress is maximum principal (brittle) while all others are von Mises equivalent (ductile). Tungsten peak tensile stress is above irradiated ultimate at EOL between 100 and 200°C.

Case	Temp [°C]	IN718SA [MPa]	SS316 [MPa]	Ta [MPa]	W [MPa]
WOL	20 to 200	550	~200	280	300
WOL	20 to 100	570	~150	240	290
EOL	20 to 200	440	~180	160	430
EOL	20 to 100	385	~160	160	275

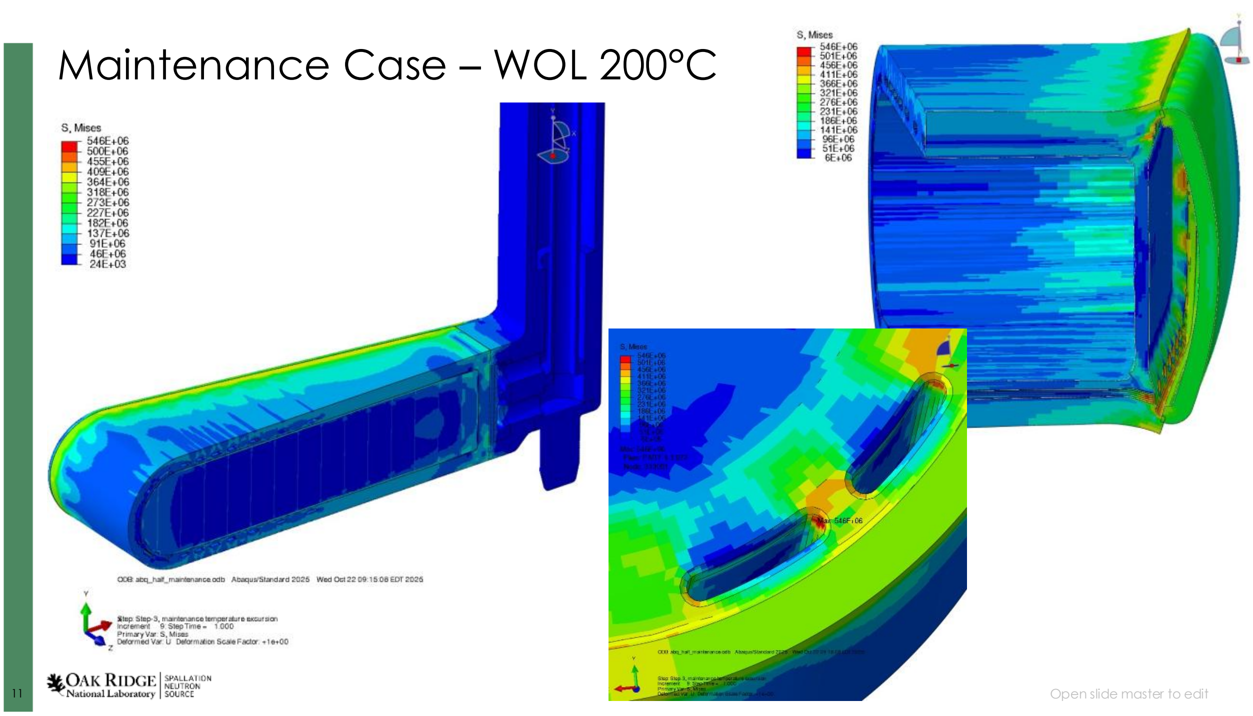

Maintenance Case – WOL 200°C

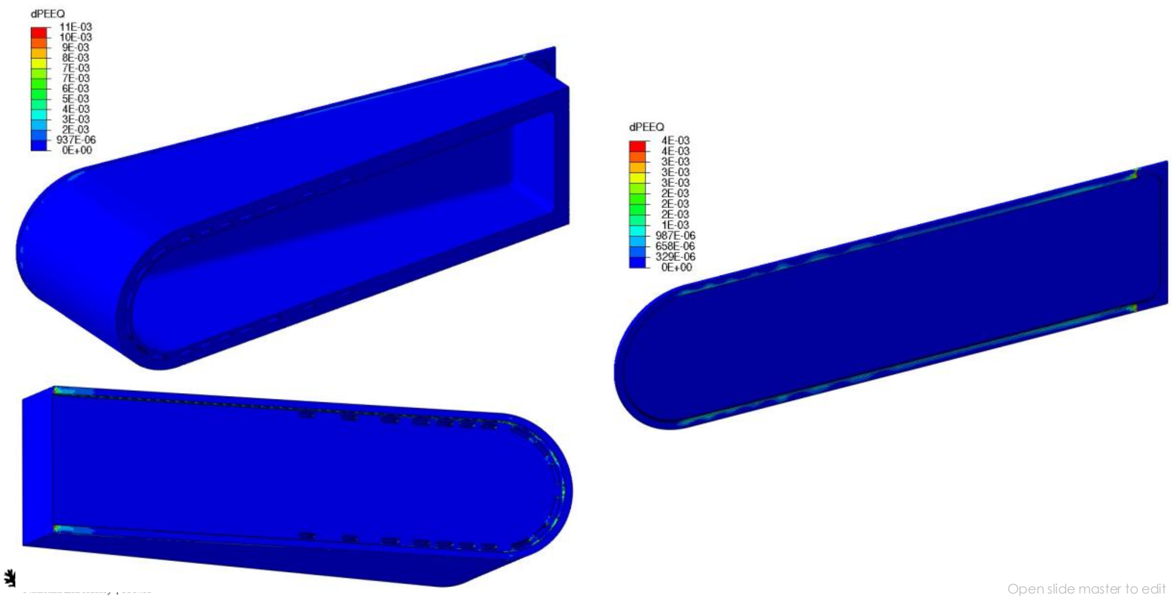

Maintenance Case – WOL 200°C

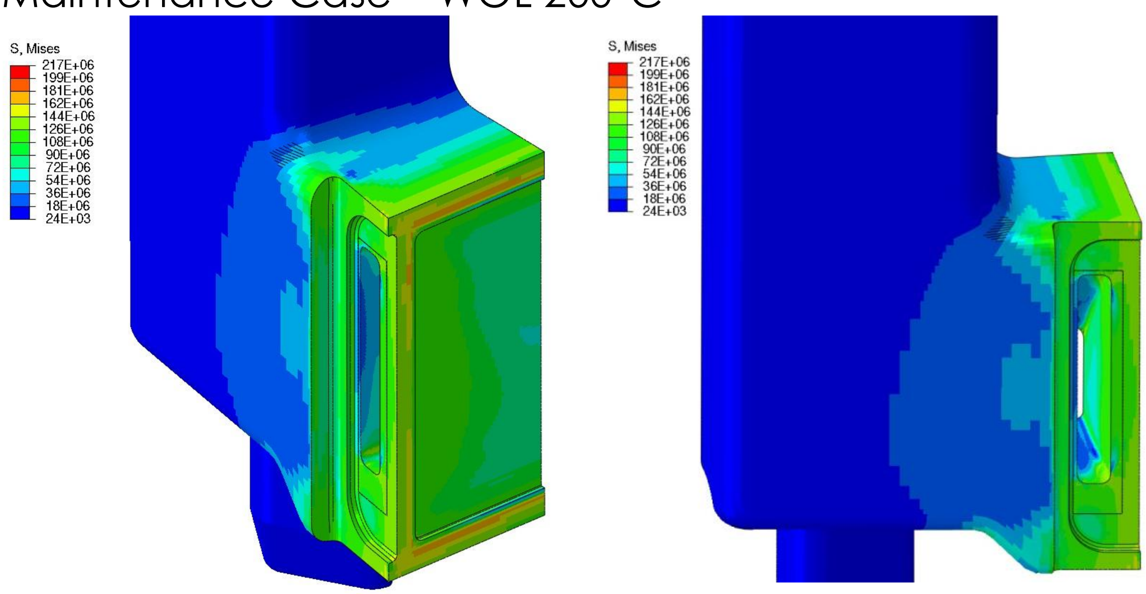

Maintenance Case – WOL 200°C

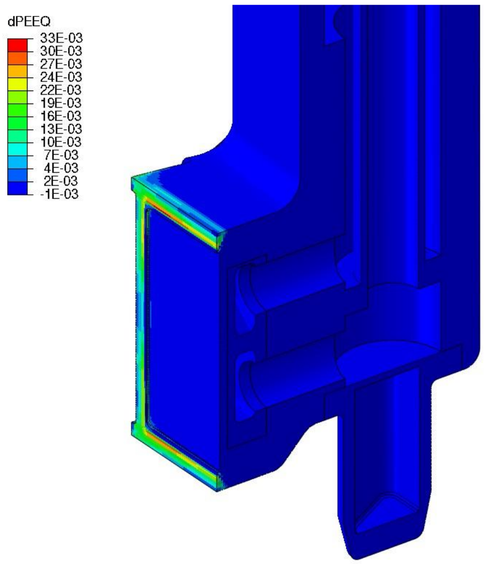

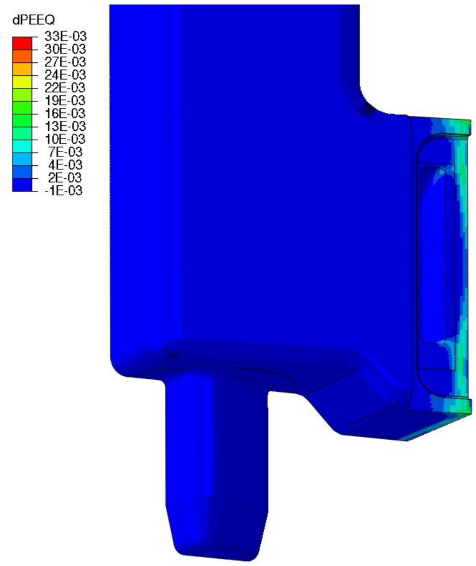

14

Open slide master to edit

Maintenance Case – WOL 200°C

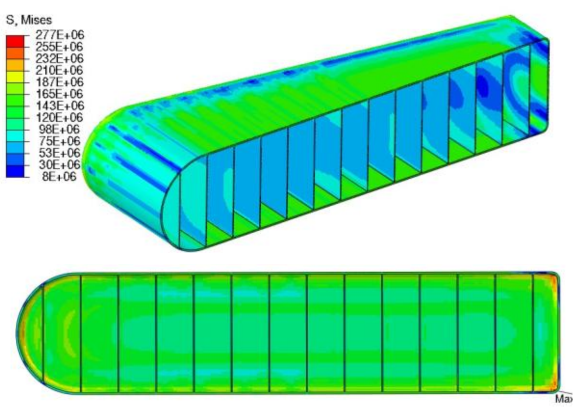

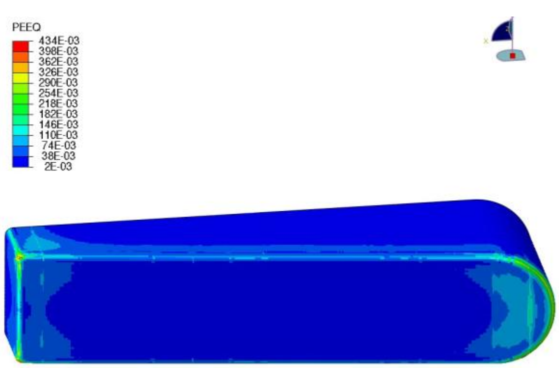

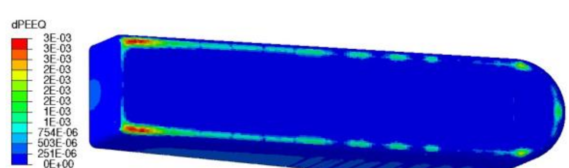

15

Maintenance Case – WOL 200°C

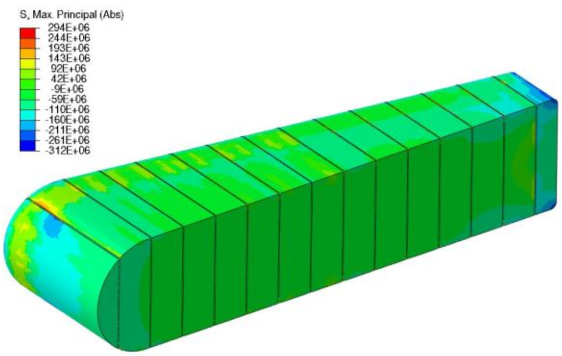

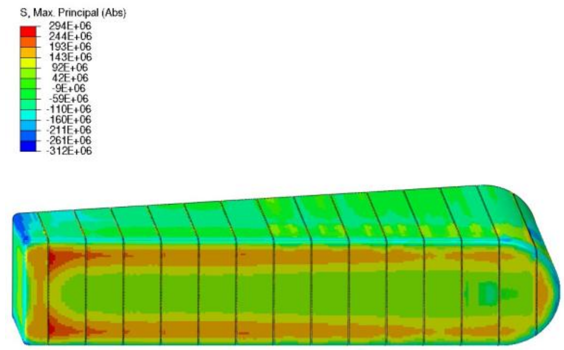

Maintenance Case – WOL 100°C

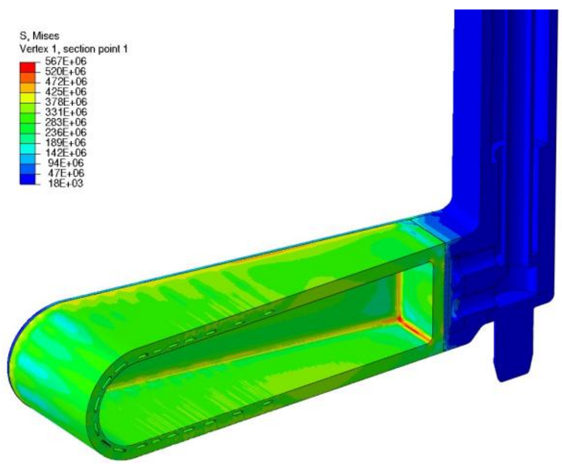

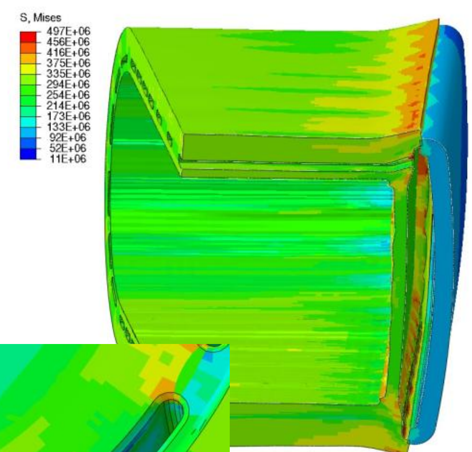

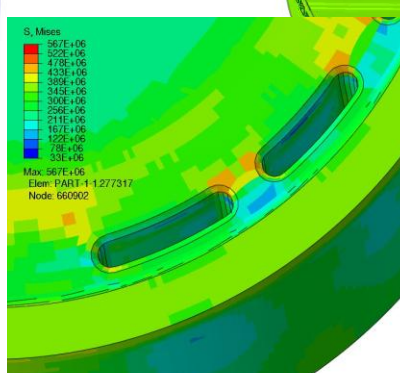

Maintenance Case – WOL 100°C

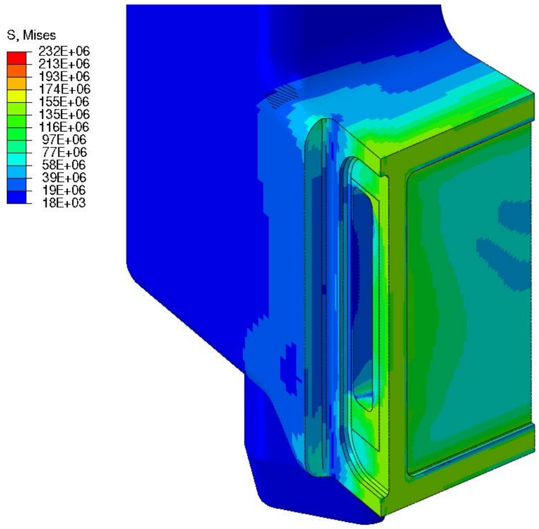

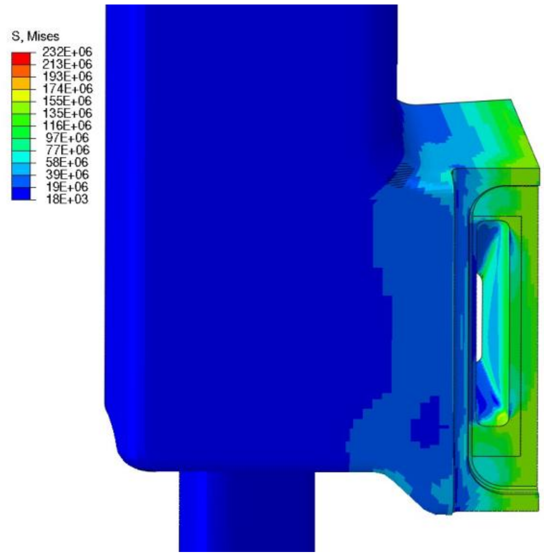

OAK RIDGE National Laboratory | SPALLATION NEUTRON SOURCE

Open slide master to edit

Maintenance Case – WOL 100°C

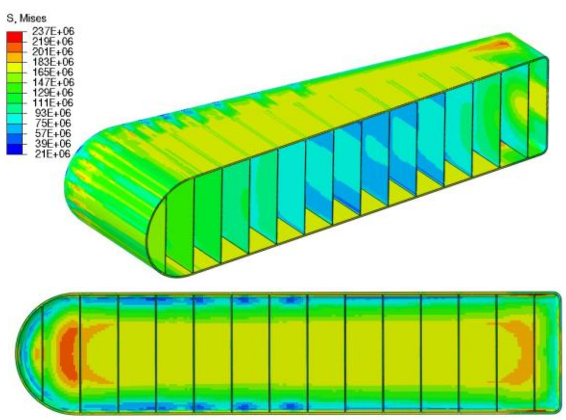

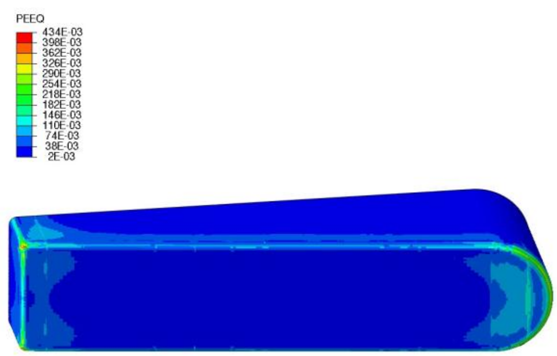

OAK RIDGE National Laboratory | SPALLATION NEUTRON SOURCE

Open slide master to edit

Maintenance Case – WOL 100°C

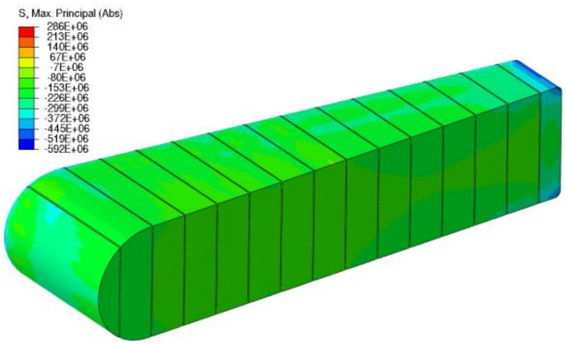

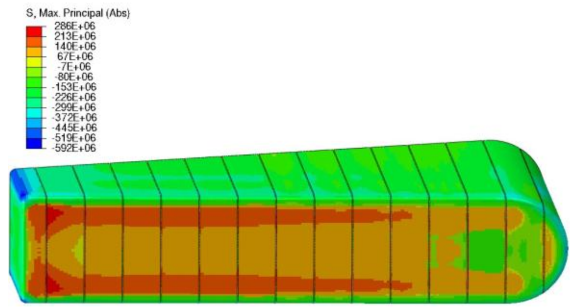

20 OAK RIDGE National Laboratory | SPALLATION NEUTRON SOURCE

Open slide master to edit

Maintenance Case – EOL 200°C

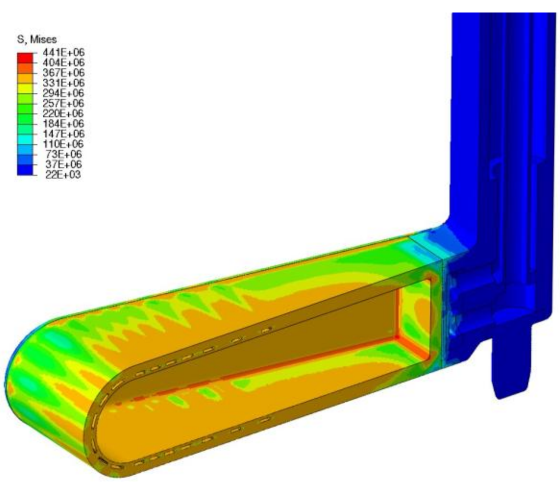

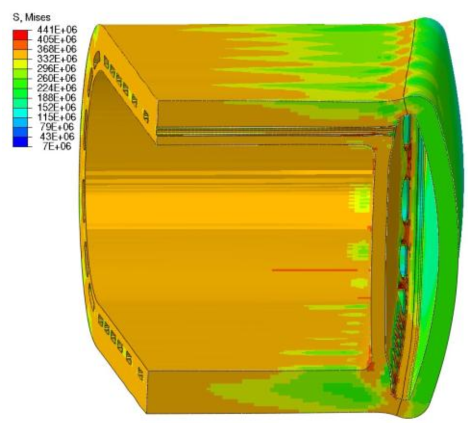

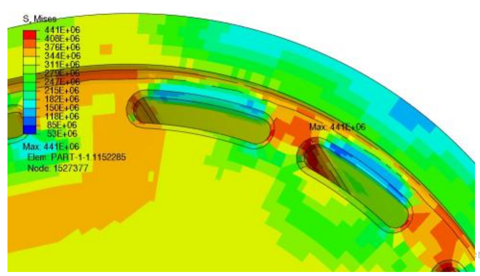

21 OAK RIDGE National Laboratory | SPALLATION NEUTRON SOURCE

n slide master to edit

Maintenance Case – EOL 200°C

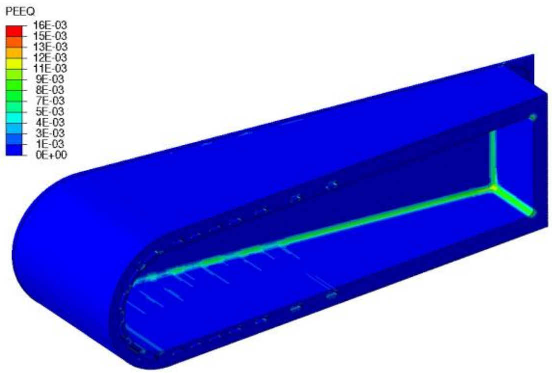

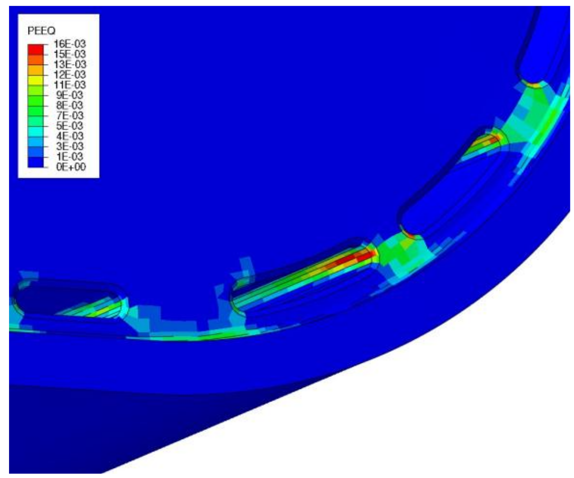

22 OAK RIDGE National Laboratory | SPALLATION NEUTRON SOURCE

Maintenance Case – EOL 200°C

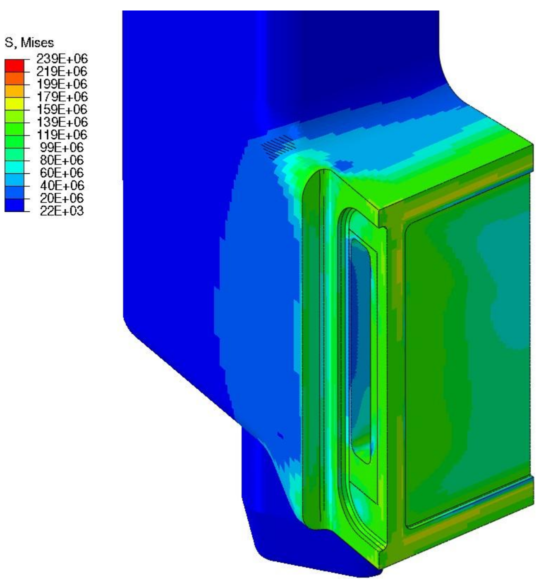

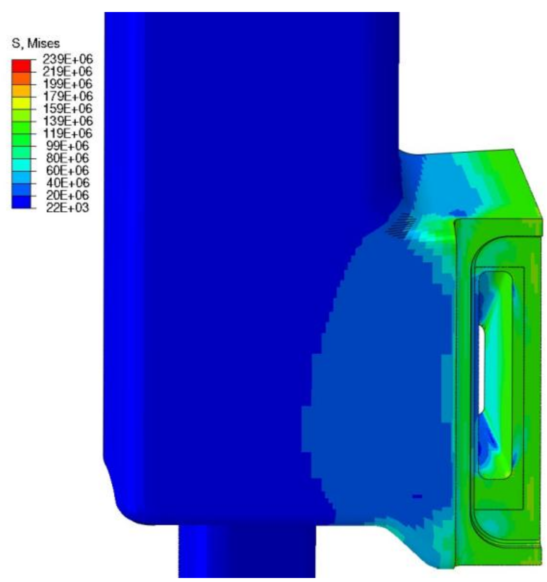

23 OAK RIDGE National Laboratory | SPALLATION NEUTRON SOURCE

Open slide master to edit

Maintenance Case – EOL 200°C

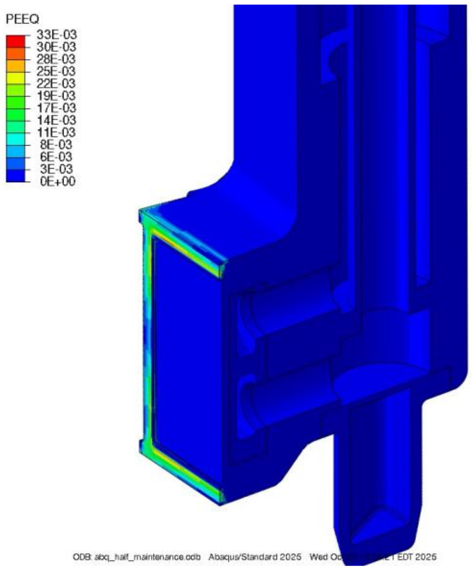

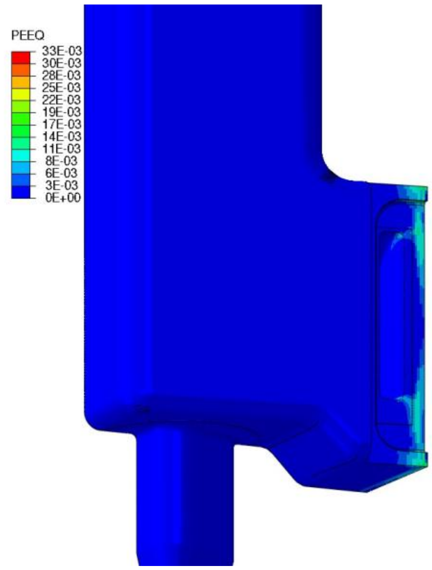

Maintenance Case – EOL 200°C

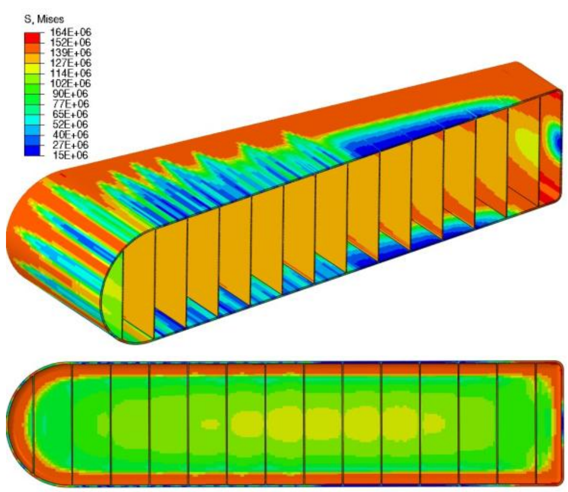

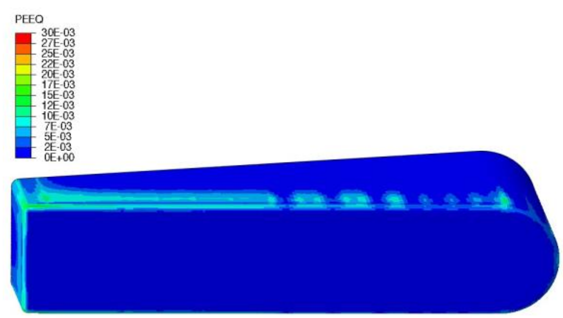

Maintenance Case – EOL 200°C

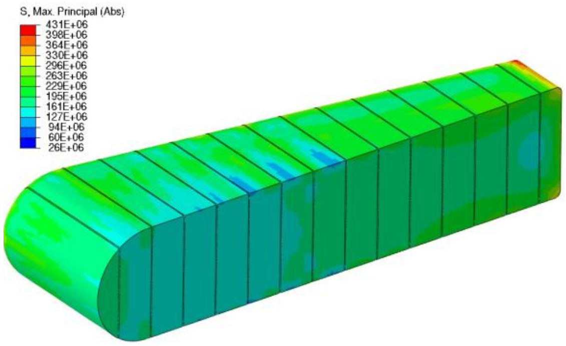

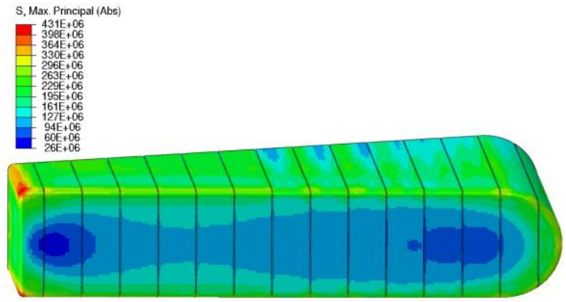

Maintenance Case – EOL 100°C

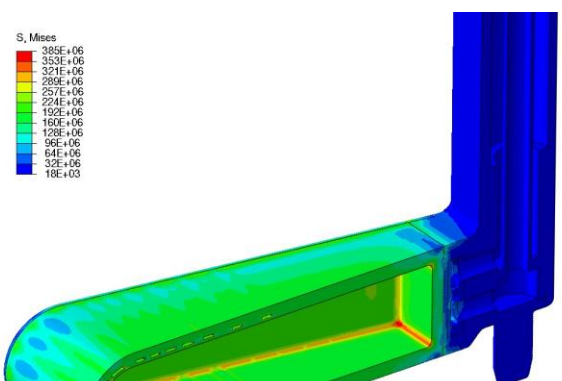

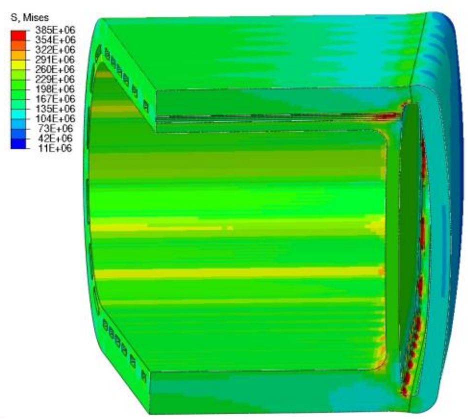

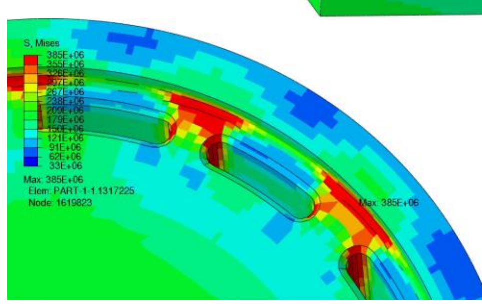

Maintenance Case – EOL 100°C

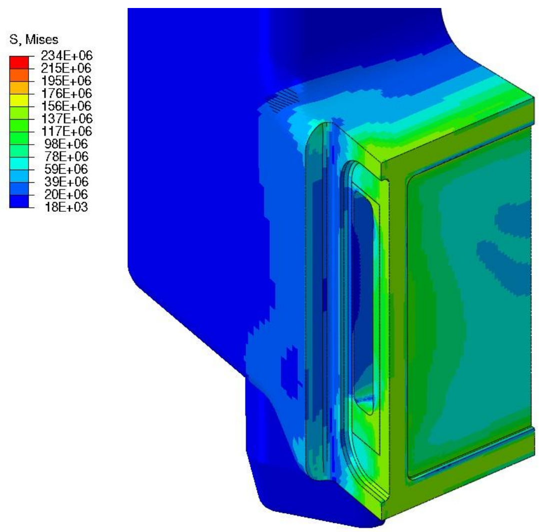

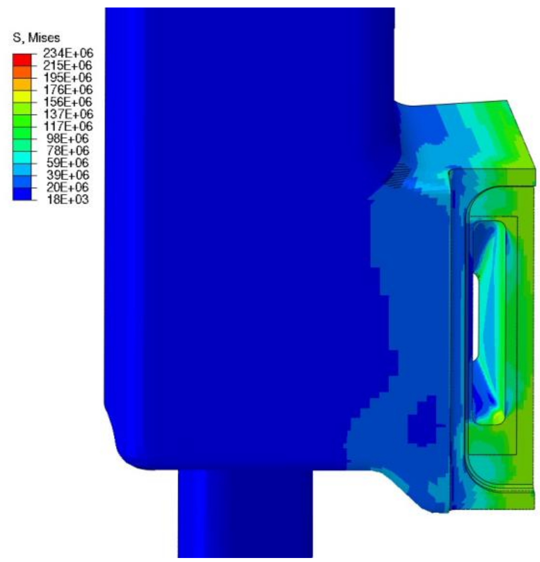

Maintenance Case – EOL 100°C

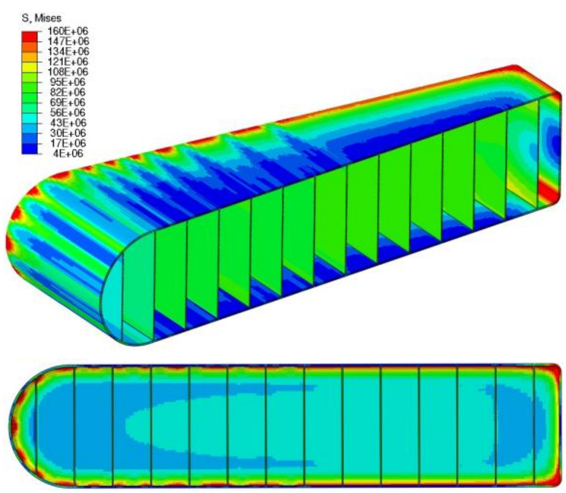

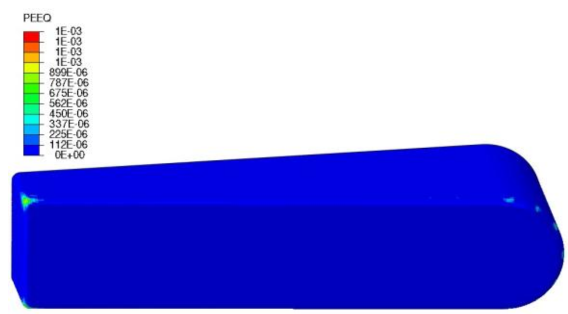

Maintenance Case – EOL 100°C

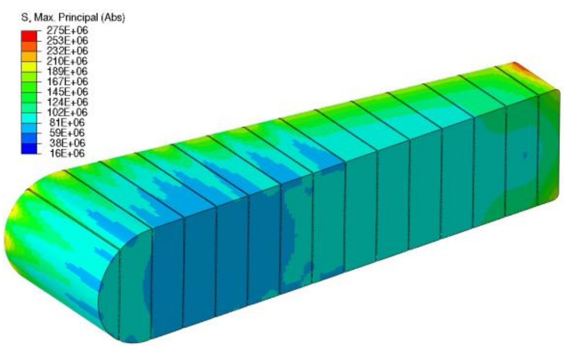

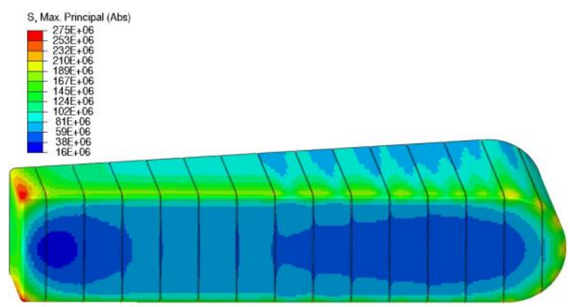

OAK RIDGE National Laboratory | SPALLATION NEUTRON SOURCE

Open slide master to edit